ANALOG/HYBRID SIMULATION OF NON-DARCY FLOW
IN ROCKFILL STRUCTURES

Peter Ludwig Kotiuga

A Thesis

in

The Faculty

of

Engineering

Presented in Partial Fulfillment of the Requirements
for the degree of Master of Engineering at
Concordia University
Montreal, Quebec, Canada

October, 1979

CONCORDIA UNIVERSITY

ABSTRACT

ANALOG/HYBRID SIMULATION OF NON-DARCY FLOW IN ROCKFILL STRUCTURES

Peter Ludwig Kotiuga

This thesis presents a one-dimensional analog/hybrid model for non-Darcy flow in rockfill structures. The model is used to determine the family of phreatic surfaces within the rockfill due to an external impact wave; the rockfill is bounded by an impervious core at the downstream end.

The impact wave is classified as "slow drop" or "fast drop" depending respectively on whether or not the fall rate of the external wave is slower or faster than the maximum seepage velocity. The movement of the outcrop point was determined for the more complex "fast drop" case for one wave period using five techniques: MIMIC, numerical, analytic, approximate, and analog. The inputs were taken from earlier experimental data (reported by Nasser [35]) for four rock types.

The outcrop point movement represents a boundary condition for the main model. The main model is based on the continuity and momentum equations for long, shallow water waves. These equations form a system of quasi-linear hyperbolic partial differential equations; the method of

characteristics is applied to render the equations stable from an error propagation point of view. The time variable is discretized to produce ordinary differential equations in the spatial variable only. These are solved iteratively to satisfy the zero normal velocity boundary condition at the core.

Comparisons with experimental results are given where applicable and readily available.

ACKNOWLEDGEMENTS

His path led through the sea
His way through the mighty waters
Though His footprints were not seen.

— Psalm 77:19

I dedicate this work to Him who comforted me in my darkest hours, who flooded my mind with love and hope and peace when fear tried to grip me, who gave me a new life and the highest principles to live by, who helps me love all people; I dedicate this to the Person and my Lord Jesus Christ.

Dr. M. S. Nasser is no ordinary person either. It has been the greatest honour to work with, study under, and share with a man of wisdom and understanding, who upholds high principles and commands the deepest respect of those who truly know him. His suggestions, moral support, his concern and thoughtfulness, his time, are immensely appreciated. His confidence in and patience with me have hopefully not gone unrewarded.

Special thanks are due to Mr. Dave Hargreaves for his technical excellence and support in programming the analog/hybrid computer. I especially thank Mrs. Julie Strick for doing a splendid job of typing, editing, and preparing the tables.

I am grateful for the National Research Council and the Civil Engineering Department for supporting me financially.

To all my friends and professors who took an interest in my progress and made my stay a pleasant one, I express my gratitude and love.

Extra special thanks are due to my family, especially my mother, who cared and encouraged and understood and prayed. They have waited for this day.

Last but certainly not least, I dedicate this work to the young woman who has captured my heart and soul and has often helped soothe a troubled mind. Grace, I love you! Thanks for sharing.

September 28, 1979
Montreal, Quebec

Peter Ludwig Kotiuga

vii

TABLE OF CONTENTS

LIST OF FIGURES

LIST OF TABLES

xvi

CHAPTER 1

INTRODUCTION

1.1 DEFINITION OF THE PROBLEM

As a wave attacks a rockfill structure, a maximum amplitude referred to as the maximum run-up and a minimum water level referred to as the limit of rush-down will be encountered on the interface; these two levels constitute the impact wave height. Part of the incident wave's kinetic energy is consumed in the uprush, part is reflected on the rock face and the remaining energy is transmitted into the rockfill. Within the rockfill the flow is usually in the non-Darcy regime and further dissipation of the wave energy occurs due to high damping effects.

The model used is based on a rockfill embankment with an impervious core (Fig. 1). By the time the wave reaches the core it will have lost most of its energy so that the transmitted wave height at the core will be significantly smaller than that of the impact wave. Simulation of the successive phreatic line profiles would provide a better understanding of interior wave motion.

1.2 OBJECTIVES

The main objective of this thesis is to develop an analog/hybrid model to simulate the phreatic line profiles within a porous breakwater
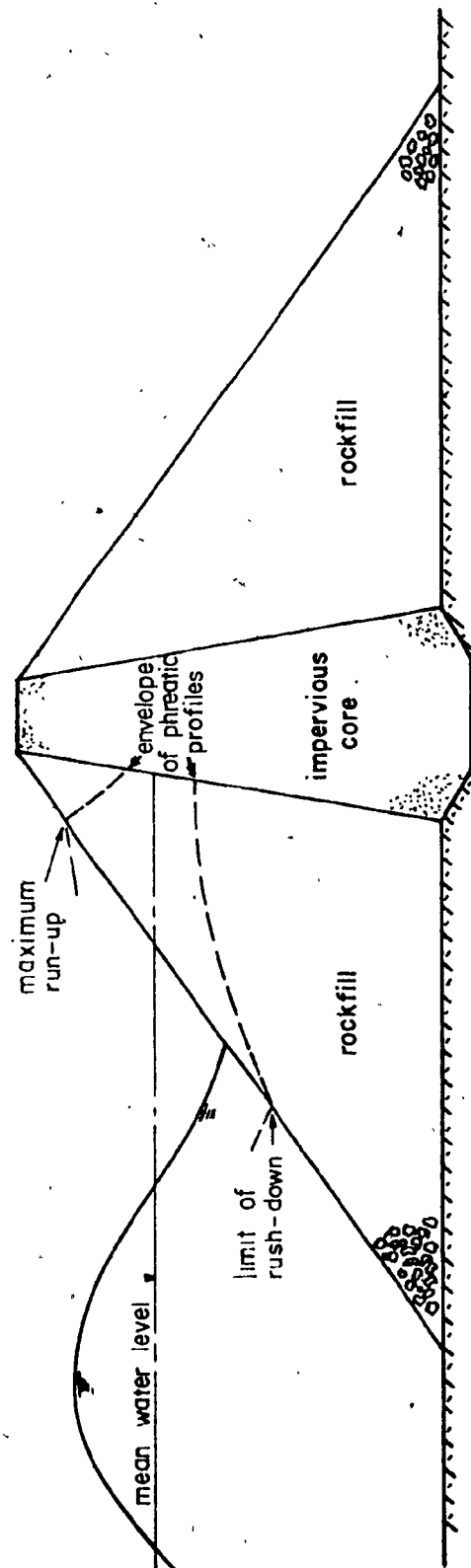
Fig. 1.1   Definition of Problem

or a rockfill dam. A Continuous-Space Discrete-Time technique is utilized
to generate a family of phreatic lines for given boundary conditions.

In determining the oscillating phreatic lines within the
structure, the movement of the outcrop point relative to an assumed sin-
usoidal impact wave is utilized as an entrance boundary condition. The
vertical rate of fluctuation of the impact wave is classified as either
"slow" or "fast" dropping. A slow drop case is one in which the oscilla-
tions of the external wave and the outcrop point are synonymous. A fast
drop case is one in which a surface of seepage occurs at the rockfill
interface because the maximum fall velocity of the internal wave is less
than that of the external wave.

This study emphasizes the digital and analog analysis of the
more complex fast drop case boundary condition and the subsequent genera-
tion of the internal phreatic surfaces for a complete wave period.

1.3 MOTIVATION

Very few attempts have been made using hybrid simulation for
specific engineering field problems governed by hyperbolic equations.
Vichnevetsky has published two excellent papers: one dealing with a
river flooding problem and another simulating electrical-transmission
lines. Civil engineers have shown very little interest in hybrid program-
ming and hence there exists a challenge to fill that vacuum. Due to lack
of exposure to hybrid computing by most engineers, the thesis will attempt
to present some of the frustrations likely to be encountered in solving
problems by this method. Since the method is solved from a civil engin-
eering point of view, many complexities of the system will not be empha-
sized.

The importance of this study is manifested in its practical application. Attainment of the stated objective could lead to a more rational approach for estimating the freeboard on the face and core of a dam, thereby resulting in better control over the maximum allowable reservoir level. Further, the height of such shore protection structures as gabion walls could more effectively be established. Tracing the unsteady water surface profiles is of value in determining the pressure distribution within the embankment.

1.4 Approach in General

Analog computers can only integrate one independent variable and since two independent variables exist (space and time), one of them must be discretized. If the time is chosen to be continuous, then the method is known as Discrete-Space Continuous-Time (DSCT) or the Parallel method. This method requires too many components if solved only on the analog computer or a special multiplexer if solved on the hybrid computer. The method chosen is the Continuous-Space Discrete-Time (CSDT) or the Serial method. There is an economy of components but error propagation becomes a problem. The two system equations are modified into characteristic equations. These resulting ordinary differential equations have characteristics of opposite sign but are integrated in the same direction. The development of the boundary conditions plays a major role in the accuracy of the solutions. A separate study of the movement of the outcrop point was made to provide the wave entrance conditions. Analytic, numeric, approximate, and analog

results are compared in the study. The continuous output derived from the plotters yields a family of curves showing the unsteady water surface profiles. These profiles are compared with the results obtained by Nasser and McCorquodale [33, 35].

CHAPTER 2

LITERATURE REVIEW

Non-Darcy flow problems have been treated by a few analytical
or numerical techniques [19, 33, 35].

2.1 SCOPE

Nasser [35] recommended that the analog simulation of long
water waves introduced by Henry [23] might be adapted to solving the
differential equations governing wave-induced unsteady non-Darcy flow.
This chapter reviews prominent contributions to the wave phenomenon of
non-linear flow in rockfill structures and the hybrid implementation of
hyperbolic partial differential equations (PDE). The governing equations
are introduced after a brief description of the nature of flow in porous
media. Different methods of solution of non-Darcy flow are then reviewed.
A summary of the various hybrid techniques developed for hyperbolic
PDE's is presented, the reasons justifying the choice of the method
employed in this work are emphasized.

2.2 FLOW REGIMES IN POROUS MEDIA

In 1856 Darcy first proposed his familiar law which expresses
the relationship between the 'macroscopic' velocity, q, and the hydraulic

gradient, i, for linear (or laminar) flow in a porous medium, viz.

$$q = ia \qquad \ldots \ldots \ldots \ldots (2.1)$$

where 'a' is a resistance coefficient.

It was not until 1901 that Forchheimer [16] published a paper indicating that Darcy flow does not universally characterize flow in porous media. He proposed the following equation which incorporates both linear and non-linear flow behaviour [1].

$$i = aq + bq^2 \qquad \ldots \ldots \ldots \ldots (2.2)$$

where 'b' is a non-Darcy resistance coefficient.

Other expressions for flow resistance in non-Darcy flow have also been proposed [11, 1▓▓▓▓, 31, 60]. In equation 2.2, a large a/b ratio suggests a predominantly laminar flow whereas a very low ratio suggests turbulent flow. Transitional flow would contain various intermediate values of a/b. There is another region of non-Darcy flow where extremely low flows exist. Kovacs [29] represents this microseepage regime by:

$$i = i_0 + aq \qquad \ldots \ldots \ldots \ldots (2.3)$$

where i_0 is a threshold gradient. The various possible regimes of flow in porous media can be represented graphically after Kovacs as in Figure 2.1.

As the flow increases in the transitional regime, the viscous effects decrease and hence the stable streamlines in the pores through which the flow propogates, start to break down and the inertial effects become predominant. In the case of rockfill structures such as break-
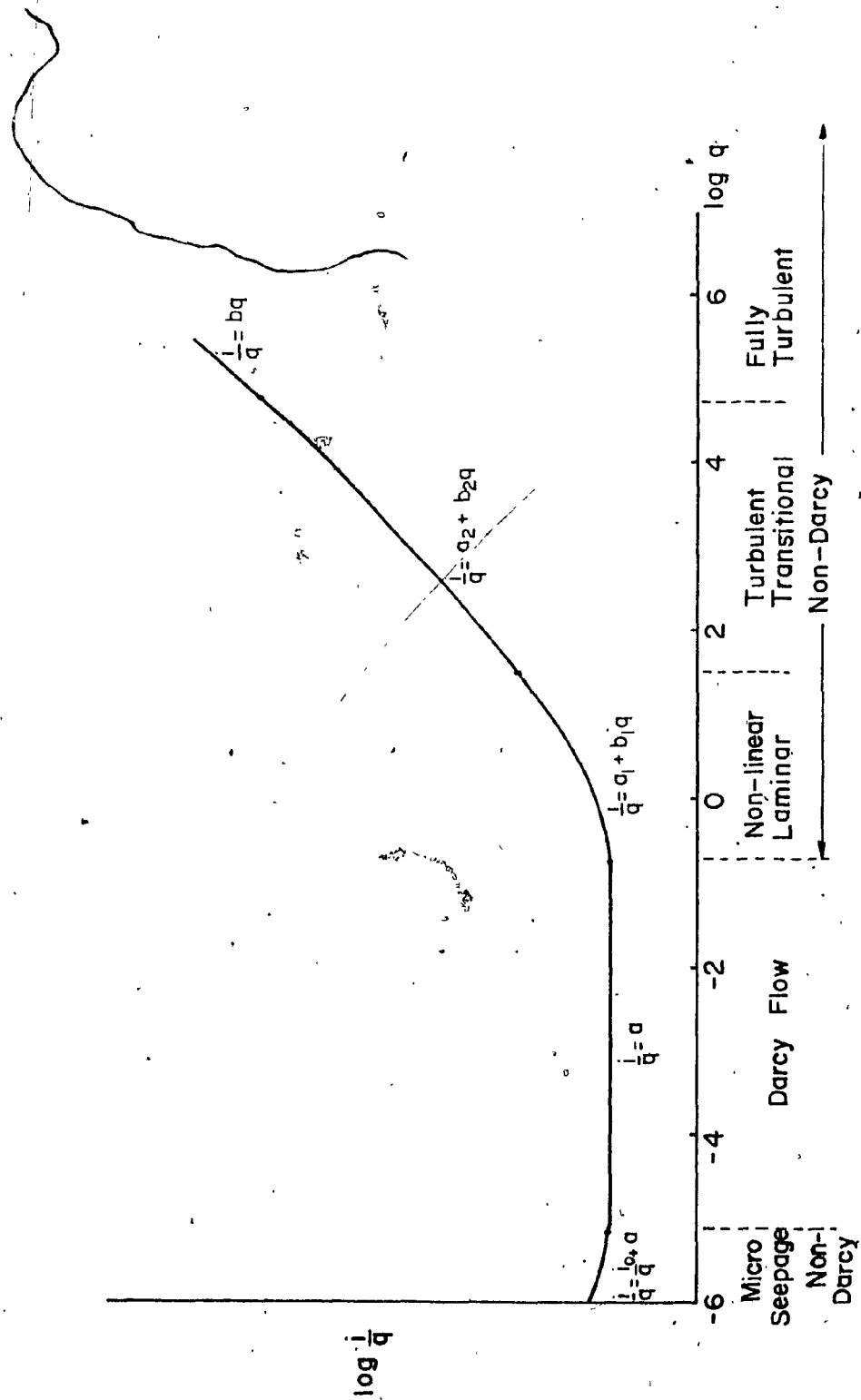
Fig. 2.1   Regimes of Flow in Porous Media

waters, the interstitial spaces tend to be quite large, thereby furnish-
ing greater propensity for inertial than viscous effects.

For the present study, both the coefficients a and b are
essential inputs. The data available on different experimental values
is very limited: the values determined by Nasser [35] were chosen for
convenience. Nasser used a steady flow permeameter to establish the
Darcy and non-Darcy coefficients, a and b. A least squares technique
was used to correlate i/q and q in Equation (2.2) and deduce the
intercept a and the slope b of the line of best fit. Nasser also
pooled his data with that of Lane, McCorquodale, Dudgeon and Ng. Empiri-
cal or semi-empirical expressions for a and b are generally considered
constants for a particular medium, fluid and flow regime.

2.2.1 State of the Art on Non-Darcy Flow

A comprehensive description of the studies performed on Darcy
and non-Darcy flows can be found in references [33, 34, 35]. The present
analysis has been mainly influenced by the work of Dracos, McCorquodale,
and Nasser.

Dracos [10] presented a study of linear flow in an infinite rectang-
ular sand medium. He uses the classical method of characteristics to
solve the Darcy flow equations:

$$\frac{\partial u}{\partial t} + u \frac{\partial u}{\partial x} + g \frac{\partial \eta}{\partial x} + gm \frac{u}{K} = 0 \qquad \ldots \ldots \ldots \quad (2.4)$$

$$\frac{\partial \eta}{\partial t} + u \frac{\partial \eta}{\partial x} + (h_0 + \eta) \frac{\partial u}{\partial x} = 0 \qquad \ldots \ldots \ldots \quad (2.5)$$

where m = porosity

g = acceleration due to gravity

u = horizontal pore velocity

η = perturbation height with respect to the mean water level

h_0 = mean water level

K = conductivity for Darcy flow.

His solution is verified by experiments performed in a Hele-Shaw apparatus. He presents the analysis of the movement of the outcrop point, i.e., the point at which the phreatic line intersects the boundary of the sand medium. Dracos shows that the outcrop point movement may undergo different phases depending on whether the maximum fall rate of the phreatic line within the rockfill structure is faster or slower than the fall rate of the free water level. Nasser [35] extended Dracos' analysis to the more complex non-Darcy flow regimes. Appendices A and B give the detailed analysis and solution of the initial value problem. Five solution methods are investigated and compared with special emphasis on the general analog solution. Computer programs and plots illustrate the types of possible initial conditions.

McCorquodale [33] uses a finite element model to study the problem of wave propagation through a rectangular rockfill embankment with an impervious core. He represents the tailwater piezometric boundary condition by a periodic function and uses triangular elements in discretizing his solution domain. After each time increment, the position of the free surface is calculated from the known previous value and the surface particle velocity during that increment.

Nasser [35] uses the method of characteristics coupled with a finite difference technique to treat wave motion in porous structures.

More recently, Hannoura and McCorquodale [19] combine the finite element and method of characteristics to determine the phreatic line and internal pressure distribution corresponding to maximum run-up. The results provide useful information for studying the stability of seawalls under both static and dynamic loading conditions. They indicate that about 60% less CPU time is required in comparison to the implementation of a purely finite element method.

The use of analog/hybrid techniques to solve this problem is missing from the literature. Some hyperbolic wave-type systems have been solved on the hybrid computer but none for porous media problems.

2.2.2 The Nature of the System Equations

Henry [23] presents the digital applications of a method devised originally to facilitate the analog and hybrid simulation of hyperbolic PDE's. The method was originally used to discretize the space variable and integrate with respect to time. He considers the problem of tidal motions in rivers and estuaries and the response of coastal inlets to tsunamis, both of which are long wave phenomena governed by hyperbolic equations. He introduces the continuity and general dynamic equilibrium equations respectively as:

$$\frac{\partial h}{\partial t} + u \frac{\partial h}{\partial x} + h \frac{\partial u}{\partial x} = q \qquad \ldots \ldots \ldots \ldots (2.6)$$

$$\frac{\partial u}{\partial t} + u \frac{\partial u}{\partial x} + g \frac{\partial h}{\partial x} = g(S_0 - S_f) - \frac{qu}{h} \qquad \ldots \ldots \ldots (2.7)$$

where   h = water level

       u = horizontal velocity

       q = lateral inflow

       S_0 = channel slope

       S_f = friction slope.

Nasser [35] introduces a porosity term and a representative resistance term in the momentum equation. His equations in a matrix form are:

$$
\begin{bmatrix}
\dfrac{h_0 + \eta}{m} & 0 & u/m & 1 \\[2ex]
u/m & 1 & gm & 0 \\[2ex]
dx & dt & 0 & 0 \\[2ex]
0 & 0 & dx & dt
\end{bmatrix}
\begin{Bmatrix}
\dfrac{\partial u}{\partial x} \\[2ex]
\dfrac{\partial u}{\partial t} \\[2ex]
\dfrac{\partial \eta}{\partial x} \\[2ex]
\dfrac{\partial \eta}{\partial t}
\end{Bmatrix}
\begin{Bmatrix}
0 \\[2ex]
-gmFu \\[2ex]
du \\[2ex]
d\eta
\end{Bmatrix}
$$

$$\dots\dots\dots\dots\dots (2.8)$$

where   F = a + bq

This is a hyperbolic system of equations; setting the 4 x 4 determinant of the matrix of coefficients to zero yields the positive and negative characteristic equations:

$$\alpha = \left.\frac{dx}{dt}\right|_{+} = \frac{u}{m} + \sqrt{g(h_0+\eta)} \qquad \ldots\ldots\ldots (2.9)$$

$$\beta = \left.\frac{dx}{dt}\right|_{-} = \frac{u}{m} - \sqrt{g(h_0+\eta)} \qquad \ldots\ldots\ldots (2.10)$$

Nasser then determines the equations of motion along the characteristic directions, α and β, respectively as:

$$\frac{d}{dt}\left(\frac{u}{m} + 2\sqrt{g(h_0+\eta)}\right) = -gFu \quad \text{on} \quad \alpha \qquad \ldots\ldots\ldots (2.11)$$

$$\frac{d}{dt}\left(\frac{u}{m} - 2\sqrt{g(h_0+\eta)}\right) = -gFu \quad \text{on} \quad \beta \qquad \ldots\ldots\ldots (2.12)$$

He utilizes a finite difference approach to reduce the time consumption on a digital computer.

Nasser's basic equations will also be used in this study with the appropriate manipulation for a hybrid procedure.

2.3. HYBRID METHODS FOR HYPERBOLIC PDEs

In the 1950s when computers were beginning to develop; the power and relative ease of programming of analog computers in simulation studies presented a sustantial advantage over digital computers. Analog computers were known for their speed, their parallel nature of operation, their man-machine interaction, the continuous output produced and their ability to integrate, a feature of prime importance in differential equations [4].

Throughout the 1950s and 1960s, great strides were made in reducing digital hardware and increasing the speed, accuracy and memory

capabilities of the digital computers. The theoretical aspects of numerical solutions of differential equations were developed so rapidly that the digital computer was accepted as the general-purpose research tool. More time and money was invested into the digital market so that the analog simulations became obsolete to most researchers. There are virtually only a handful of analog computer producing companies today compared with the many in existence in the 1950s.

Hybrid computers were produced in the early 1960s basically out of economic motivation. Analog methods tended to require large amounts of hardware while numerical techniques were often too time consuming. Hybrid computers combine the advantages of the analog computer, i.e., speed and integration, with those of the digital computer, i.e., accuracy and memory capabilities. It must be remembered that the analog computer can integrate with respect only to one independent variable. Therefore, all the hybrid techniques for treating PDEs involve the reduction of the PDEs into a system of ordinary differential equations (ODEs). These techniques will be described shortly.

Vichnevetsky [54] suggests two reasons for preferring a hybrid solution of PDEs to the numerical solution:

a. the PDEs are only a part of a larger system, where some other parts are represented by ODEs and the use of an analog/hybrid system has been dictated by over-all economic requirements;

b. the numerical implementation of the PDE, more or less by itself, is prohibitively long and expensive.

In these cases, hybrid computers have been shown to have the potential to be several hundreds of times faster and cheaper (per solution) than

digital computers.

It is emphasized that the primary concern in this study is not the economic justification of the use of a particular method but rather the exploration of the potential for utilizing a technique not commonly adopted today in civil engineering practice. More detail regarding the advantages and disadvantages of analog computers as well as a description of their major components can be found in Appendix C.

2.3.1 Methods of Lines [54, 62].

Methods of lines are those where PDEs are approximated by ODEs along a certain uni-directional path of integration or 'line' within the space-time domain. The path of integration may be along one of the following directions (considering the space-time domain):

a. parallel to the time axis

b. parallel to the space axis

c. along a characteristic direction.

The first method is the classical analog discrete-space continuous-time (DSCT) method. It is also referred to as the Parallel method since the whole system is analyzed with increasing time. Its hybrid nature is mainly associated with the multiplexing of components.

The second method is commonly referred to as the CSDT or serial method. This method, which is truly hybrid in nature, will be discussed later in greater detail.

The method of characteristics (MOC) has not seen much direct application in analog/hybrid computation. However, the theory associated with the characteristics and their properties in hybrid problems

has been an important tool in the analysis and development of other methods of lines (mainly for CSDT methods).

Schuchmann [46] presents a general paper covering all aspects of analog, hybrid and digital simulation of PDEs. The PDE must be reduced to ODEs since only one continuous variable can be treated by the analog computer. Independent variables can be classified as continuous (C), discretized (D), or transformed (T).

McCann [32] observes that two independent variables with the above three classifications result in nine combinations as shown in Table 2.1.

Since only one variable can be represented continuously, the first combination is no longer valid. The transformation of variables (T) by Laplace or Fourier series was not considered in the present problem since the method did not get support from any of the simulations of practical problems in the literature. A DSDT (discrete-space discrete time) framework would be handled more easily on a digital computer. This leaves the two main methods already mentioned: DSCT and CSDT.

Schuchmann [46] concludes that the DSCT method seems too coarse for an application to flow and wave-type systems and that the hybrid CSDT method seems to be the best for real time simulations of systems containing flow terms, i.e., hyperbolic equations.

2.3.2 DSCT (Parallel) Method [62].

This is the traditional technique used for solving PDEs. The equations are reduced to a set of ODEs in time by using a suitable numerical approximation for the space derivative and the resulting set of equations are solved in parallel.

TABLE 2.1

CLASSIFICATION OF 2-D PROBLEMS

Combination	Space Variable	Time Variable
1	C	C
2	C	D
3	C	T
4	D	C
5	D	D
6	D	T
7	T	C
8	T	D
9	T	T

C = continuous

D = discrete

T = transformed

In principle this method offers the fastest solution yielding time histories of the system behaviour at selected points in the domain. The resulting equations are normally stable and the boundary conditions are rapidly solved on the analog computer. The main difficulty arises in the amount of analog equipment needed. Adequate accuracy requires that a sufficient number of spatial grid points be provided, each of which must be represented by a set of differential equations. Even for simple problems, the equipment requirements can become excessive making the method suitable only to the largest analog installations.

Two important contributions are worth noting; Henry [23] refers to a paper by Hsu and Howe [24] in deriving his numerical sectioning procedure. Hsu and Howe replaced the all-parallel analog solution with a series-parallel combination. Instead of using many analog components, by their multiplexed DSCT method, they employ a relaxation technique. Their method involves integrating a subset of the continuous time finite difference differential equations for the whole period of time and then iterating through the different subsets to satisfy the coupling solution. This method is a special form of cell multiplexing; it retains most of the advantages of the DSCT method except that the speed of solving the problem is reduced due to the iterative process. Hsu and Howe use the iterative DSCT method to solve various diffusion-type equations. Due to the lack of a suitable hybrid computer system, their solution is simulated on a digital computer. Since their work is a preliminary investigation with many unanswered questions regarding implementation of field problems, it was not seriously considered as a method of solution.

Wright and Mutfi [62] utilized a multiplexed DSCT method to model the hyperbolic nature of unsteady fluid flow systems. Their problem dealt with systems subjected to time-varying flow of compressible fluids (quasi-linear hyperbolic PDEs). Because of difficulties encountered in the breakdown of solutions at sonic flow or stagnation points (i.e. fluid velocity is zero), they concluded that the CSDT method is unsatisfactory for unsteady compressible fluid flow problems. The general consensus is to try the CSDT method first and then switch to other methods if it is not applicable.

2.3.3 Method of Characteristics

In the method of characteristics, at every point in the space-time (x-t) plane, there are two characteristic directions in which the PDEs reduce to equations involving total differentials only. In these directions, the equations are not complicated by the presence of partial derivatives in other directions. This method is especially suited for the analyses of hyperbolic PDEs since the two characteristic directions are real and of opposite sign (whereas for elliptic equations, there are two imaginary directions and parabolic equations yield two real and equal directions) [48].

The standard hybrid MOC solution involves integration along one family of characteristics with finite differencing along the other family [62]. A subcomputer block of computing elements is required to integrate along one characteristic and hence N blocks are necessary to handle N characteristics. In addition to the minimum number of blocks needed to maintain numerical accuracy, the number of computing elements per subcomputer block can become large when the characteristics are functions of

the solutions. Therefore, the MOC as a hybrid technique reassembles the DSCT method in that it requires a large number of analog components.

Paul and Ahmed [43] developed a continuous-characteristics approximation technique that slightly differs from the finite difference-differential method described. In their procedure, the characteristics of the equation are used to scan and give data on the initial line, thereby allowing the boundary conditions of the problem to be introduced.

Although their subcomputer blocks contain more complicated set-ups than the standard method, they note that there is a saving in the use of fewer blocks and claim that their method is an improvement upon similar digital techniques because of the increased speed of integration and the continuous nature of integration along one of the characteristics. Paul et al present worked examples which deal with supersonic and compressible flows. The CSDT method is not recommended for solving such problems as was noted earlier.

McAvoy's [31] uses a modification of an error analysis developed by Bosgra and Buis [5] which results in a perfect frequency response relative to the exact solution. He concludes that the MOC can handle problems where discontinuities may arise in the solution. The drawback of McAvoy's method is that it does not use the full potential of the hybrid computer, i.e., the integration process. In his somewhat unusual hybrid implementation, the digital computer is used for function storage and playback while the analog computer solves a system of algebraic equations and determines whether a storage point has been reached. It is only hybrid in the sense that the algebra is performed in parallel.

A mechanical distributed parameter system with a non-linear force was studied by Fugita et al [17] using the theory of characteristics and a finite difference approximation technique. He comments that his method is very useful to such practical problems: his method is not outlined in the paper but in essence it resembles the MOC finite difference differential equations. Upon determining the characteristic lines and making some substitutions, the second order system is reduced to simultaneous first order PDEs. These are then reduced to simultaneous difference equations by using certain transformations and finite difference approximations. Repetitive corrections are then carried out on the non-linear friction force term. This method is not generally applicable as Fugita suggests.

Gentina and Cleret [18] propose a method of solving hyperbolic equations using quasi-linear hybrid methods. They use McAvoy's characteristic method to yield the boundary conditions of the problem. They then use a second method of integration using the boundary conditions stored by the MOC solution to yield the total solution. The second method of resolution incorporates various speeds of integration and track/store devices. The method is not clearly presented.

In summary, the MOC hybrid technique can be used in problems where discontinuities may arise or in scanning the domain of a problem to determine the boundary conditions. This method is not generally pursued due to its limited applications and the quantity of analog components required. Thus, the most viable and truly hybrid technique remains to be discussed.

2.3.4 CSDT (Serial) Method

Since its introduction [26] in 1961, the serial method has steadily been growing in popularity to the point that today it is the standard hybrid approach of computation. The method consists of reducing the PDEs to ODEs in space by a suitable numerical representation of the time derivative. This reduces to a boundary value problem which must be solved at each time step of the time-marching integration process [52].

CSDT methods are inherently dependent on the capability of store and playback functions. This severely taxes the hybrid interface hardware and the high speed of the analog computer is only possible to the degree allowed by the time for information to be read in and out of the digital computer. Therefore, this method is usually reserved for complex PDEs.

This method has the following advantages over the classical DSCT method [20]:

1. It allows for higher resolution and accuracy without a proportional increase in equipment and as such is important in dealing with non-linearities in equations.

2. Greater use is made of the high-speed computational capabilities of the analog computer.

3. The integration interval of the continuous space variable can be controlled so that problems with moving boundaries are easily solved.

The major set-back with CSDT methods is the problem of error propagation. Typical hybrid errors result from truncation of results and inaccuracies in analog equipment. These errors can be controlled to a certain degree and do not drastically change the results. The CSDT

method has the disadvantage that the system equations are inherently
unstable, i.e., the errors will accumulate rapidly and become substantial.
Various techniques have been developed to overcome this drawback.

The target-shooting method consists mainly of iteratively
correcting guessed values. It suffers from serious error instability
properties and is not frequently used.

Calza-Bini et al [52] used a superposition technique whereby
the solution of the homogeneous equation is added to the computed solu-
tion so that the boundary condition is satisfied. The error instability
is reduced because there is no iteration but the problem still exists.

Witsenhausen [52] expressed the solution as a functional or
definite integral of the space variable with the use of Green's functions.

Vichnevetsky's paper [51] introduced the Decomposition Method
in 1968 and was instrumental in establishing the CSDT method as the
standard hybrid approach. His method decomposes an unstable problem of
the second order into problems of the first order that can be made stable
by the proper choice of the spatial direction of integration.

The method can be best illustrated using a linear coefficient
parabolic equation, viz.,

$$\frac{\partial u}{\partial t} = K \frac{\partial^2 u}{\partial x^2} \qquad \ldots \ldots \ldots \ldots \quad (2.13)$$

Discretizing the time yields

$$\frac{d^2 u^{j+1}}{dx^2} - \frac{u^{j+1}}{k\Delta t} = -\frac{u^j}{k\Delta t} \qquad \ldots \ldots \ldots \ldots \quad (2.14)$$

The operator of this equation,

$$L = \frac{d^2}{dx^2} - \frac{1}{K\Delta t} \qquad \ldots \ldots \ldots \ldots (2.15)$$

may be decomposed into the product:

$$L = \left(\frac{d}{dx} - a_F\right)\left(\frac{d}{dx} - a_B\right) = L_F \cdot L_B \qquad \ldots \ldots \ldots \ldots (2.16)$$

where $\quad a_F = \dfrac{-1}{\sqrt{K\Delta t}} \quad ; \quad a_B = \dfrac{+1}{\sqrt{K\Delta t}}$

A particular solution of the system may be obtained by solving two computationally stable initial value problems:

$$L_F y_1 = \frac{dy_1}{dx} - a_F y_1 = -\frac{u^j}{K\Delta t} \qquad \ldots \ldots \ldots (2.17)$$

integrated in the forward direction ($x = 0$ to xmax) and

$$L_B y_2 = \frac{dy_2}{dx} - a_B y_2 = y_1 \qquad \ldots \ldots \ldots \ldots (2.18)$$

integrated in the backward direction (x = xmax to 0) or

$$\frac{dy_2}{d(-x)} + a_B y_2 = -y_1(x) \qquad \ldots \ldots \ldots \ldots (2.19)$$

The same analog cell can be used twice to represent these equations as can be seen in Figure 2.2.

Vichnevetsky also introduced an interpolated form of Equation 2.13 to reduce the time-skew effect which results in a truncation error of order Δt.
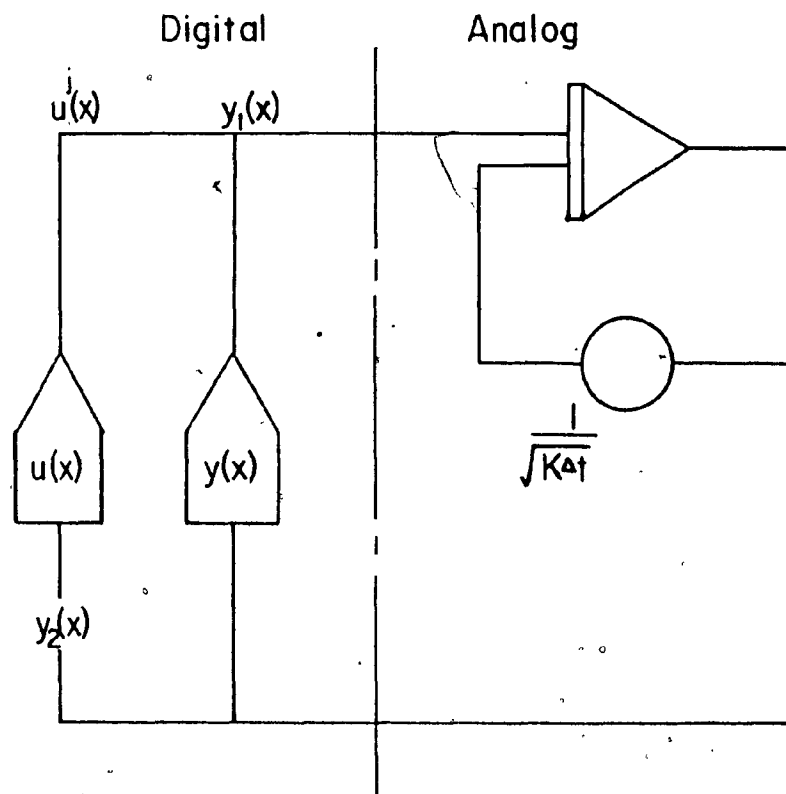
Fig. 2.2 Typical Analog Cell for a Parabolic System

$$\frac{d^2u^{j+1}}{dx^2} - \frac{u^{j+1}}{\theta K \Delta t} = -\frac{u^j}{\theta K \Delta t} - \left(\frac{1-\theta}{\theta}\right)\frac{d^2u^j}{dx^2} \quad \dots \text{(2.20)}$$

where θ is the interpolation factor,

which is reduced to

$$\frac{d^2u^{j+1}}{dx^2} - \frac{u^{j+1}}{K\theta\Delta t} = -\frac{\tilde{u}^j}{\theta K \Delta t} \quad \dots \dots \dots \dots \dots \text{(2.21)}$$

$\tilde{u}$ satisfies the recurrence relation

$$\tilde{u}^{j+1} = \tilde{u}^j + \frac{1}{\theta}\left(u^{j+1} - \tilde{u}^j\right) \dots \dots \dots \dots \dots \dots \dots \text{(2.22)}$$

A detailed analysis of this process would show that a necessary and sufficient condition for time-marching stability is $1/2 < \theta < 1$.

Later in 1968, Hara and Karplus [20] introduced their CSDT version for solving PDEs with stable equations. A control function is digitally generated and is imposed as a forcing function upon the analog circuit. A steepest descent optimization routine is then used to minimize the errors of the control forcing function. They feel that the high speed computational capabilities of the hybrid computer can offset the more complicated functional optimization problem and hence more hardware, introduced by their method.

The introduction of novel computing serial schemes reached a peak in 1970. Vichnevetsky and Tomalesky [58] solved a time dependent river pollution problem which was basically an extension of Vichnevetsky's previous work. In order to reduce the computer time consumption, they introduced a technique by which truncation errors induced by taking larger grid-time steps could be corrected for in a semi-exact fashion.

In 1969, Vichnevetsky [53] introduced a different method applicable only to quasi-linear hyperbolic problems. He presented a second

order hyperbolic system, viz:

$$\frac{\partial u}{\partial t} = f(u) \frac{\partial u}{\partial x} + g(x,t) \qquad \ldots \ldots \ldots \ldots (2.23)$$

where u is a two dimensional vector of dependent variables, f is a square matrix of functions of u and $g(x,t)$ is the external or forcing function, thus,

$$u = \begin{vmatrix} u_1(x,t) \\ u_2(x,t) \end{vmatrix} \quad ; \quad f(u) = \begin{vmatrix} f_{11}(u) & f_{12}(u) \\ f_{21}(u) & f_{22}(u) \end{vmatrix} \quad ; \quad g = \begin{vmatrix} g_1(x,t) \\ g_2(x,t) \end{vmatrix}$$

$$\ldots \ldots \ldots \ldots (2.24)$$

The system can be transformed to its characteristic form:

$$\frac{\partial W}{\partial t} = \lambda I \frac{\partial W}{\partial x} + G(x,t) \qquad \ldots \ldots \ldots \ldots (2.25)$$

where W is the vector of transformed dependent variables

   I is the identity matrix

   λ is the vector of eigenvalues

   G is the resulting forcing functions, i.e.,

$$W = \begin{vmatrix} W_1(u_1, u_2) \\ W_2(u_1, u_2) \end{vmatrix} \qquad \lambda = [\lambda_1(W_1, W_2) \quad \lambda_2(W_1, W_2)] \ldots \ldots (2.26)$$

Upon discretizing the time variable in Equation 2.25, the resulting boundary value problem reduces to two initial value ODEs with stable error propagation properties. The equations are decoupled by a time interlaced integrated scheme which can be seen in the computer block diagram in Figure 2.3.

$$\frac{dW_1^j}{dX} - \frac{W_1^j}{\lambda_1 \Delta t} = -\frac{W_1^{j-1}}{\lambda_1 \Delta t} - \frac{G}{\lambda_1}$$

Boundary Condition
in $X = 0$

$$W_1^{j+\frac{1}{2}} = \frac{3}{2} W_1^j - \frac{1}{2} W_1^{j-1}$$

$$\frac{dW_2^{j+1}}{d(-X)} + \frac{W_2^{j+\frac{1}{2}}}{\lambda_2 \Delta t} = \frac{W_2^{j-\frac{1}{2}}}{\lambda_2 \Delta t} + \frac{G}{\lambda_2}$$

Boundary Condition
in $X = X_{max}$

$$W_2^{j+1} = \frac{3}{2} W_2^{j+\frac{1}{2}} - \frac{1}{2} W_2^{j-\frac{1}{2}}$$

$$W_1^j \simeq W_1(X, t^j)$$

$$W_2^{j+\frac{1}{2}} \simeq W_2(X, t^{j+\frac{1}{2}})$$
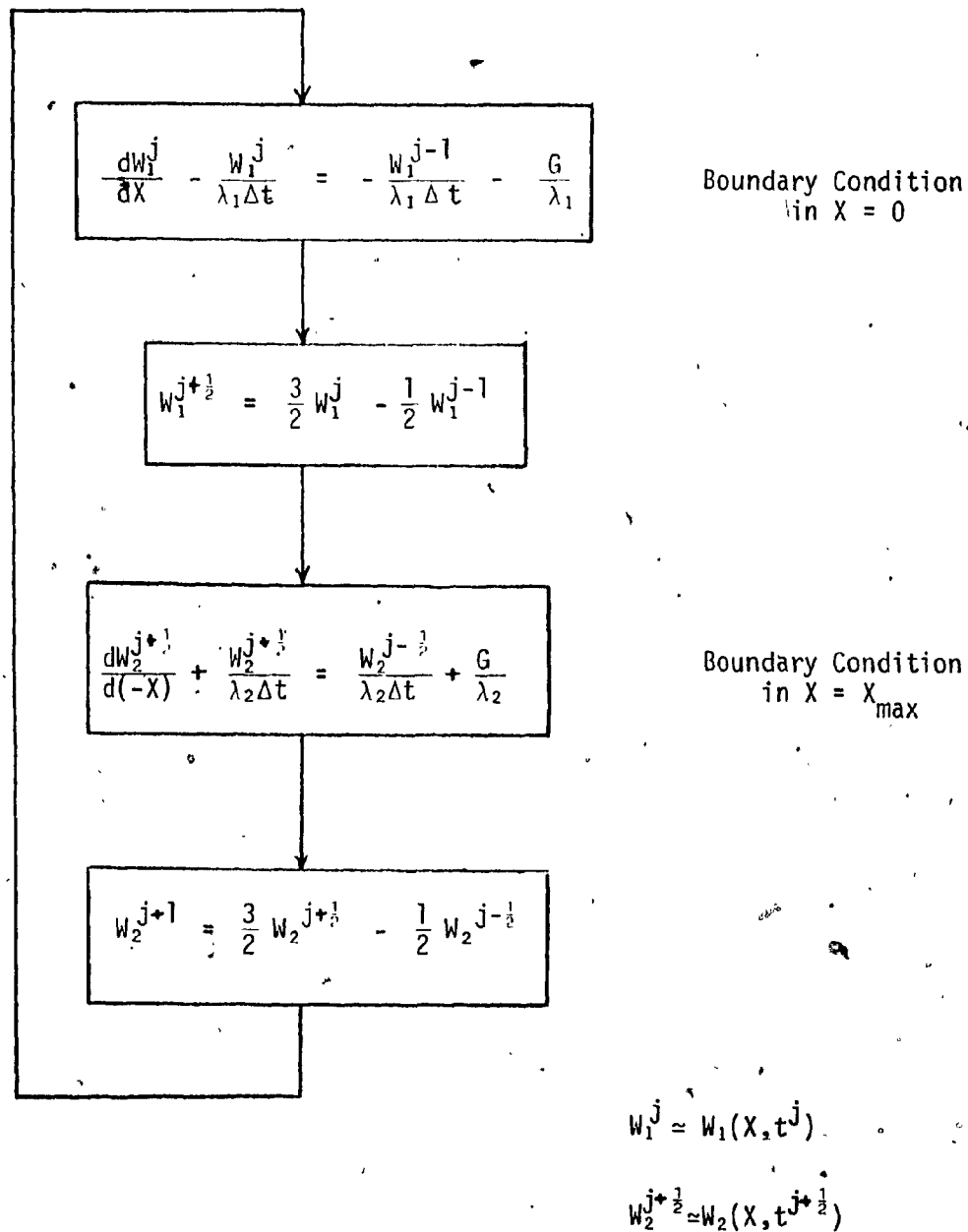
Fig. 2.3 — Computer Block Diagram of Interlaced Integration
Scheme.

Vichnevetsky uses a river flooding problem to illustrate his method. This method cannot indiscriminately be applied to the present study despite the similarity in the problem definitions. This is due to the fact that Vichnevetsky's flood wave has no downstream constraint, i.e., the wave is allowed to freely dampen out along its course whereas the solution domain in the present study is constrained by the core which not only inhibits further flow but also introduces wave reflection.

Vichnevetsky's method permits the decoupling of the discretized characteristic equations because the wave disturbances propagate in different directions. His initial value equations are simpler than the two point boundary value problem at hand. An iterative procedure was found necessary to evaluate the downstream condition in this study.

André [2] suggested two methods similar to Vichnevetsky's. In the first method, given first order PDEs, a similarity transformation is carried out whereby the equations to be solved at each time period on the analog are totally decoupled and hence solved simultaneously. In the second method, he applies the method of characteristics (MOC) to quasilinear hyperbolic equations. He uses increments in both time and space dimensions and claims that accuracy is not sacrificed at discontinuities.

Nelson [38] presented a preliminary study into the use of invariant bedding. This technique is essentially a method of converting a two-point boundary value problem for a linear system of ODEs to an equivalent initial value problem for an associated non-linear system of ODEs. A progress report on a digital solution appeared later in the year [39]. They felt it was a highly effective method for solving some types of PDEs.

Silvey and Barker [47] presented a decomposition-iterative method that uses one trial run and two correcting runs at each time step to satisfy the boundary conditions to within 0.1 per cent. They felt their method was more accurate than Vichnevetsky's decomposition-superposition method but at the expense of computing time.

Bosgra and Buis [5,6,7,8] introduced a directional difference method which was generally applicable to sets of hyperbolic equations. They found the decomposition-iterative method very impractical and searched therefore for a better method of solution. Assuming a sufficiently smooth function, they chose a point lying on a straight line joining two solution points for which the mean value theorem was valid. This method involved taking both time and spatial increments (as did André) and could be considered more general than Vichnevetsky's scheme. By choosing the proper ratio of space-to-time grid sizes, stability could be ensured for the finite difference-differential equations. Bosgra et al present error analysis in both the physical and numerical sense: the suitability of the method as a tool for the development of new classes of methods, etc. is discussed in subsequent papers. A complex multi-point hybrid CSDT difference approximation is introduced that eliminates the problem of inversion of the coefficient matrix as well as the suitability problem.

In 1971, Nelson and Altom [40] published their hybrid solution using their method of invariant imbedding. For the parabolic problem considered, they found their technique slightly less efficient (efficiency being measured by the number of operations) than the decomposition-superposition method but considerably more efficient than the decomposition-iteration method. They feel their method is at least competitive with

other stable serial methods for some problems.

Appolovicova and Babirad [3] in 1973 solved a general hyperbolic system by a method of distribution. The resulting equations and formulations closely parallel the decomposition-superposition method. The difference lies in their definition of two optional and arbitrary functions in the solution that must be chosen in such a way that the final solution must fulfill the initial and boundary conditions. This method does not appear generally applicable to this study.

In 1974, Vichnevetsky and Tomalesky [59] presented a computer algorithm for treating hyperbolic PDEs with special application to the simulation of electrical transmission lines. Truncation errors cause a spurious diffusion term to be introduced into the problem. This paper, similar to the one in 1969, introduces a time-centered approximation which results in a new recurrence algorithm. Incremental values are transferred across the interface to alleviate the effects of round-off errors.

O'Brien and Edge [42] in 1975 extended Vichnevetsky's work to yield a hybrid solution of the water quality in an estuary. Their graphical results were very instructive.

Stockton [49] solved the wave equation in isotropic and anisotropic media by employing MOC. He obtains satisfactory results for the isotropic case by using a predictor/corrector estimator for the unknown boundary conditions. For the anisotropic case, he implements a method whereby a solution is obtained from two computationally independent solutions. He indicates that the hybrid procedure is significantly superior to the digital procedure with respect to execution time.

In 1976, Janac [25] presented CSDT methods to solve PDEs in several space dimensions. The schemes are unconditionally stable with no truncation error in relation to the space variables. He makes use of the 'weak approximation' theory to approximate two-dimensional problems (in space) by two one-dimensional problems. He then uses a Crank-Nicolson scheme [48] to develop the recursive equations. He solves the boundary value problems for a system of ODEs (these can be solved in parallel). He claims that a very fine space discretization is possible without accumulating larger errors and without the need for more accurate computations.

In summary, the CSDT method is the most versatile, truly hybrid technique but has a problem of computational instability. Numerous techniques have been developed to overcome this problem, some highly specialized, others very general in application. In particular, the work of Vichnevetsky and O'Brien et al have influenced the present study. .

Chapter 3

THEORETICAL DEVELOPMENTS

This chapter will describe the development and modification of the non-Darcy flow equations to suit the CSDT method of analysis. The theory presented considers a rectangular embankment; however, sloping configurations would basically differ in the geometric treatment.

3.1 Governing Equations

The derivation of the basic continuity and momentum equations for unsteady flow can be found in numerous references [9, 22, 35].

Fig. 3.1 shows an impact wave with a mean water level, h_o, and a maximum amplitude, A_o, attacking a rockfill structure; the resultant interior flow has a horizontal velocity, u. Within the porous media, the wave gradually loses its kinetic energy due to friction; the height of the phreatic surface with respect to the mean water level is termed η, so that the actual depth, y, of the phreatic surface is

$$y = h_o + \eta \qquad \ldots \ldots \ldots \ldots \ldots (3.1)$$

Since h_o is constant, the differential height of the phreatic surface is

$$dy = d\eta \qquad \ldots \ldots \ldots \ldots \ldots (3.2)$$
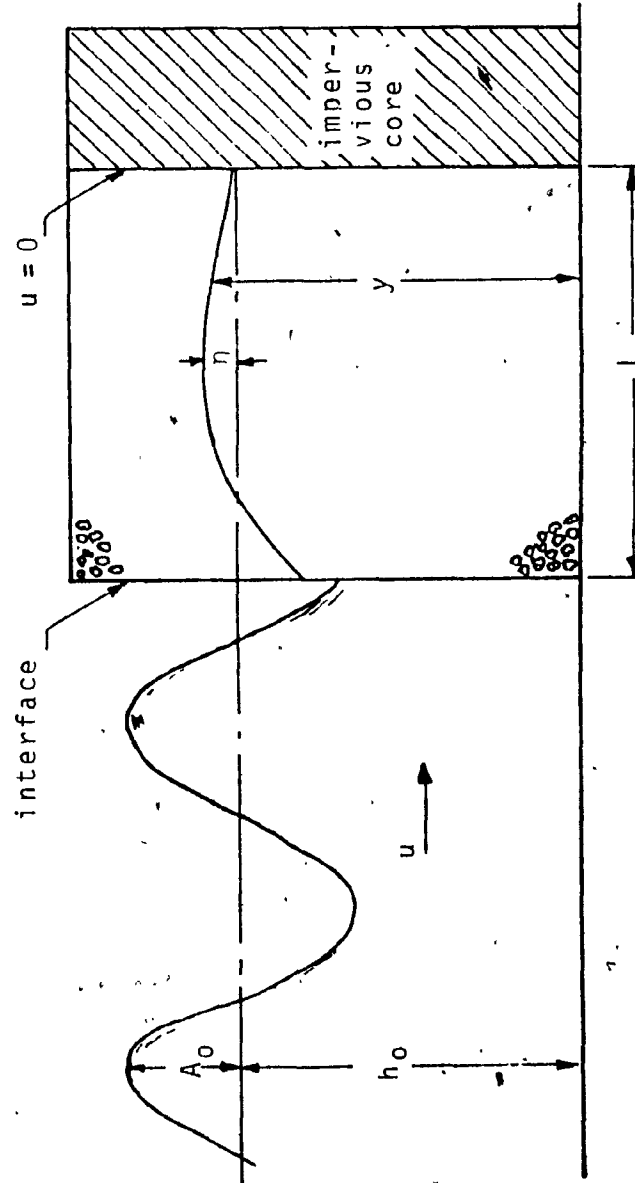
Fig. 3.1 Problem Definition

The porosity, m, is the ratio of the volume of the voids to the total volume of the medium and can therefore be taken as a measure of the actual cross-sectional area through which the water can flow. Hence, the actual pore velocity, $\underline{V}$, is

$$\underline{V} = u/m \qquad \qquad \ldots \ldots \ldots \ldots (3.3)$$

3.1.1 Continuity Equation

Henderson [22] gives the continuity equation for a long shallow water wave (Fig. 3.2), i.e.

$$\frac{\partial y}{\partial t} + \underline{V} \frac{\partial y}{\partial x} + D \frac{\partial \underline{V}}{\partial x} = 0 \qquad \ldots \ldots \ldots \ldots (3.4)$$

where:

D = hydraulic depth = y for rectangular channels

x = spatial horizontal direction

t = time variable.

Substituting Equations 3.1, 3.2, and 3.3 into the above equation yields the continuity equation for wave motion in rockfill:

$$\frac{\partial \eta}{\partial t} + \left(\frac{u}{m}\right) \frac{\partial \eta}{\partial x} + (h_0 + \eta) \frac{\partial(u/m)}{\partial x} = 0 \qquad \ldots \ldots \ldots (3.5)$$

or the equation given by Nasser [35], viz.

$$\frac{\partial \eta}{\partial t} + \left(\frac{u}{m}\right) \frac{\partial u}{\partial x} + \frac{(h_0 + \eta)}{m} \frac{\partial u}{\partial x} = 0 \qquad \ldots \ldots \ldots (3.6)$$

To simplify the analysis, it is helpful to introduce the celerity, c, being the velocity of a wave relative to the velocity of flow. For small gravity waves, the celerity is defined as:
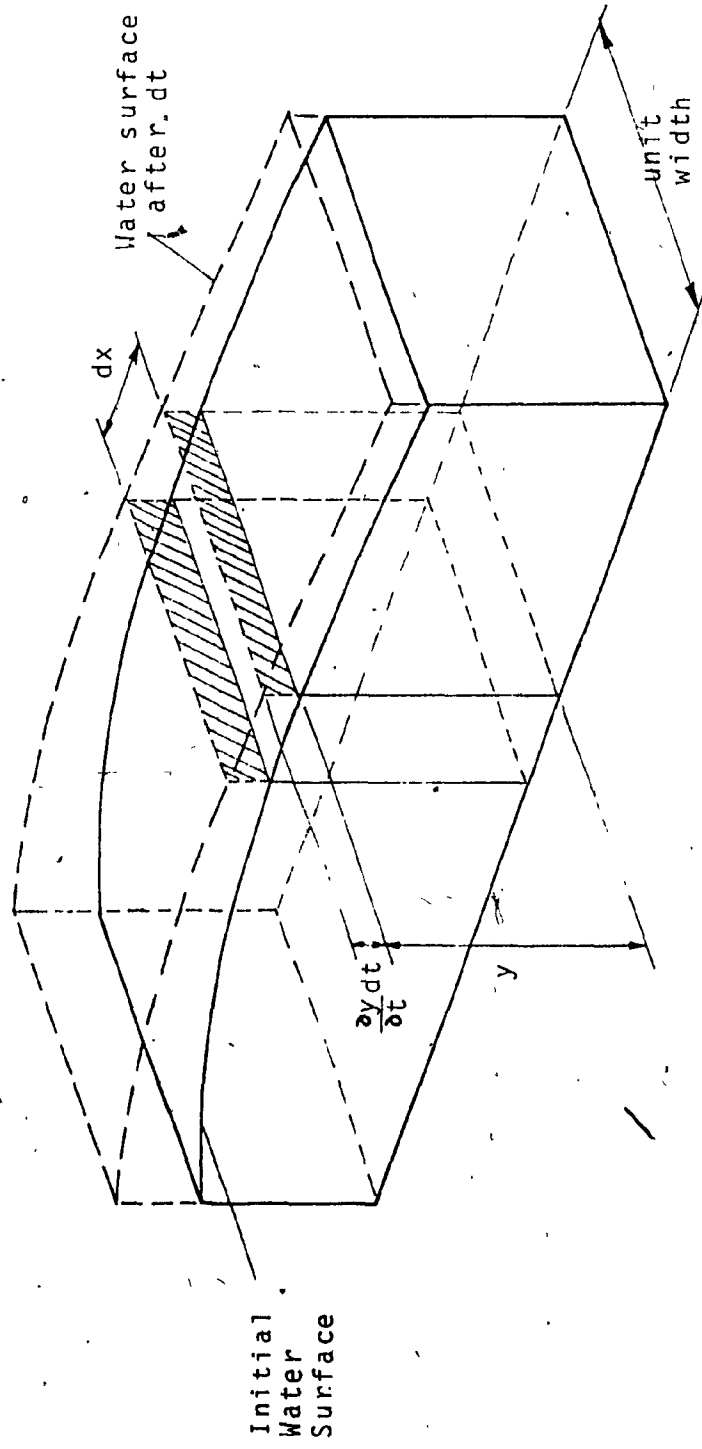
Fig. 3.2 Continuity of Unsteady Flow in an Open Channel.

$$c = \sqrt{g(h_0 + \eta)} \qquad \ldots \ldots \ldots \ldots (3.7)$$

where   g = acceleration due to gravity

   = 980.6 cm/sec^2

or

$$c^2 = g(h_0 + \eta) \qquad \ldots \ldots \ldots \ldots (3.8)$$

Taking the differential of both sides of the equation results in:

$$2 \ c \ dc = d(g(h_0 + \eta)) = g \ d\eta \qquad \ldots \ldots \ldots (3.9)$$

or

$$d\eta = \frac{2c}{g} \ dc \qquad \ldots \ldots \ldots \ldots (3.10)$$

Upon substitution of equations 3.7 through 3.10 into equation 3.6, the continuity equation reduces to the form:

$$\frac{\partial c}{\partial t} + \frac{c}{2m} \ \frac{\partial u}{\partial x} + \frac{u}{m} \ \frac{\partial c}{\partial x} = 0 \qquad \ldots \ldots \ldots (3.11)$$

3.1.2 Equation of Motion

Assuming a prismatic channel, Henderson [22] gives the equation of motion for unsteady, open channel flow (Fig. 3.3) as:

$$\frac{1}{g} \ \frac{\partial V}{\partial t} + \frac{\alpha V}{g} \ \frac{\partial V}{\partial x} + \frac{\partial y}{\partial x} = S_0 - S_f \qquad \ldots \ldots \ldots (3.12)$$

where α is the energy coefficient (assumed to be unity)

   S_0 is the channel bed slope

   S_f is the energy line slope.
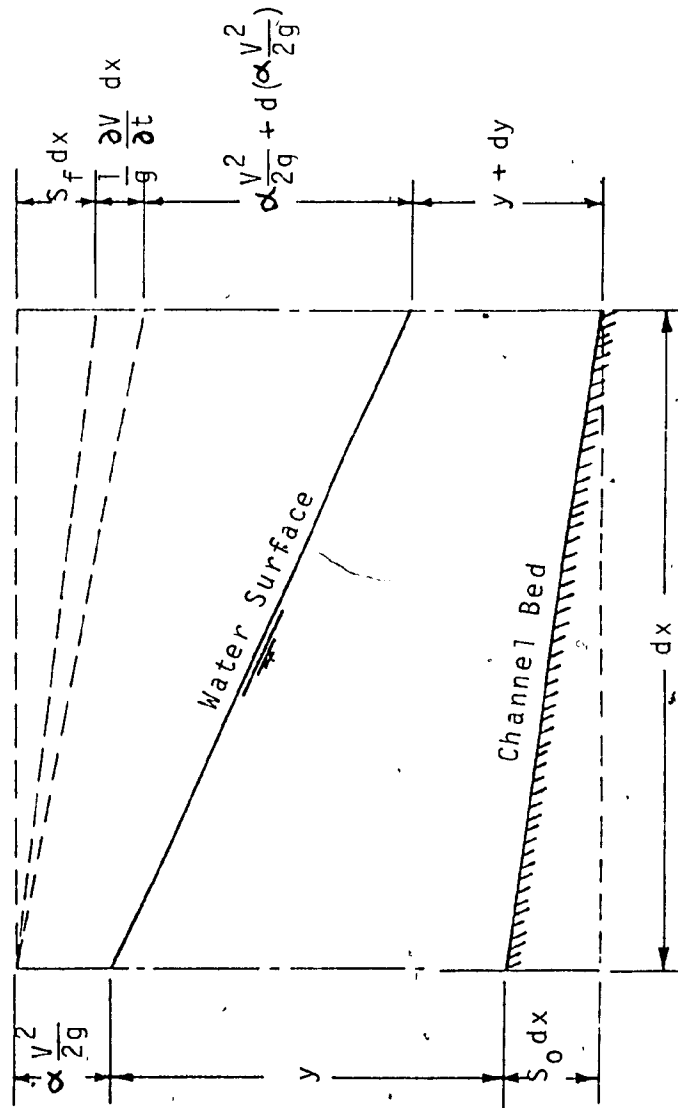
Fig. 3.3. Representation of Energy in Open Channel Flow.

Substituting equations 3.1, 3.2, and 3.3 into 3.12 and rearranging results in the following interior flow equation:

$$\frac{\partial u}{\partial t} + \frac{u}{m}\frac{\partial u}{\partial x} + gm\frac{\partial \eta}{\partial x} = gm(S_0 - S_f) \qquad \ldots \ldots \ldots (3.13)$$

The right hand side resistance term must be a function of the porosity, gravity, hydraulic gradient i, particle properties and velocity. Among the various resistance formulae available, it has been determined [1, 34, 35] that the Forchheimer equation is the most convenient expression available, i.e.

$$i = aq + bq^2 \qquad \ldots \ldots \ldots (2.2)$$

Since the hydraulic gradient is dimensionless and suitably describes the energy loss, it will be used to describe the slope terms in equation (3.13), viz.

$$\frac{\partial u}{\partial t} + \frac{u}{m}\frac{\partial u}{\partial x} + gm\frac{\partial \eta}{\partial x} = -gmi \qquad \ldots \ldots \ldots (3.14)$$

The hydraulic gradient can also be expressed as:

$$i = Fu \qquad \ldots \ldots \ldots (3.15)$$

where $F = a + b|u|$.

The equation of motion can easily be expressed in terms of velocity and celerity:

$$\frac{\partial u}{\partial t} + \frac{u}{m}\frac{\partial u}{\partial x} + 2cm\frac{\partial c}{\partial x} = -gmFu \qquad \ldots \ldots \ldots (3.16)$$

Both equations 3.11 and 3.16 are quasilinear partial differential equations which when coupled form a hyperbolic system. This suggests that Vichnevetsky's [53] special procedure for solving quasilinear hyperbolic PDE's is applicable to this study.

3.2 BOUNDARY CONDITIONS

A time dependent function that describes the movement of the outcrop point is used as the boundary condition at the water rockfill interface. The derivation and solution of this time dependent function is given in Appendix A. Five solution methods are presented. The discrete points comprising the outcrop point curve are stored and used as the input data for the boundary conditions described by the hyperbolic system.

At the impervious core, the boundary condition of no normal flux is stated, i.e., the horizontal velocity must be zero; thus

$$u(t, x_{max}) = 0 \qquad \ldots \ldots \ldots \ldots \ldots \quad (3.17)$$

Because a boundary condition is specified at each end of the solution domain, the phenomenon is a bounday value problem and therefore an iterative procedure may be used to satisfy the downstream condition of zero velocity.

3.3 Initial Conditions

Originally the water is considered to be at rest with the reservoir. Therefore, the velocity is zero and there will be no perturbation. Therefore the celerity of the wave initially is given as:

$$c(0,0) = \sqrt{g\,h_0} \qquad \ldots \ldots \ldots \ldots \ldots (3.18)$$

3.4 Hybrid Formulation

There exists a wide range of hybrid techniques to solve the existing problem but due to constraints of analog hardware, efficiency, complexity, etc., the CSDT method was chosen. For the reasons mentioned in Chapter 2, Vichnevetsky's method of lines [53] was deemed best suited in analyzing the governing equations.

3.4.1 Characteristic Transformation

The conservation of mass (3.11) and momentum (3.16) equations can be written in matrix notation, viz.

$$\frac{\partial}{\partial t}\begin{vmatrix} u \\ c \end{vmatrix} + \begin{vmatrix} u/m & 2cm \\ c/2m & u/m \end{vmatrix}\frac{\partial}{\partial x}\begin{vmatrix} u \\ c \end{vmatrix} = \begin{vmatrix} -gmFu \\ 0 \end{vmatrix} \qquad \ldots \ldots (3.19)$$

The eigenvalues are determined by solving for:

$$\det\begin{vmatrix} u/m - \lambda & 2cm \\ c/2m & u/m - \lambda \end{vmatrix} = \lambda^2 - 2\lambda\frac{u}{m} + \frac{u^2}{m^2} - c^2 = 0$$

$$\ldots \ldots (3.20)$$

or

$$\lambda_{1,2} = u/m \pm c \qquad \ldots \ldots (3.21)$$

The adjoint-eigenvectors, w^1 and w^2 are defined as:

$$cw_1^1 + \frac{c}{2m} w_2^1 = 0$$

$$-cw_1^2 + \frac{c}{2m} w_2^2 = 0 \qquad \dots\dots\dots \quad (3.22)$$

which yield

$$w^1 = \begin{vmatrix} 1 \\ \\ 2m \end{vmatrix}$$

$$w^2 = \begin{vmatrix} 1 \\ \\ -2m \end{vmatrix} \qquad \dots\dots\dots \quad (3.23)$$

These two real matrices are linearly independent vectors. By multiplying 3.19 by the transpose of w^1 and w^2, two equivalent equations are obtained but in a new set of dependent variables. This yields the characteristic form of the equations. For example, multiplying the transpose of w^1 by 3.19 yields:

$$\frac{\partial u}{\partial t} + \frac{u}{m} \frac{\partial u}{\partial x} + 2mc \frac{\partial c}{\partial x} + 2m \frac{\partial c}{\partial t} + c \frac{\partial u}{\partial x} + 2u \frac{\partial c}{\partial x} = -gmFu$$

$$\dots\dots\dots\dots \quad (3.24)$$

Rearranging the terms and performing a little algebra yields the integrable form:

$$\frac{\partial}{\partial t} (u + 2mc) + (u/m + c) \frac{\partial}{\partial x} (u + 2mc) = -gmFu \quad \dots\dots\dots \quad (3.25)$$

A similar expression can be obtained by multiplying the transpose of w^2 and rearranging the terms, viz.

$$\frac{\partial}{\partial t}(u - 2mc) + (u/m - c)\frac{\partial}{\partial x}(u - 2mc) = -gmFu \quad \ldots \ldots (3.26)$$

Equations 3.25 represents the forward propagation of a wave, $W_1 = u-2mc$, at a velocity of $u/m+c$, whereas 3.26 represents a backward wave propagation, $W_2 = u-2mc$, at a wave velocity of $u/m-c$.

The original variables and the characteristics can now be expressed in terms of the new independent variables W_1 and W_2:

$$u = \frac{W_1 + W_2}{2} \quad \ldots \ldots \ldots \ldots (3.27)$$

$$c = \frac{W_1 - W_2}{4m} \quad \ldots \ldots \ldots \ldots (3.28)$$

$$n = \frac{1}{g}\left[\frac{W_1 - W_2}{4m}\right]^2 - h_o \ldots \ldots \ldots \ldots (3.29)$$

$$\lambda_1 = \frac{u}{m} + c = \frac{3W_1 + W_2}{4m} \quad \ldots \ldots \ldots (3.30)$$

$$\lambda_2 = \frac{u}{m} - c = \frac{W_1 + 3W_2}{4m} \quad \ldots \ldots \ldots (3.31)$$

Equations 3.25 and 3.26 can be expressed in terms of the new independent variables, ie.

$$\frac{\partial W_1}{\partial t} + \frac{3W_1 + W_2}{4m} \frac{\partial W_1}{\partial x} = \frac{-qmF}{2}(W_1 + W_2) \quad \ldots \ldots \ldots \quad (3.32)$$

$$\frac{\partial W_2}{\partial t} + \frac{W_1 + 3W_2}{4m} \frac{\partial W_2}{\partial x} = \frac{-qmF}{2}(W_1 + W_2) \quad \ldots \ldots \ldots \quad (3.33)$$

Vichnevetsky states that an equation of the form of 3.22 is computationally stable from the error propagation point of view when integrated in the forward direction, i.e. from $x = 0$ to $x = x_{max}$. Equation 3.33 would then have to be integrated in the backward direction, i.e. from $x = x_{max}$ to $x = 0$. In his example, the equations can be decoupled but in the present study such is not the case and therefore his serial interlaced integration is not applicable. The two characteristic equations must be solved simultaneously either by a matrix method or by an iterative procedure.

3.4.2 CSDT Formulation

Since the CSDT method is being applied, the time is discretized by intervals of Δt. A typical time frame is expressed as:

$$t^j = j\Delta t \quad \ldots \ldots \ldots \quad (3.34)$$

where $j = 0, 1, 2, \ldots$

The waves are denoted as:

$$W_1^j = W_1(x, t^j)$$

$$W_2^j = W_2(x, t^j) \quad \ldots \ldots \ldots \quad (3.35)$$

Introducing a backward finite difference scheme for the two time derivatives results in the following discretization:

$$\frac{\partial W_{1,2}}{\partial t}\bigg|_{t^j} = \frac{W^j_{1,2} - W^{j-1}_{1,2}}{\Delta t} \qquad \ldots\ldots\ldots\ldots\ldots (3.36)$$

where   subscripts $_{1,2}$ indicate the applicability of equation 3.36

   to W_1 and W_2.

Upon substitution of equation 3.36 into 3.32 and 3.33 and rearranging, the following equations are obtained:

$$\frac{dW^j_1}{dx} + \frac{W^j_1}{\lambda_1 \Delta t} = \frac{1}{\lambda_1 \Delta t} W^{j-1}_1 - \frac{gmF}{2\lambda_1} (W_1 + W_2) \quad \ldots \quad (3.37)$$

$$\frac{dW^j_2}{dx} + \frac{W^j_2}{\lambda_2 \Delta t} = \frac{1}{\lambda_2 \Delta t} W^{j-1}_2 - \frac{gmF}{2\lambda_2} (W_1 + W_2) \qquad \ldots \quad (3.38)$$

At time t^j, both equations 3.37 and 3.38 become ordinary differential equations with respect to the spatial direction x.

3.4.3 Solution Method

Equations 3.37 and 3.38 state that the dependent variables are coupled with respect to wave velocities and the resistance term. This suggests that the equations must be solved simultaneously. This is achieved on a digital computer by utilizing a Runge-Kutta and/or a predictor-corrector method for a system of ODE's. On an analog computer, the two equations are patched up with the proper cross connections of the two variables and solved in a continuous fashion because only one independent.

variable exists. Both variables are updated from one time frame to another.

The initial condition, ie. $t = t^0$, for the system in terms of W_1 and W_2 is:

$$W_1(0) = u(0) + 2mc(0) = \quad 2m\sqrt{gh_0}$$

$$W_2(0) = u(0) - 2mc(0) = \quad -2m\sqrt{gh_0} \quad \ldots\ldots\ldots (3.39)$$

Because of the time differencing, the system can only begin to be solved at $t = t^1$. At this second time frame, the celerity is known from the outcrop point movement but the macroscopic velocity is unknown, ie.

$$W_1(t^1) = u(t^1) + 2m\sqrt{g(h_0 + \eta(t^1))}$$

$$W_2(t^1) = u(t^1) - 2m\sqrt{g(h_0 + \eta(t^1))} \quad \ldots\ldots\ldots (3.40)$$

Since $u(t^1)$ is not known, it must be given a trial value such that at the end of the integration of the two equations, 3.37 and 3.38, the downstream boundary condition is satisfied, viz.

$$W_1(t^j, x_{max}) = -W_2(t^j, x_{max}) \quad \ldots\ldots\ldots (3.41)$$

If the trial value does not satisfy equation 3.41, a new guess is required. On the digital computer, this is achieved by specifying the limits on the velocity, entering an initial guess and changing one limit depending on whether the velocity u (or $(W_1 + W_2)/2$) is positive or negative, and thereby converging to the correct solution. This Bisector Search Method can yield a solution quickly if the initial guess is close enough (Fig. 3.4).

- 47 -

1. Initial   2. Adjusting   3. Adjusting
   guess.   lower limit and   upper limit and
                 obtaining new   obtaining new
                 guess for velocity. guess for velocity.

4. Assumed
   final solution
   after x iterations.
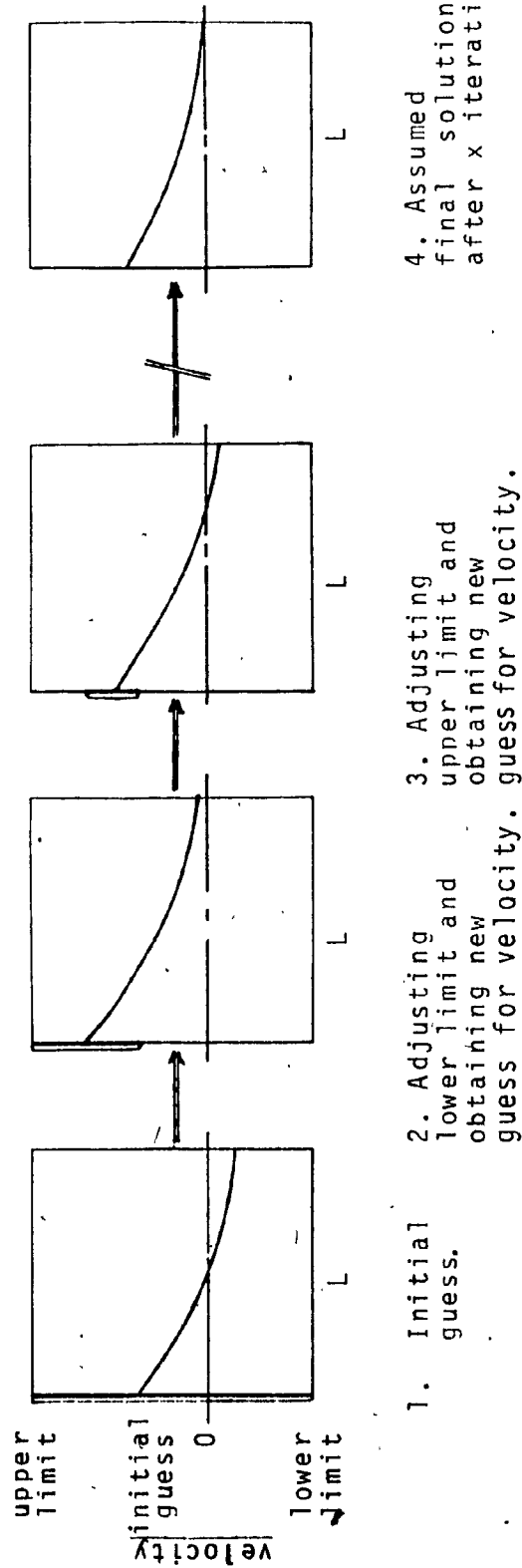
Fig. 3.4 A Possible Sequence of Events for the Bisector Search Method

Once a solution is obtained·for a particular time frame, the variables are converted back to the original parameters to yield a plot of the variation of the water level with distance, ie. the phreatic surface within the rockfill structure. The time advances one frame, using the reference values of W_1 and W_2 at the mean water level, and the procedure is continued until a family of phreatic surfaces is obtained for one complete period of the outcrop point movement.

This method was first programmed on a CDC 6600/Cyber digital computer to remove all the programming obstacles and then was implemented on the EAI 690 analog/hybrid computer.

CHAPTER 4

ANALYSIS

A number of methods were attempted to solve the characteristic equations of this study (Eqs. 3.32 & 3.33). Vichnevetsky [53] suggested that his serial-interlaced solution could easily be implemented using a standard Runge-Kutta 4th order subroutine. This would enable the programmer to obtain a fully digital solution from which proper scaling of the analog circuit could be established; thus, an accurate solution could be determined and used as a check against the hybrid solution. This technique proved helpful in this study since the hybrid program was not conveniently edited with the existing facilities. It was assumed that once the numerical program was correctly formulated, transferrring the functioning algorithm to the hybrid computer would be relatively easy. Hence, it is imperative that the digital formulation be emphasized as a prelude to the hybrid solution; obtaining the proper algorithm presented the biggest challenge.

4.1 PROGRAMMING CONSIDERATIONS

Vichnevetsky's [53] serial-interlaced solution was attempted first to obtain some more information on the nature of the problem. It was quickly realized that a purely Runge-Kutta solution would be quite time

consuming because the method utilized four function evaluations for each
value calculated. However, the method is a self-start one and can easily
be programmed. Predictor/Corrector methods only required two function
calls for each value calculated for the same order of accuracy. Thus,
they were less time consuming but were not self-starting. Therefore,
the numerical integration was performed utilizing a Runge-Kutta method
to obtain the first four integration values and the solution was then
propagated using an Adams-Moulton predictor/corrector method; the computer
programs are given in Appendix D.

It was also found that one defining function statement could
be used to model both characteristic equations.

Vichnevetsky's method did produce a propagating solution but
it was noticed that: (a) the velocity term, u_* was not satisfying the
zero velocity criterion at the core; (b) the velocity generated was too
high, in fact unrealistic; (c) the damping of the water-wave at the
maximum run-up was minimal and in some cases the phreatic surface even
sloped upwards (a physical impossibility). Further, the W_2 wave was
not adequately accounted for.

In order to satisfy the downstream boundary condition, a term
was introduced to force the velocity to zero at the core. This method
was not acceptable even though it appeared to generate a plausible solu-
tion, because the system behaviour was far more complicated than the
forcing function indicated and there was instability in the equations
that required very small space increments. To this end, it was decided
to re-evaluate Vichnevetsky's work.

Vichnevetsky's claims were based on the definition of his problem: the routing of a flood wave. Since he had no downstream constraint, an input wave was allowed to dampen out to its steady state value sufficiently far downstream. His problem statement was consistent with the hydraulics of a flood disturbance generating wave fronts upstream and downstream (W_2 and W_1 waves respectively). He integrated the W_1 wave in the positive downstream direction and the W_2 wave in the negative upstream direction beginning with his input at his original axis as in Fig. 4.1. Hence, his W_1 and W_2 waves were also independent of each other which was not the case in the present study.

Because of the interdependence of the equations in this study, both the variables W_1 and W_2 were needed simultaneously to satisfy the downstream condition; this is a typical boundary value problem as opposed to Vichnevetsky's initial condition problem. Because both variables had to be solved simultaneously, a more elaborate integrating subroutine had to be devised. Instead of solving for each variable separately in a serial fashion, both variables had to be updated simultaneously. This called for a matrix solution method or a trial and error procedure. The latter method was used because of its convenient implementation in the present study. A typical slow drop case was used, for comparison purposes, in modelling all the problem features correctly. The range or the envelope of the phreatic lines for one reference slow drop case is given in Fig. 4.2.

Experimental findings [10, 35] indicated that the water wave continued to enter the breakwater even after the maximum run-up has been reached, i.e., the water wave velocity changes direction some time after the crest has been reached. This can be seen in Fig. 4.3 which shows the

Fig. 4.1 — Definition of Vichnevetsky's Flood Routing Problem.
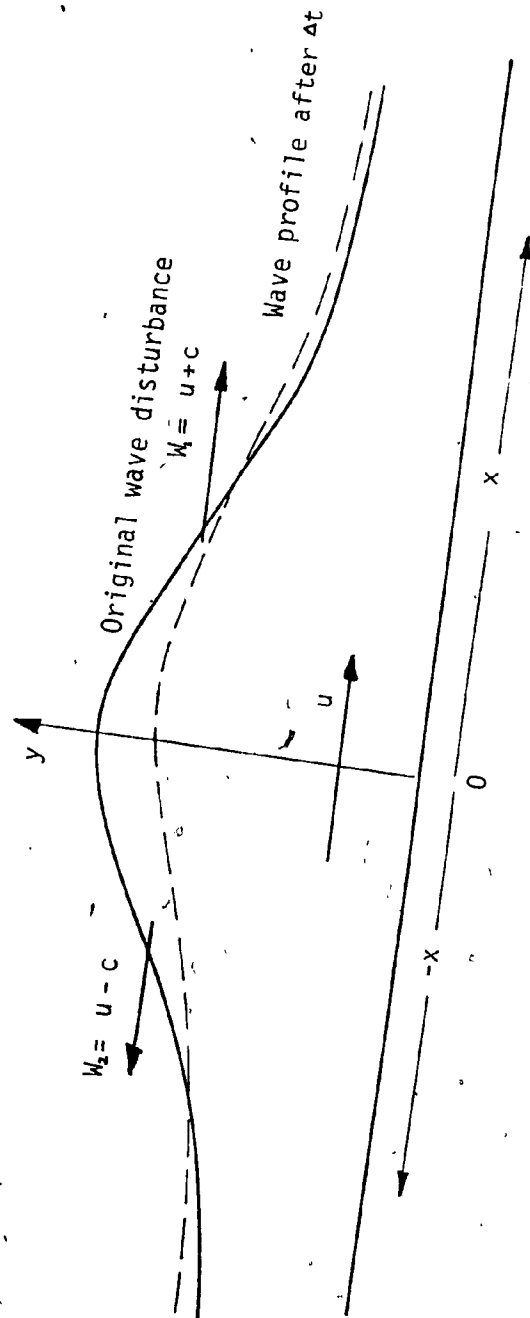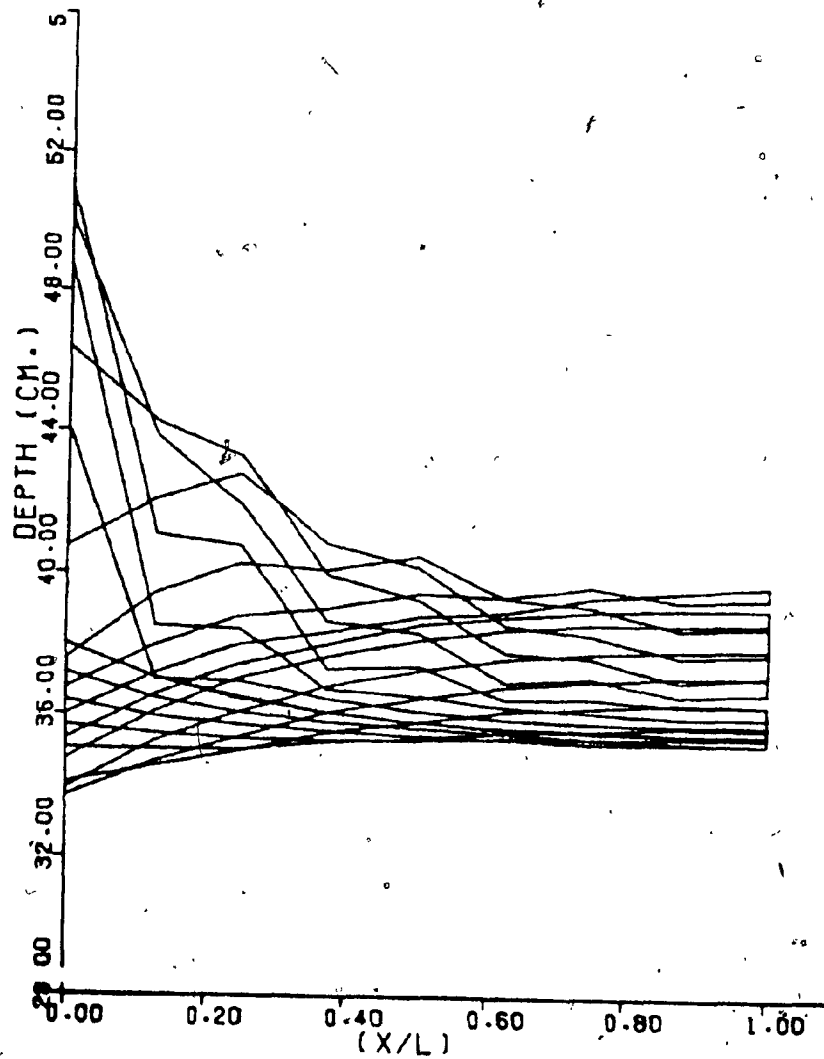
Fig. 4.2 — Typical Envelope of Phreatic Lines for a Slow
Drop Case.
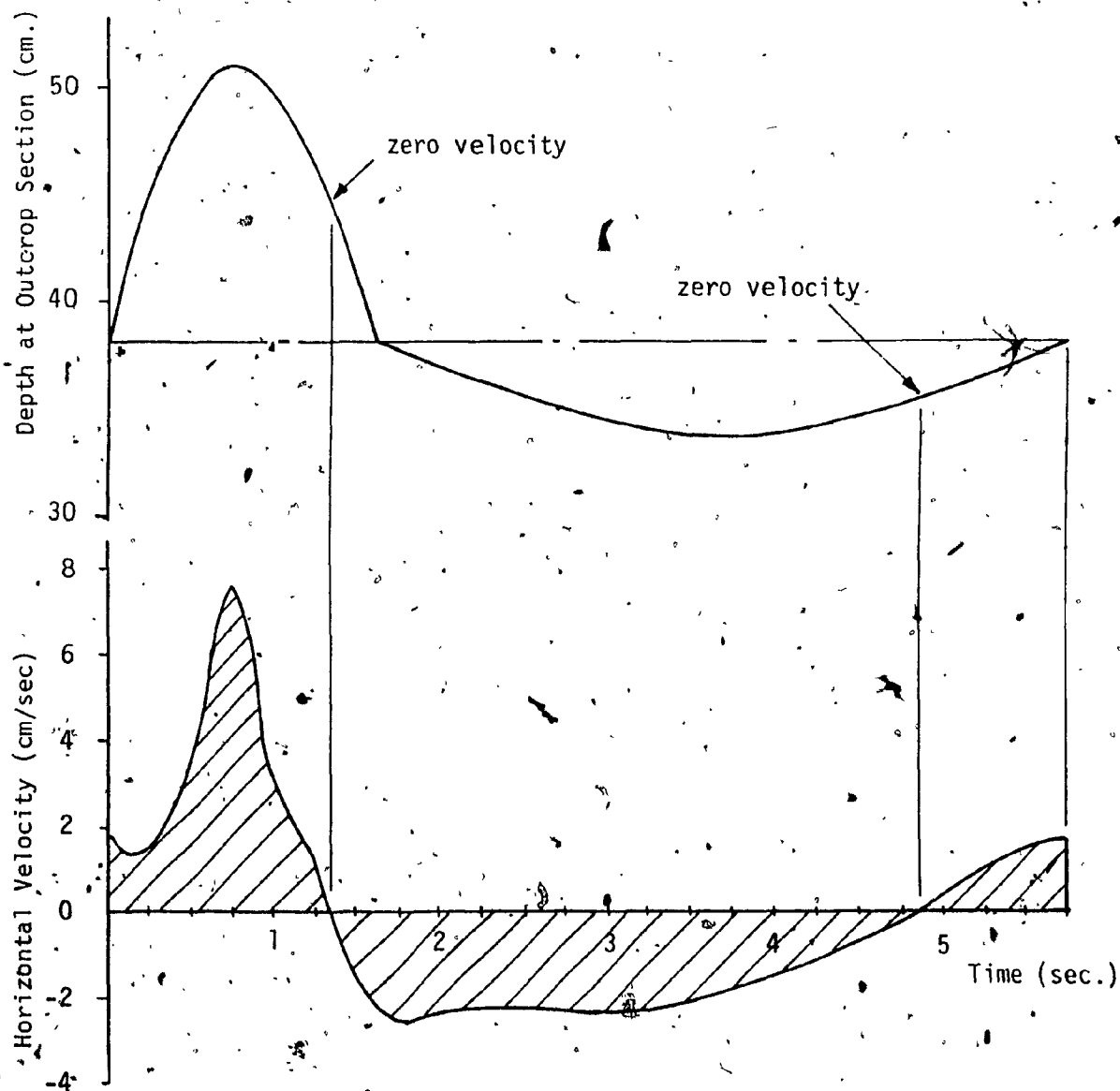
Fig. 4.3 — Typical Velocity Variation at Outcrop Section for a Slow Drop Case.

variation of the sign and magnitude of the velocity at the outcrop section with respect to the input wave profile.

The definition of the velocity, $u = (W_1 + W_2)/2$, suggests that the W_1 and W_2 terms reach the same magnitude at the core where the resultant velocity is zero. Fig. 4.4 serves to illustrate how the W_1 and W_2 waves of representative time exposures A and B must have equal magnitude but opposite signs, i.e., $W_1 = -W_2$.

As noted previously, Vichnevetsky integrated his waves in their respective forward directions. When this same procedure was used in the present study, it was found that the velocity at the outcrop had to be zero to satisfy the downstream conditions. This was not acceptable. However, upon integrating the equations in the same positive downstream direction, realistic velocity distributions but unrealistic W_2 profiles resulted.

Based on the previous discussion, a qualitative description of the phenomenon can be formulated. The solution must satisfy the following conditions: (1) the velocity within the rockfill must be less than the maximum fall rate, V; (2) the horizontal velocity must change direction at a time delay after the maximum run-up or minimum rush down; (3) the wave must necessarily dampen towards the core, and (4) zero velocity at the core must be maintained.

4.2 TIME DISCRETIZATION

Explicit numerical techniques for solving PDE are generally hampered by instability problems. Nasser [35] adopted the following stability criterion for his finite difference formulation, viz.
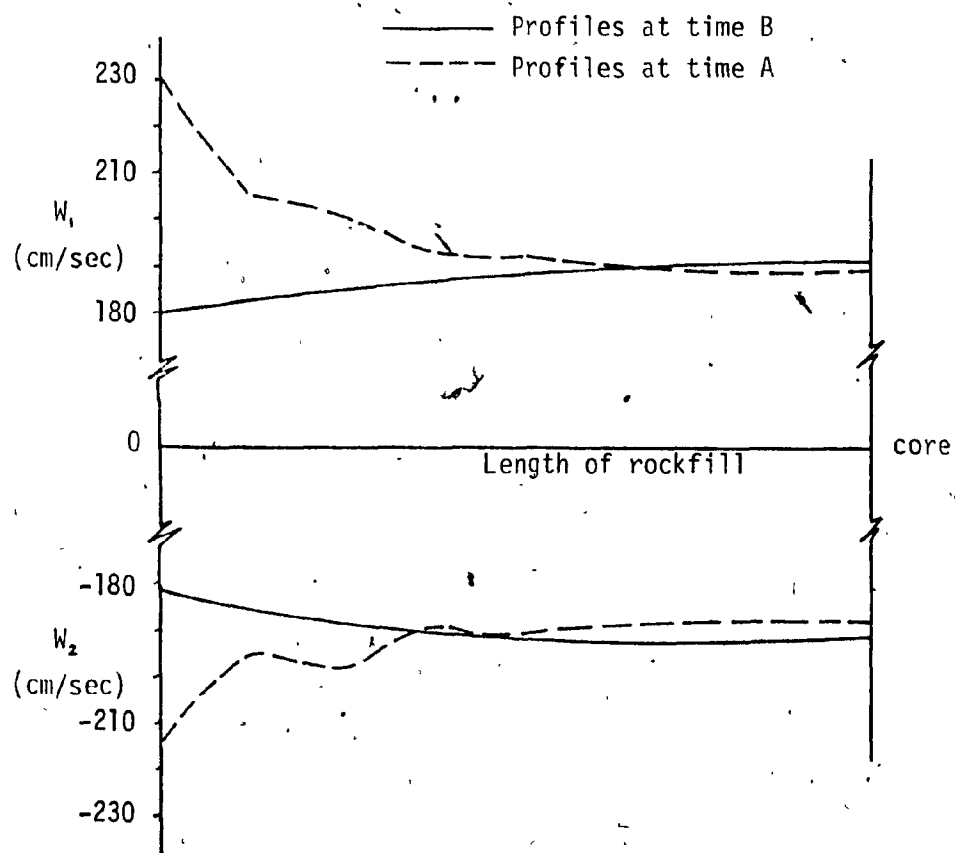
Fig. 4.4 — Typical W_1 and W_2 Profiles at Different Time Frames.

$$\frac{\Delta t}{\Delta x} < \frac{1}{2} \left(\frac{u}{m} + c \right)^{-1} \qquad \ldots \ldots \ldots \ldots (4.1)$$

where Δt and Δx are the respective time and spatial increments. This criterion was not applicable in this study.

The numerical integration necessitated small spatial increments but time increments were determined separately for the outcrop point movement. It was difficult to determine an upper limit on the size of Δt. The value of Δt used, based on experimentation, ranged between .022 sec. and .114 sec., depending on the value of the wave period, the average Δt used was in the neighbourhood of .05 sec. The value of Δt was kept relatively constant for any solution case to minimize velocity fluctuations. With finite difference techniques, the solution should continue for a few wave periods to ensure that the non-linearities are properly accounted for. The nonlinearities associated with the equations and downstream conditions were determined, in this study, by direct integration and iteration, respectively. The time effect was more difficult to analyze.

Originally, it was felt that a backward differencing scheme would logically account for the $\partial W/\partial t$ term in the governing equation:

$$\frac{\partial W}{\partial x} = -\frac{1}{\lambda} \left(\frac{\partial W}{\partial t} - gmE\sigma \right) \qquad \ldots \ldots \ldots \ldots (4.2)$$

The main difficulty was associated with the proper differencing of the term:

$$\frac{\partial W}{\partial t} \cong \frac{\Delta W}{\Delta t} \bigg|_{j} = \frac{W_I^j - W_I^{j-1}}{\Delta t} \qquad \ldots \ldots \ldots \ldots (4.3)$$

where j denotes the time period under study.

Since the first term, i.e., W_I^j, would be the continuous variable, the problem shifted to the definition of the previous value, W_I^{j-1}. This

term was investigated in numerous ways. Originally, W_1^{j-1} was taken as the previous initial value of W_1^{j} for a working solution. This yielded unreasonable answers; only the criteria of zero velocity at the core and reasonable velocities in the solution were realized.

The next step was to store the complete previous profile to better simulate the continuous nature of the problem. This did not improve the solution but did increase the memory storage requirements and time consumption.

It was then reasoned that since all systems when left alone, seek the stable state, then successive profiles should not be compared with each other but rather with the mean water level. This resulted in more reasonable profiles but there was no time lag of the change in the direction of the horizontal velocity. A sample output showing typical results for a half wave period using this method is given in Fig. 4.5.

The final solution utilized a term that needs special explanation. It is difficult to determine the point at which the horizontal velocity changes direction but it is known that at the time constant t_1, (see Appendix A), the water begins to leave the rockfill embankment. It is assumed that this is the point at which the horizontal velocity will change. Similarly, the time constant t_c defines the point at which the external wave meets the outcrop point and both rise together. Thus, this is the point at which water will re-enter the rockfill, provided that t_c is greater than three quarters of the wave period. Fig. 4.6 represents the region in which the water is leaving the rockfill at its maximum vertical velocity (not necessarily at a maximum horizontal velocity).
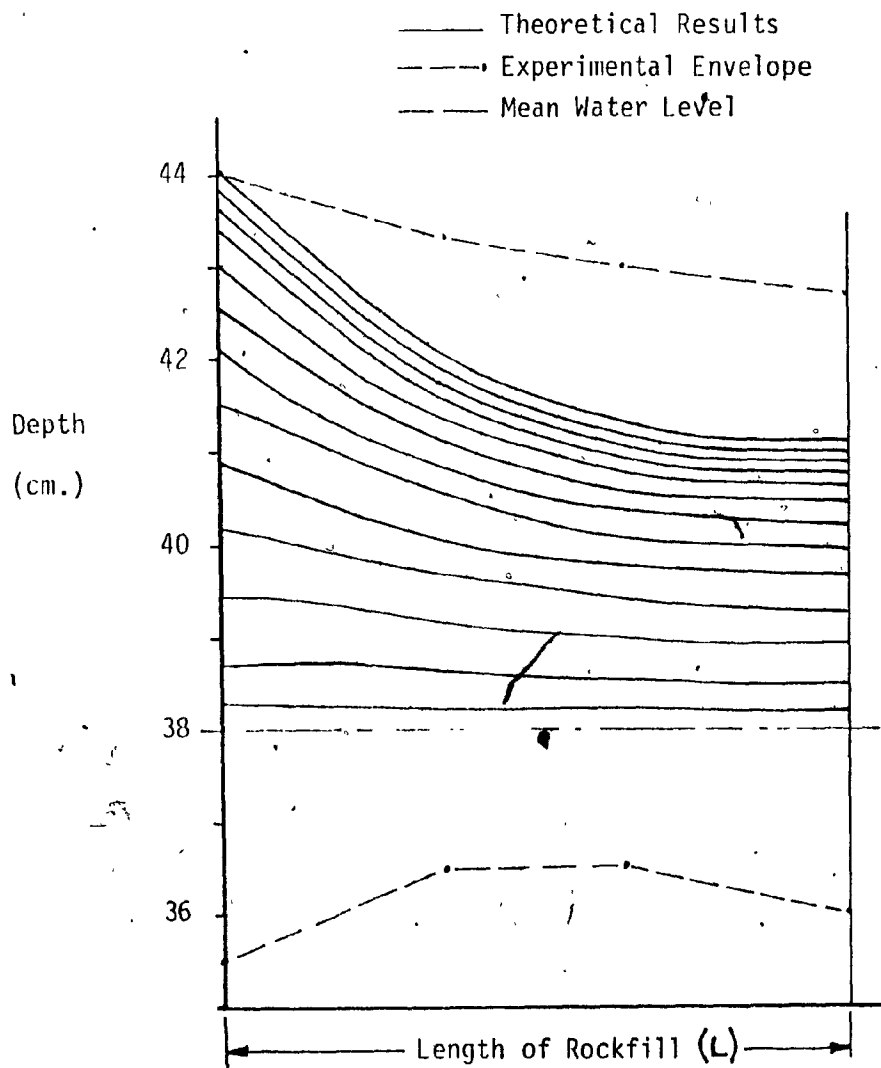
Fig. 4.5 — Sample Phreatic Profiles for a Half Wave Period with $W_1^{j-1} = h_0$.
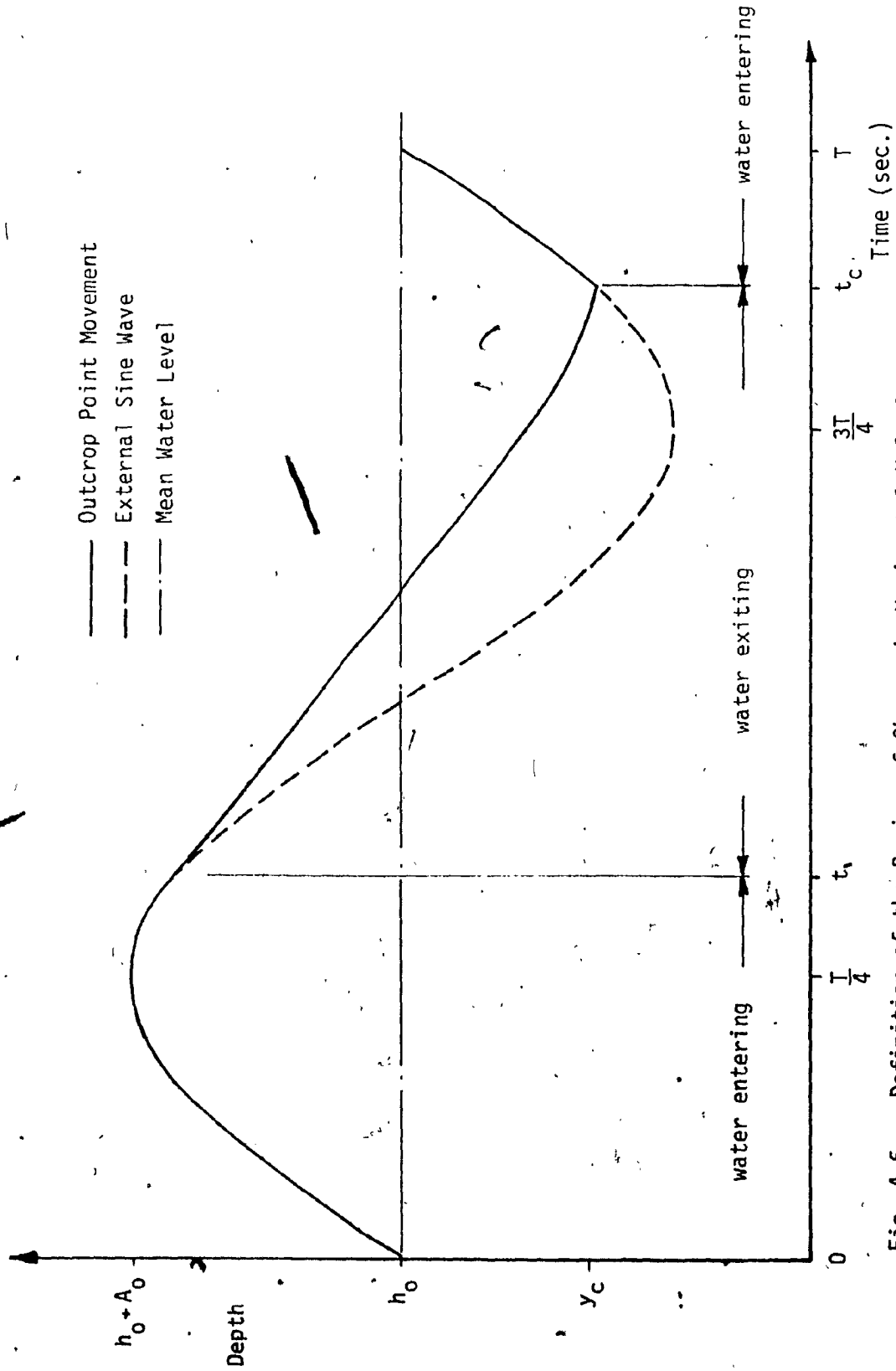
Fig. 4.6 — Definition of the Region of Change in Horizontal Velocity.

Based on the assumption of change of velocity direction at times t_1 and t_c, W_1 and W_2 can be determined, viz.

$$W_1(t_1) = -W_2(t_1) = 2m \sqrt{gh(t_1)} \qquad \ldots \ldots \ldots \ldots \ldots (4.4)$$

$$W_1(t_c) = -W_2(t_c) = 2m \sqrt{gh(t_c)} \qquad \ldots \ldots \ldots \ldots (4.5)$$

The initial conditions are also known, i.e.,

$$W_1(0) \neq W_2(0) = 2m \sqrt{gh_0} \qquad \ldots \ldots \ldots \ldots (4.6)$$

An assumption is made of a constant W_1^{j-1} along the length of the embankment at each time increment since its variation with length cannot be known in advance. According to the preliminary investigations attempting the storage of complete wave profiles, the difference in result did not seem to indicate any significant change. To simulate a change in the variation between the known values of W_1 and W_2, linear interpolations of the W_1^{j-1} term were used. These modifications were introduced into the hybrid model. The following three conditions pertain to the time discretization:

$$W_1^{j-1} = (W_1(0) \cdot (t_1 - t) + W_1(t_1) \cdot t_1)/t_1 \qquad \text{for } t \leqslant t_1 \quad \ldots \ldots (4.7)$$

$$W_1^{j-1} = (W_1(t_1) \cdot (t_c - t) + W_1(t_c) \cdot (t - t_1))/(t_c - t_1) \cdot$$
$$\text{for } t_1 < t \leqslant t_c \ldots \ldots (4.8)$$

$$W_1^{j-1} = (W_1(t_c) \cdot (t_1 + T - t) + W_1(t_1) \cdot (t - t_c))/(t_1 + T - t_c)$$
$$\text{for } t_c < t < t_1 + T \ldots \ldots (4.9)$$

A curve representing the variation of W_1^{j-1} for one wave length is given in Fig. 4.7. The value of t_c should not be below 3/4 T.
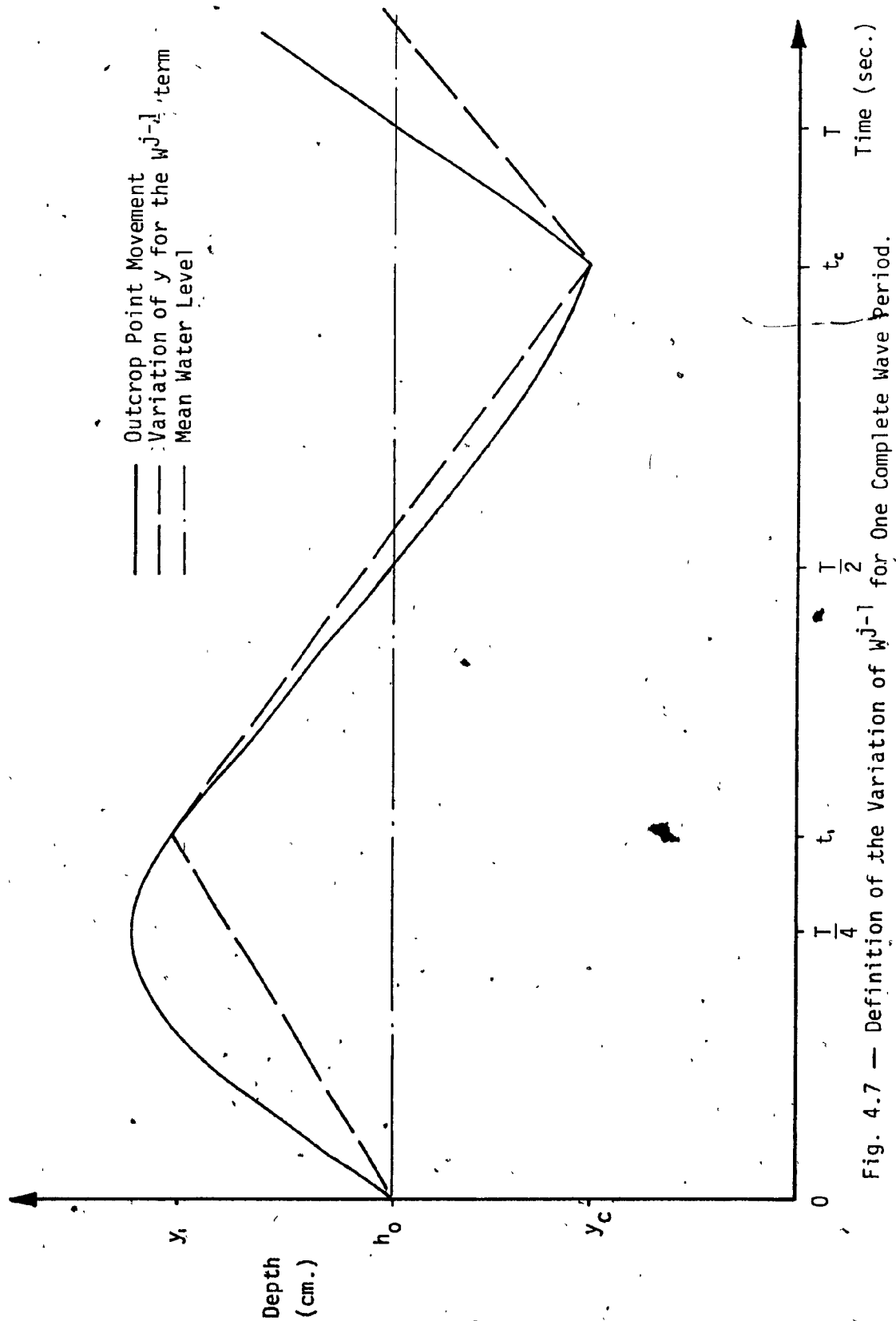
Fig. 4.7 — Definition of the Variation of W_j^{j-1} for One Complete Wave Period.

4.3 ANALOG/HYBRID PROGRAM

The hybrid program differs from the numerical program in that the analog circuit replaces the integration routine and special library subroutines must be called to activate the EAI 693 Interface Unit. References 12, 13 and 14 give all the explanations of the use of the hybrid FORTRAN software used.

The digital program reads in all the relevant parameters encountered in the program, makes any necessary calcuations or checks, provides a means of printing out digital answers, and controls the operation of the analog computer. The analog computer, besides integrating the characteristic equations simultaneously, provides the means for obtaining the continuous plot of any of its variables for a given time increment.

4.3.1 Analog Circuitry

Fig. 4.8 shows the pot and amplifier components comprising the analog circuit used in this study. The circuit can be subdivided into five sections as illustrated in Fig. 4.9. Box B contains the A/D and D/A signals required; boxes A and E contain the circuits for W_1 and W_2 respectively; box D shows the components shared commonly in the characteristic equations by A and E; and box C illustrates some components required for plotting. Select variables are included at the output of certain amplifiers to acquaint the reader with the functions performed.

4.3.2 Analog Scaling

At the outset, amplitude scaling posed a problem due to the large values of W_1 and W_2 and their small summations. The resistance term also presented a challenge. In this study, the values of $W_{1,2}$ never
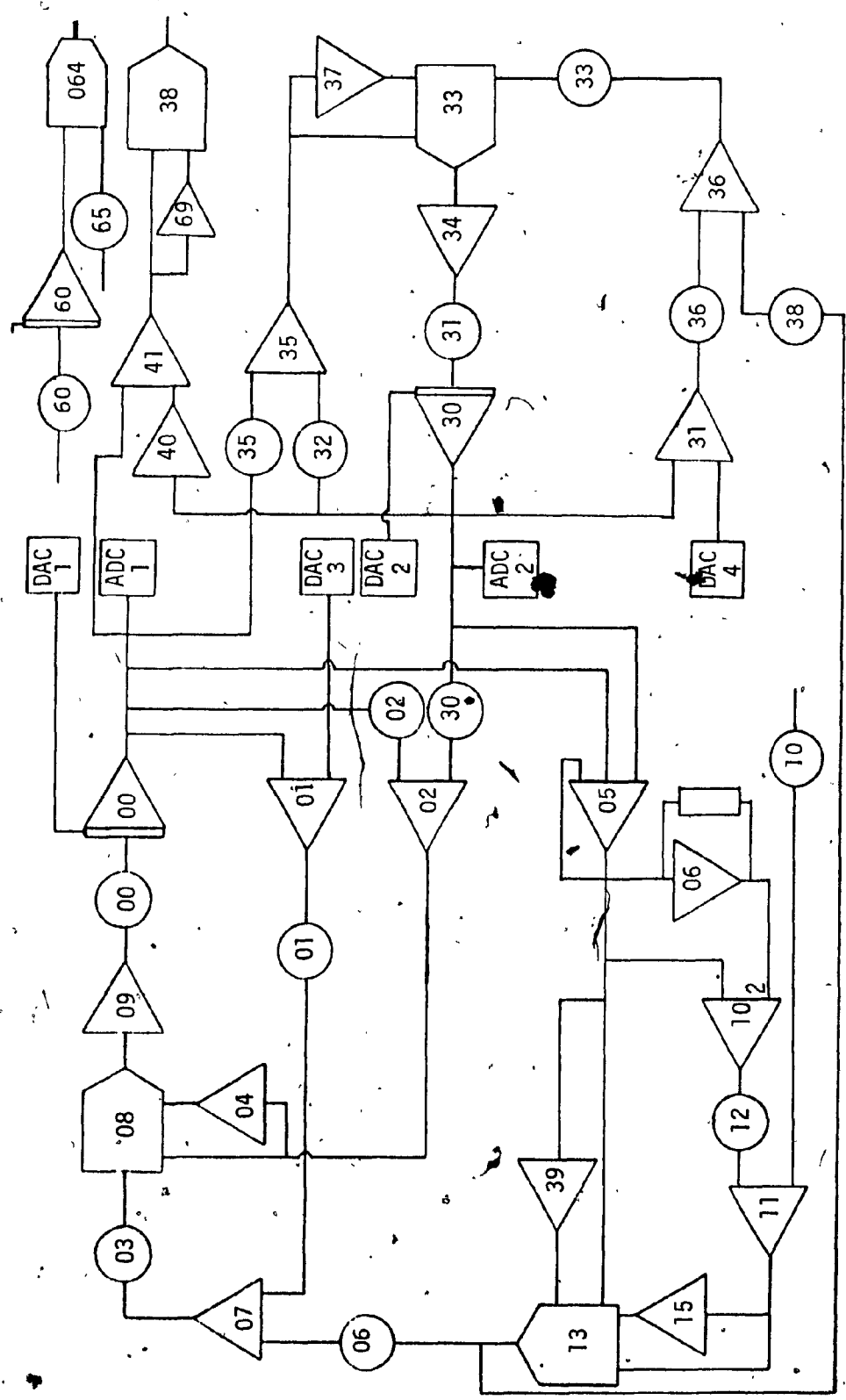
Fig. 4.8 — Analog Circuit Diagram for the Hybrid Program.
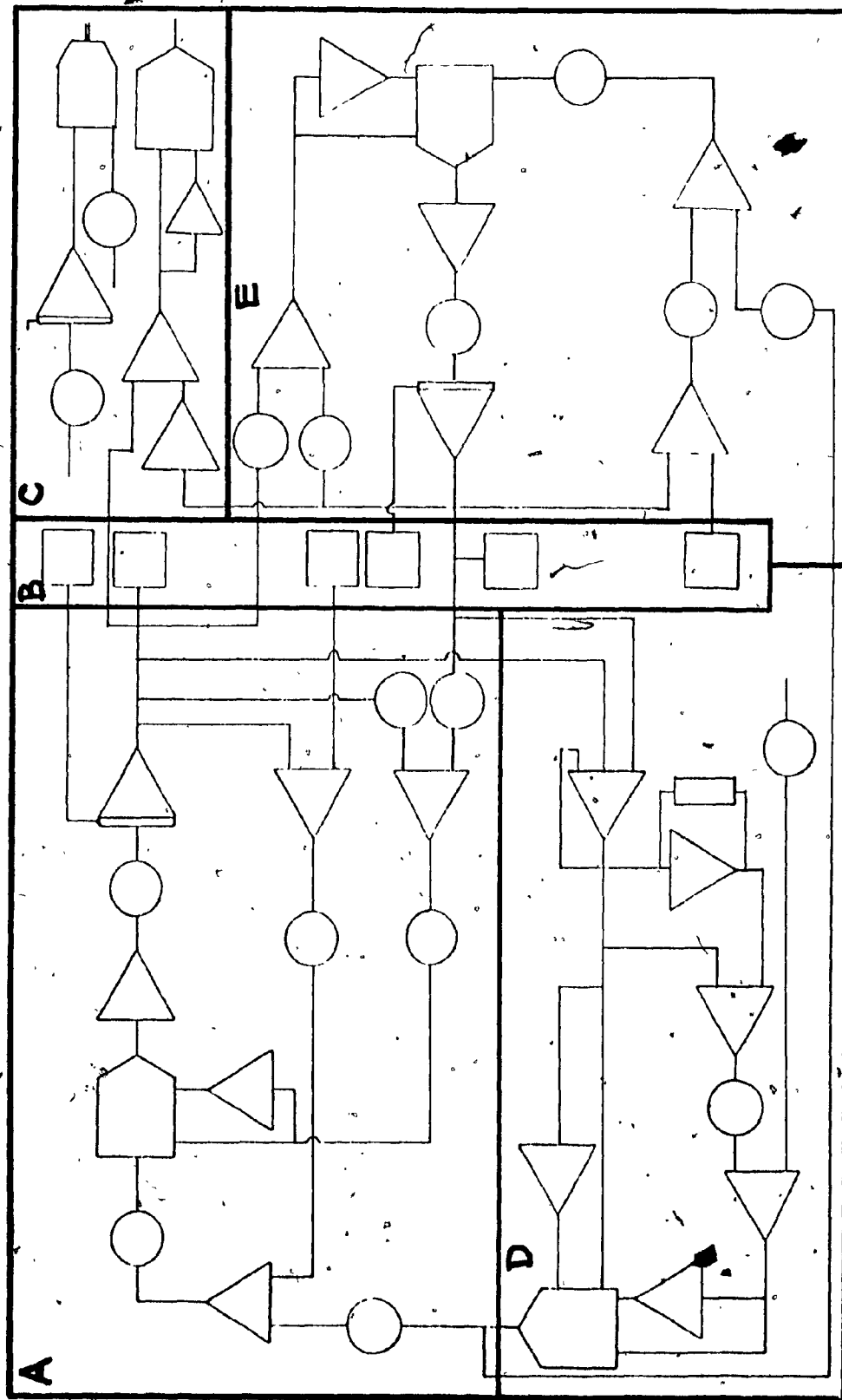
Fig. 4.9 —. Components of the Hybrid Characteristic Equations.

greatly exceeded the value of the celerity which was directly related to

the depth of flow. It was decided that a scale factor of 1/300 would

suffice in dealing with the most extreme cases. This scale was thus intro-

duced throughout the solution. Since the output at amplifier A05 was

always small, its gains were increased to 10. Potentiometer P12 was then

multiplied by 30 to yield a scaled value of $a + b |u|$ at the output of

A11. Potentiometer P06 had to be divided by 500 to obtain a pot coeffic-

ient less than 1.0. Thus, the scaling at the output of P06 was 1/15,000.

This necessitated P01 to be divided by 50 to yield a similar scaling. P00

had a value of 1/6 to maintain a consistent scale factor through integrator

A00. Fig. 4.10 displays the scaling fractions at the appropriate loca-

tions in the circuit.

The problem did not need to be time scaled. It was decided to

use a slow integration time to better analyze the problem and obtain

adequate plots. The time of integration can be chosen according to the

needs of the problem.

The output of the analog computer could be measured continuously

by a strip chart recorder, or occasionally by an XY recorder. The output

would have to be properly scaled to give accurate results. There are two

sets of scaling in determining the output of a particular component: the

scalings introduced by amplitude scaling and those introduced by the plot-

ting machine itself. For instance, amplifier A38 yields a scaled fraction

of the term y, the depth to be solved for. The circuit currently takes

an average of the difference of W_1 and W_2. Thus, a reading off the digital

voltmeter of A38 would have to be interpreted as:
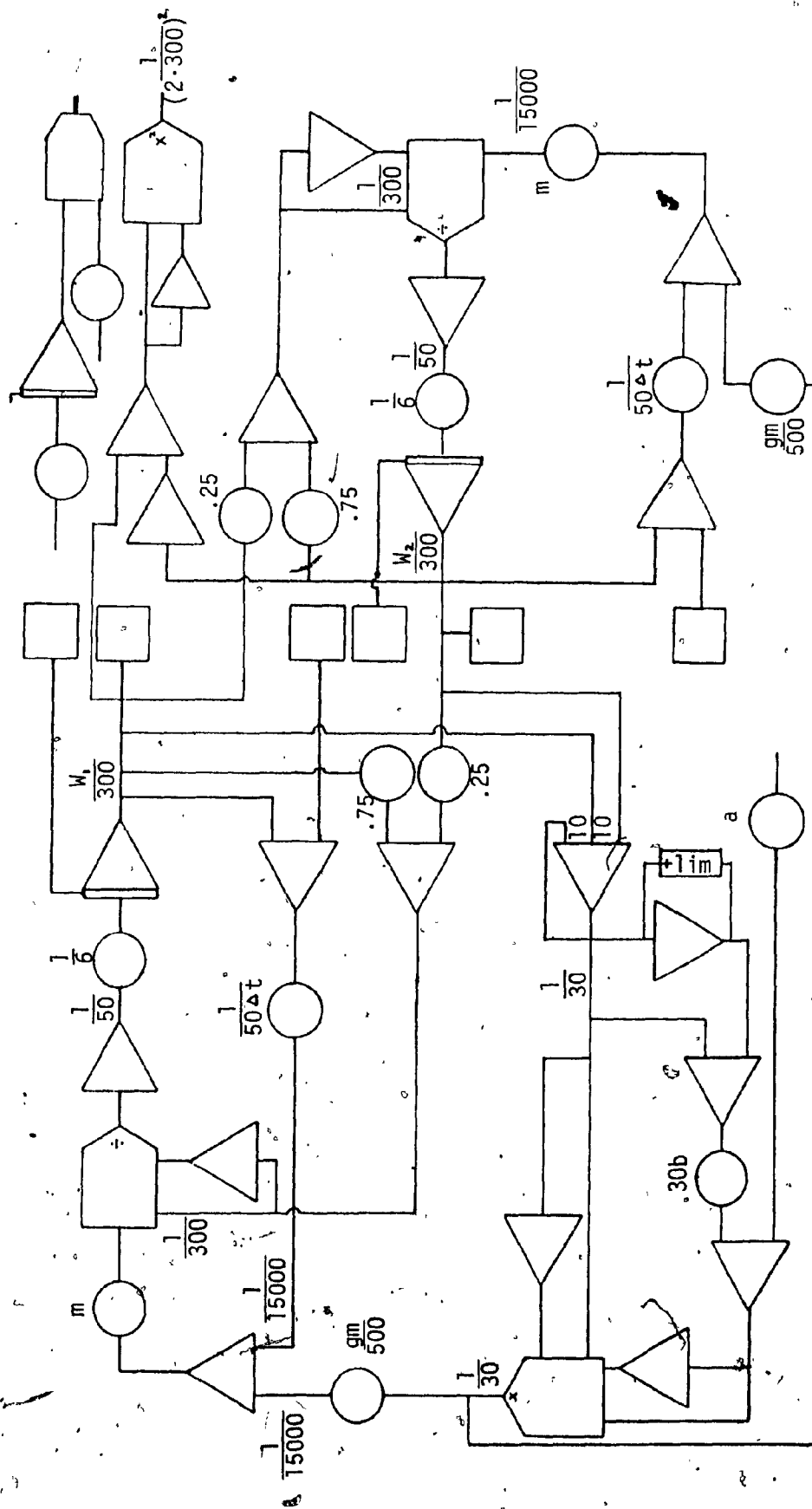
Fig. 4.10 — Amplitude Scaling in the Analog Circuit

$$y = \frac{c^2}{g} = \frac{1}{980.6} \cdot \left[\text{output of A38}\right] \frac{1}{16\ m^2} \cdot 4 \cdot (300)^2$$

$$= \frac{22.945}{m} \left[\text{output of A38}\right]$$

$$\dots\dots\dots (4.15)$$

The individual graph would have to be scaled to the sensitivity and speed of the chart recorder or pen on the XY recorder. The whole aspect of determining the scaling factors and interpreting output causes a great inconvenience. This also introduces greater chance for errors to be introduced into the solution.

The pot coefficients for this hybrid program are automatically determined in Subroutine Pots included in the computer listings of Appendix D.

4.4 RESULTS

The analysis of the outcrop point movement, covered in greater detail in Appendices A and B, provided excellent results. The success of the analog solution in treating the full range of fast drop cases studied proved the worth of the method as a viable alternative to other more popular techniques. Comparison of the results indicate consistently excellent agreement among the various methods applied.

The analog solution nevertheless had an advantage over the digital solution in that the contributions of the various parameters of the damping equation (A.12) could be analyzed. In particular, an investigation carried out determined the roles of each of the two resistance coefficients a_1 and b_1. This was easily done by disconnecting the outputs of pots P03 and P02 representing a_1 and b_1 respectively (see Fig. B.1). Disconnecting

pot PO3 had no apparent effect while disconnecting PO2 completely altered the viscous damping curve. (A typical case is depicted in Fig. 4.11). This indicates that the non-linear damping term b_1 is more prominant in the solution and therefore the interior flow is truly non-Darcy. This behaviour could be determined from the digital solution but not in the same dramatic fashion. This is attributed to the fact that analog computers, once properly scaled, would be more flexible in studying changes in the parameters. The analog solution was more interactive and better simulated the physical nature of the outcrop point movement.

With the encouraging results of the outcrop point movement, a limited attempt was made to proceed to show how the hybrid analysis can be extended to simulate the interior wave motion. A digital formulation was then developed to furnish a basis for the hybrid simulation (see Appendix D). It is noted that the digital program in its present form can only treat embankments of short lengths.

The results of two typical cases are presented. Fig. 4.12 gives pertinent information about case H-2 (see Appendix E for details on the organization of the data); and Fig. 4.13 shows a plot of its Outcrop Point Movement; Fig. 4.14 illustrates the family of phreatic profiles obtained from one wave period. Similarly, Figs. 4.15 through 4.17 represent results for case K-2.

The general nature of the phreatic profiles confirms the trends observed by Nasser [35]. Fig. 4.18 shows the variation of velocity at the outcrop section for one period. Sample output of the wave profile is given in Table 4.1. It can be seen that the velocity never exceeds the maximum fall rate.

Depth (cm.)

h_o

Outcrop Point Movement (OPM)
External Sine Wave
OPM without coefficient a_1
OPM without coefficient b_1

Time (sec.)

t

t_c
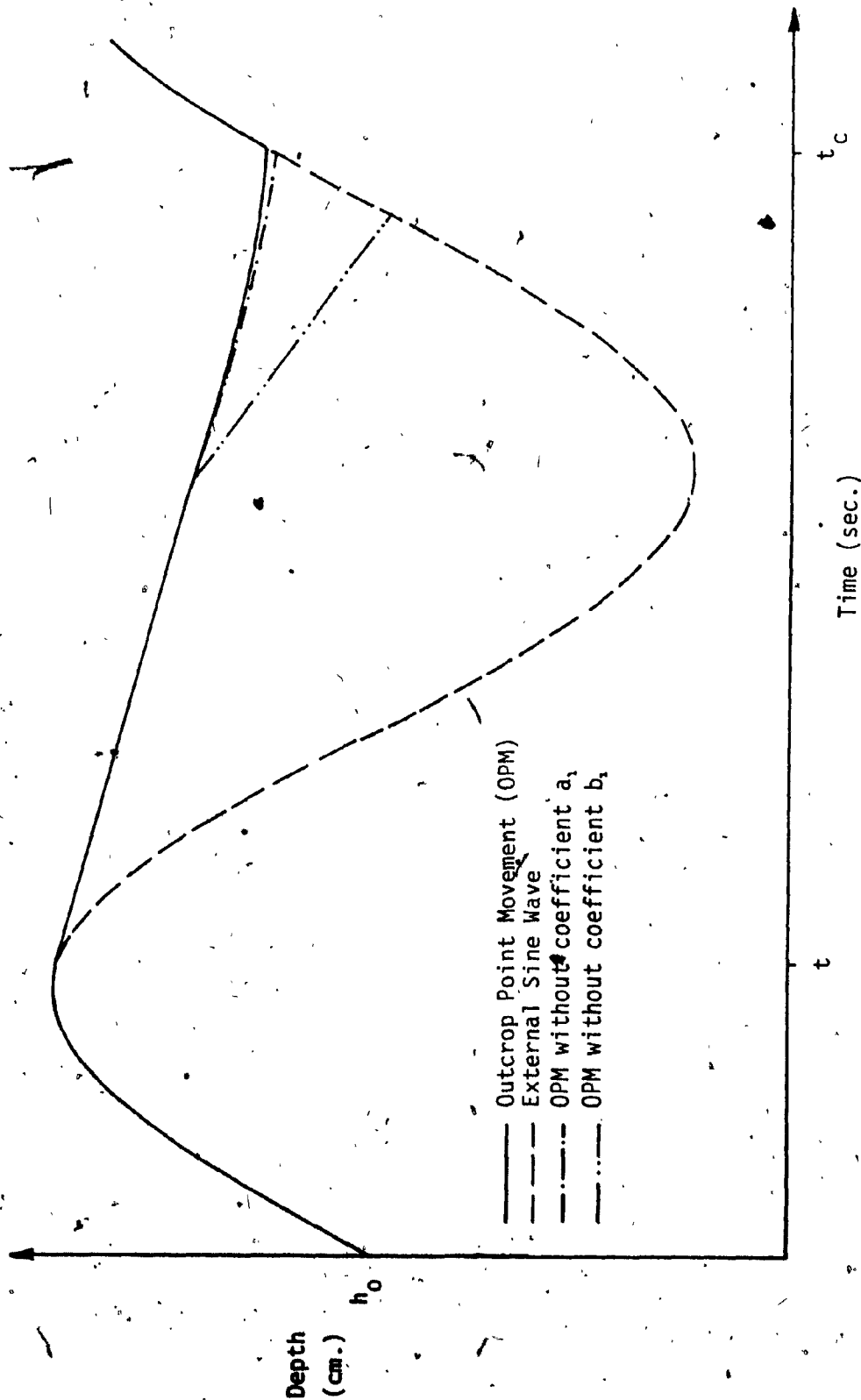
Fig. 4-11 — Influence of Coefficients a_1 and b_1 on the Outcrop Point Movement.

CASE H-2

G I V E N		CALCULATED
A =	.0170	APRIME = 8.1017
B =	.0330	BPRIME = 7.6433
PERIOD =	2.6300	TSR = 1.0151
POROSITY =	.4860	TSR1 = 1.6149
GRAVITY =	980.6000	HYD. COND.(K) = 5.2533
SLOPE (RAD) =	1.5708	FREQUENCY = 2.3890
AMPLITUDE (A0) =	6.0000	TANGENT PT. = 41.9407
DEPTH (H) =	38.0000	MAX. DEVIATION = 1.3974

Y(0) = 35.4567   VEL(0) = -10.8092   ACCEL(0) = .0168

W = .7541   DEL = 701.7189   PK (%) = 11.6452

****

POT	SETTING	KO = 1/(45.)
		K1 = 1/(15.)
		BETA = 10.
PC0	.0333	
PC1	.7206	
PO2	114.6488	
PO3	8.1017	
PO5	2.3890	
Q07	2.3890	
PO7	.1333	
PO8	.2402	
P10	.8444	
P31	.1000	
P35	.1000	
P36	210.5157	
P62	.1000	
P64	.1015	
P94	.1615	

****

SECOND ORDER DIFFERENTIAL DAMPING

FOR H = .00800 AND N = 7

					% DIFF	
TIME	NUM	ANAL	APPROX	YDOT	ANAL.	APPROX
1.6149	35.4567	35.4603	35.4567	-.7206	-.01	0.00
1.6709	34.8534	34.7815	35.0027	-.7128	.21	.43
1.7269	34.2643	34.1564	34.5487	-.6867	.31	.83
1.7829	33.7050	33.5962	34.0948	-.6418	.32	1.16
1.8389	33.1914	33.1110	33.6408	-.5774	.24	1.35
1.8949	32.7410	32.7097	33.1868	-.4910	.10	1.36
1.9509	32.3740	32.3995	32.7328	-.3779	-.08	1.11
2.0069	32.1168	32.1860	32.2788	-.2263	-.22	.50
2.0629	32.0150	32.0731	31.8248	.0067	-.18	-.59

Fig. 4-12   Perinent Data for Case H-2

CASE H-2

M= .4850
A= .0170
B= .0330
THETA= 90.0000 (DEGREES)

DEPTH (CM.)

44.00   36.00   28.00

0.00   0.80   1.60   2.40   3.20

TIME (SEC.)
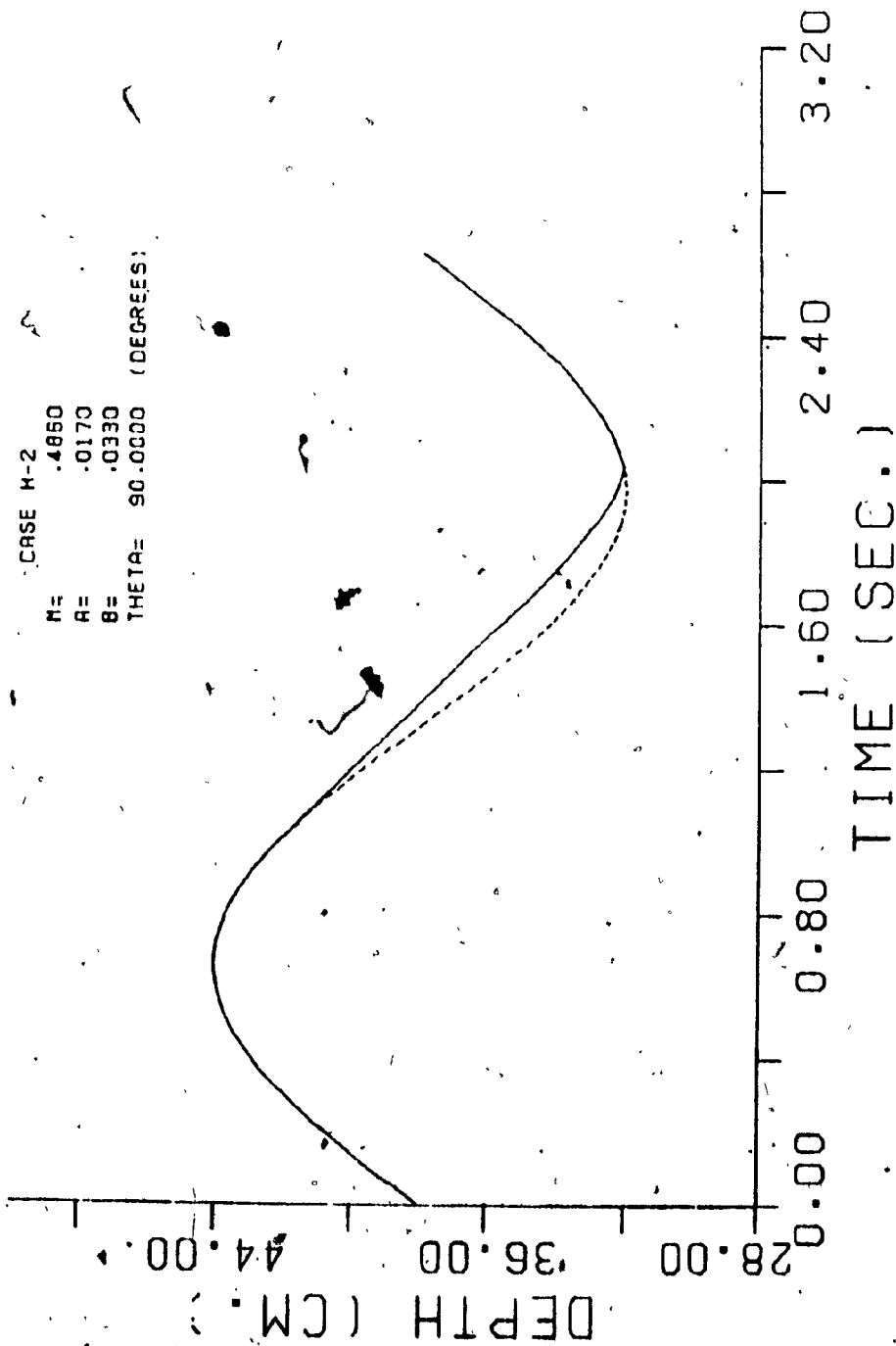
Fig. 4.13 — Outcrop Point Curve for Case H-2.
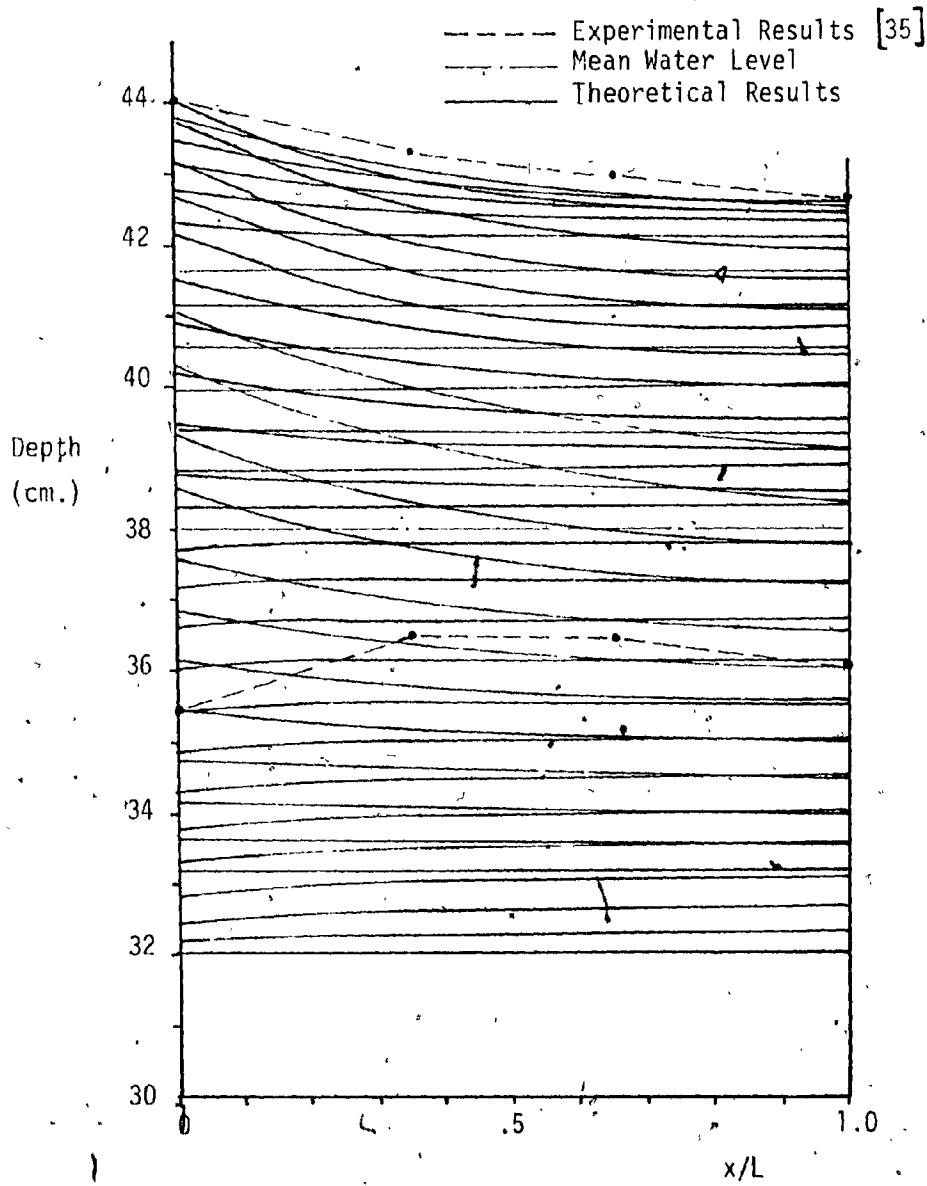
Fig. 4.14 — Envelope of Phreatic Profiles for Case H-2.

CASE K-2

GIVEN		CALCULATED	
A =	.0100	APRIME =	3.6969
B =	.0210	BPRIME =	2.9268
PERIOD =	2.6200	TSR =	.9065
POROSITY =	.3770	TSR1 =	1.7135
GRAVITY =	980.6000	HYD. COND.(K) =	6.6667
SLOPE (RAD) =	1.5708	FREQUENCY =	2.3982
AMPLITUDE (A0) =	13.0000	TANGENT PT. =	40.7065
DEPTH (H) =	30.0000	MAX. DEVIATION =	7.1420

Y(0) = 26.4356   VEL(0) = -17.6835   ACCEL(0) =   .0054

W =   .5672   DEL =   137.3000   PK (%)   =   27.4693

****

POT	SETTING	
		K0 = 1/(45.)
		K1 = 1/(25.)
		BETA = 10.
P00	.0556	
P01	.7073	
P02	73.1701	
P03	3.6969	
P05	2.3982	
Q07	2.3982	
P07	.2889	
P08	.3930	
P10	.6667	
P31	.1000	
P35	.1000	
P36	24.7140	
P62	.1000	
P64	.0906	
P94	.1714	

****

SECOND ORDER DIFFERENTIAL DAMPING

FOR H = .00900   AND N =   6

					% DIFF	
TIME	NUM	ANAL	APPROX	YDOT	ANAL	APPROX
1.7135	.5875	.5876	.5875	-.7073	-.02	.00
1.7675	.5663	.5640	.5715	-.7040	.39	.93
1.8215	.5453	.5413	.5556	-.6915	.73	1.89
1.8755	.5249	.5199	.5397	-.6690	.95	2.83
1.9295	.5053	.5002	.5238	-.6361	1.01	3.67
1.9835	.4868	.4826	.5079	-.5918	.87	4.33
2.0375	.4699	.4674	.4920	-.5345	.53	4.70
2.0915	.4549	.4549	.4761	-.4618	-.01	4.65
2.1455	.4424	.4455	.4601	-.3691	-.70	4.01
2.1995	.4331	.4392	.4442	-.2462	-1.43	2.58
2.2535	.4282	.4363	.4283	-.0624	-1.89	.03

Fig. 4.15   Pertinent Data for Case K-2
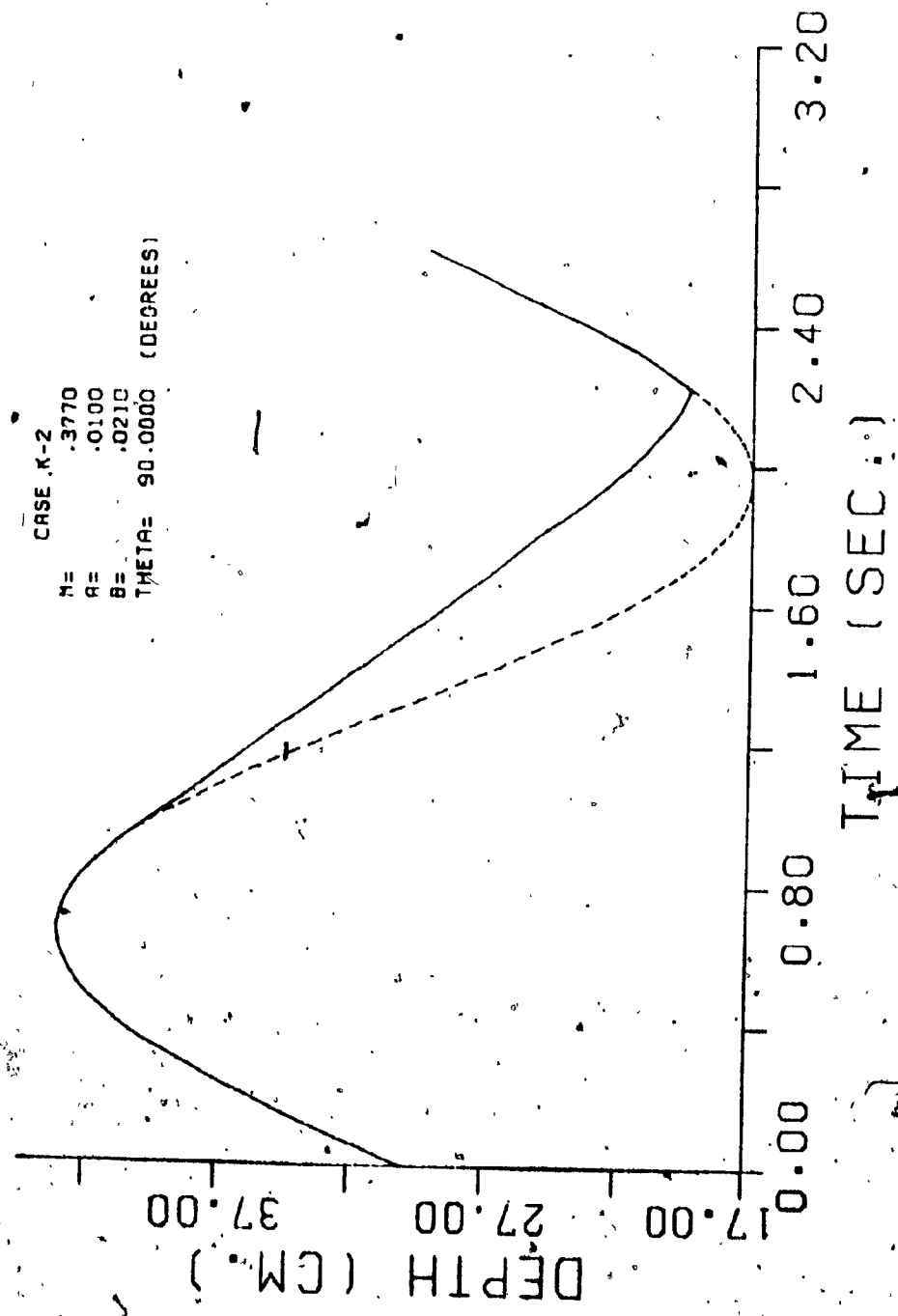
Fig. 4.16 — Outcrop Point Curve for Case K-2.
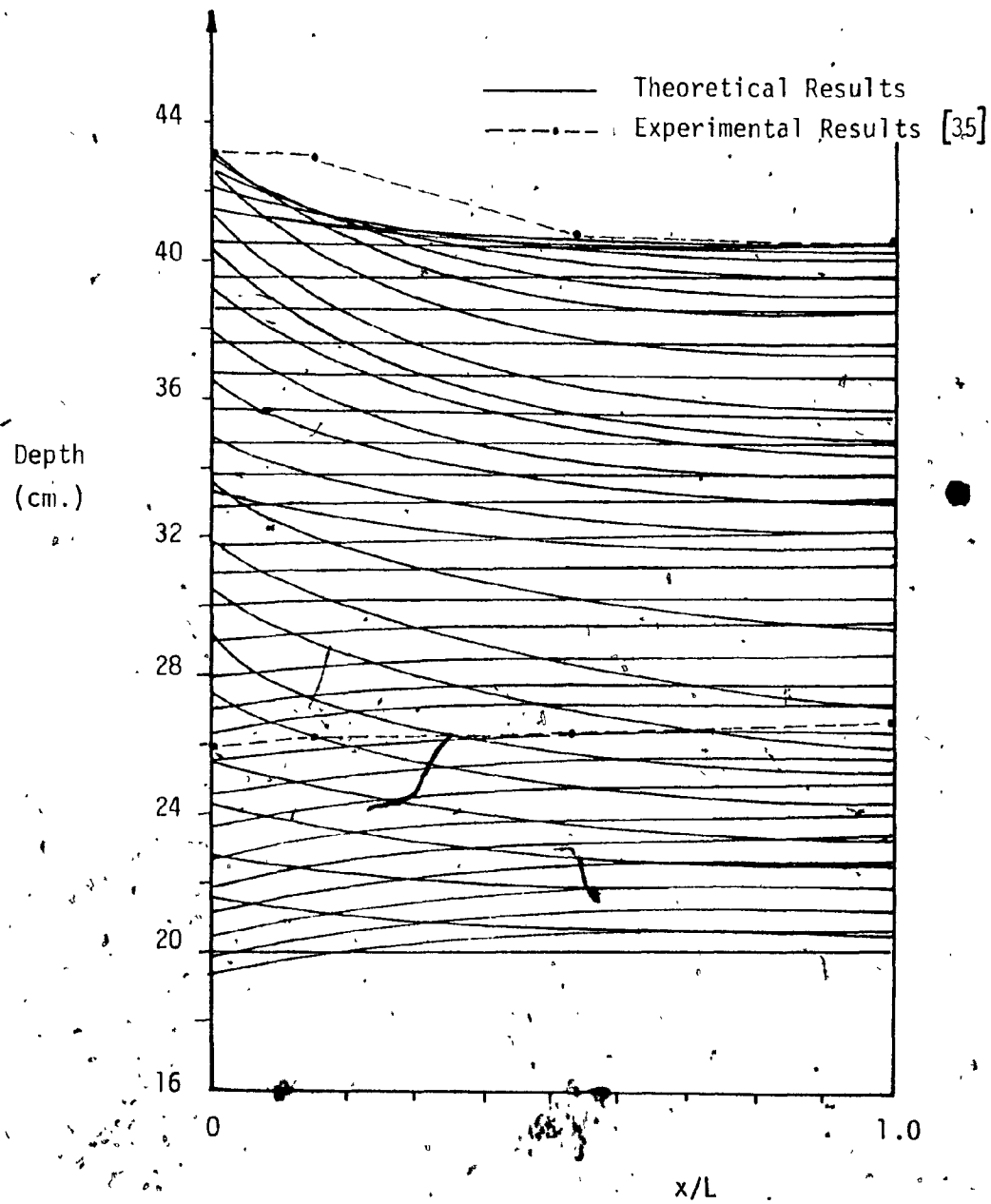
Fig. 4.17 — Envelope of Phreatic Profiles for Case K-2.
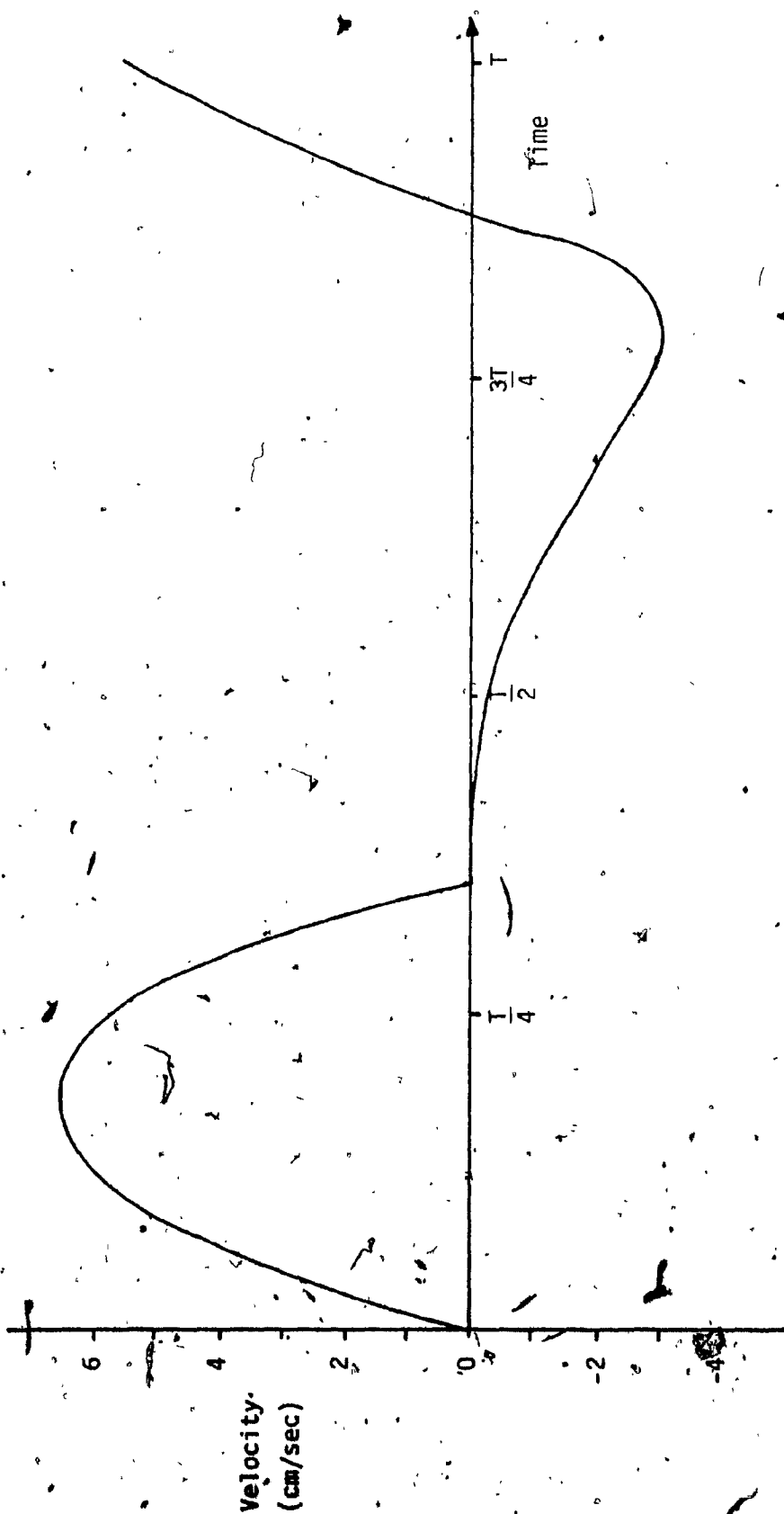
Fig. 4.18 — Velocity Variation at Outcrop Section for Case K-2.

Table 4.1   Sample Output of Wave Profile (Case K-2)

STEP NO. 9 REQUIRED 10 ITERATIONS

X	Y	J	C	W1	W2
0.0000	41.9468000	6.5596	202.8128	159.4734	-146.3623
1.6500	40.7350970	5.2104	198.6341	154.9805	-144.5597
3.3000	39.0519906	4.1335	195.7043	151.6945	-143.6275
4.9500	38.2419992	3.2720	193.6494	149.2837	-142.7397
6.5000	37.4478222	2.5745	192.2029	147.4955	-142.3465
8.2500	37.7755735	1.9992	191.1869	146.1542	-142.1567
9.9000	37.0014275	1.5128	190.4825	145.1367	-142.1110
11.5500	36.8180468	1.0890	190.0099	144.3565	-142.1788
13.2000	36.7035704	.7057	189.7143	143.7513	-142.3179
14.8500	36.6427434	.3493	189.5570	143.2753	-142.5768
16.5000	36.6243452	.0030	189.5695	142.8931	-142.8871

STEP NO. 10 REQUIRED 9 ITERATIONS

X	Y	J	C	W1	W2
0.0000	42.5087000	6.6590	204.1667	160.4007	-147.4827
1.6500	40.8385477	5.1392	200.1157	156.0264	-145.7481
3.3000	39.4445553	4.0832	197.2680	152.8233	-144.6569
4.9500	38.8830292	3.2347	195.2657	150.4671	-143.9936
6.6000	38.3224644	2.5496	193.8531	148.7144	-143.6156
8.2500	37.9304969	1.9811	192.8591	147.3969	-143.4347
9.9000	37.4597162	1.4991	192.1695	146.3949	-143.3967
11.5500	37.4786038	1.0774	191.7069	145.6249	-143.4692
13.2000	37.3657541	.5969	191.4180	145.0251	-143.6323
14.8500	37.3061956	.3400	191.2654	144.5541	-143.8741
16.5000	37.2888618	-.0053	191.2208	144.1742	-144.1868

STEP NO. 11 REQUIRED 10 ITERATIONS

X	Y	J	C	W1	W2
0.0000	42.8611000	6.2041	205.0112	160.7826	-148.3743
1.6500	41.2360235	4.9451	201.2334	156.6751	-146.7849
3.3000	40.2841358	3.9358	198.5676	153.6547	-145.7832
4.9500	39.4508673	3.1256	196.6851	151.4271	-145.1740
6.6000	38.9151701	2.4670	195.3514	149.7520	-144.8279
8.2500	38.5477265	1.9199	194.4094	148.5065	-144.6548
9.9000	38.2830493	1.4545	193.7533	147.9445	-144.6355
11.5500	38.1087502	1.0459	193.3118	146.8039	-144.7102
13.2000	37.9997841	.5776	193.0352	146.2252	-144.8709
14.9500	37.4420330	.3312	192.8885	145.7691	-145.1067
16.5000	37.9250489	-.0049	192.8453	145.4004	-145.4102

The validity of the digital formulation was tested by comparing the points on the maximum and minimum phreatic envelopes with those determined experimentally by Nasser [35]. It can be seen from Table 4.2 and Fig. 4.14 that there is excellent agreement for the maximum envelope whereas the values of the minimum envelope are consistently lower than the experimental results:

Tables 4.3 and Fig. 4.17 reflect the same discrepancies for case K-2. A closer agreement with the experimental results can be obtained if an asymmetric wave form is used to describe the impact wave.

It is believed that the digital formulation can be best improved to treat wider embankments by resorting to a non-dimensionalized form of the governing equations. Further, non-dimensionalization of the equations would lead to a more versatile program. A possible non-dimensional form is given in the next section.

It was not possible to test the hybrid program for interior wave profiles because of hardware malfunction.

4.5 THE PROPOSED NON-DIMENSIONAL FORM

The original differential equation can be written as:

$$\frac{dW_{1,2}}{dx} = \frac{-m}{.75W_{1,2} + .25W_{2,1}} \left[\frac{\Delta W_{1,2}}{\Delta t} + gm\left(a+b \left|\frac{W_1+W_2}{2}\right|\right)\left(\frac{W_1+W_2}{2}\right) \right]$$

$$............ (4.10)$$

The variables, W_1 and W_2, have the units of a velocity. Thus, the best term to serve as a reference would be the celerity corresponding to the mean water level, i.e.

Table 4.2 Comparison of Results for Case H-2

Distance (cm)	Theoretical Depth		Experimental Depth	
	Maximum (cm)	Minimum (cm)	Maximum (cm)	Minimum (cm)
0.0	44.00	32.06	44.00	35.50
2.5	43.07	32.06	43.30	36.50
4.5	42.70	32.06	43.00	36.50
7.0	42.66	32.06	43.00	36.00

Table 4.3 Comparison of Results for Case K-2

Distance (cm)	Theoretical Depth		Experimental Depth	
	Maximum (cm)	Minimum (cm)	Maximum (cm)	Minimum (cm)
0.0	43.00	19.49	43.00	26.00
2.5	41.20	19.90	43.00	26.20
8.5	40.66	19.99	40.80	26.20
16.5	40.53	19.99	40.70	26.70

$$W_{1,2}^{*} = \frac{W_{1,2}}{\sqrt{g h_0}} \qquad \cdots \cdots \cdots \quad (4.11)$$

The spatial and time variables are best described in relation to the length of embankment, L, and wave period, T, respectively. Therefore,

$$x^{*} = \frac{x}{L} \qquad \cdots \cdots \cdots \quad (4.12)$$

$$t^{*} = \frac{\Delta t}{T} \qquad \cdots \cdots \cdots \quad (4.13)$$

The two remaining terms are gma and gmb with units of $(time)^{-1}$ and $(length)^{-1}$ respectively, suggesting the last two dimensionless groups to be gmaT and gmbL. Thus, the dimensionless, governing characteristic equation for W_1 is:

$$\frac{dW_1^{*}}{dx^{*}} = \frac{-m}{.75 \, W_1^{*} + .25 W_2^{*}} \left[\frac{\Delta W_1^{*}}{\Delta t^{*}} + \left(gmaT + gmbL \cdot \left| \frac{W_1^{*} + W_2^{*}}{2} \right| \right) \cdot \left(\frac{W_1^{*} + W_2^{*}}{2} \right) \right]$$

$$\cdots \cdots \cdots \quad (4.14)$$

A similar expression for W_2 can be obtained by interchanging W_1^{*} and W_2^{*}.

4.6 - GENERAL REMARKS

Chapters 1 and 2 summarize the reasons for attempting the method of solution used in this study but this section will concentrate on specific frustrations civil engineers might encounter in pursuing analog/hybrid simulation for the analysis of their problems. Some of the setbacks are localized while others are of a universal nature.

A disadvantage of the hybrid computer is that the accuracy of the solution is governed by the least accurate electronic component.

Further, a malfunction in one component can affect the entire solution.
An apparent error in the time delay subroutine call from the digital
computer prevented the reporting of any specific analog/hybrid results for
the simulation of the interior wave. The hyperbolic nature of the equations
plus the interactive procedure required prevented the manual implementation
of the program on the analog computer only. This reinforced the need for
hybrid simulation for the present study.

Literature dealing with analog/hybrid simulation has made few
inroads into making engineers aware of its potential. Most of the books
written date back to the late 50's and early 60's, suggesting no substan-
tial growth of the hybrid simulation field. Most hybrid techniques have
only been developed within the last decade so that good references are hard
to come by.

At the same time, there are few people who are actually using
hybrid computers to simulate PDEs and therefore there is little or no
exchange of ideas or feedback among the users. Further, equipment is
seldom updated and hence technological advances in hardware have very
little impact on the market.

Civil engineers would have to become more familiarized with
basic electronics just to develop a finer sense of the limitations and
the sensitivity of the analog component hardware.

A crucial feature of analog simulation is the scaling of the
circuit to ensure that no components overload. This often requires
a digital solution to determine the range of variables and hence the
scale factors. The circuit must then be scaled at every component.
This becomes difficult as the complexity of the differential equation
increases.

Since the circuits have to be physically patched on a patch panel, the program has to be checked before using. This is done by a static check test. This necessitates storing analog circuits which presents an inconvenience as far as other users are concerned.

The facilities at Concordia have rather unsophisticated methods of loading the digital programs required for the hybrid simulation. Creating or editing files are not conveniently done.

There are many questions as to the future of hybrid computation. Rubin et al [45] present a very optimistic view; they mention the development of a hybrid programming language called SIMTRAN whose objective is to lower the fixed cost of program preparation, debugging and checking. This would considerably lower the break-even point in relation to digital computers (see Fig. 4.19). SIMTRAN would enable the hybrid user to enter his source program in a remote batch terminal and have all programming and check calculations done automatically.

Rubin et al foresee the features of next generation of hybrid computers to include automatic patching, high language programmability and local and remote terminals. This would decrease the variable cost of simulation to produce even more efficient computers. Far down the road, they expect hybrid computers to contain smaller circuitry, have lower costs, more integrators and faster speeds (Fig. 4.20).
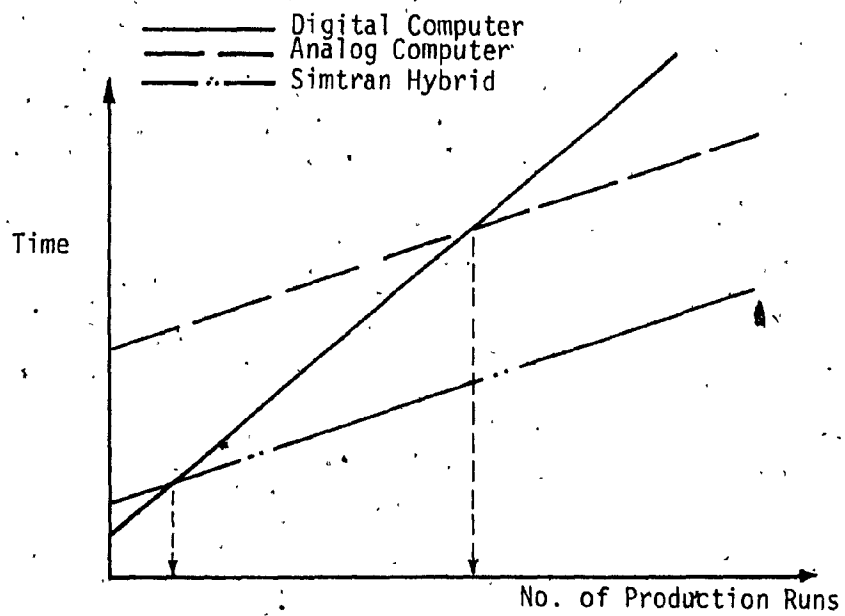
Fig. 4.19 — Break-Even Diagram Between Hybrid and Digital
Computers.
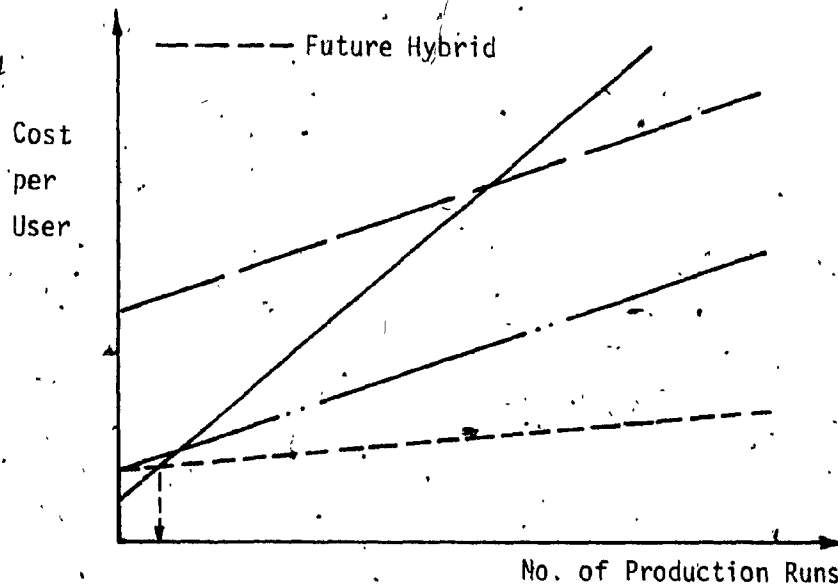
Fig. 4.20 — Cost Comparisons Between Hybrid and Digital
Computers.

CHAPTER 5

CONCLUSIONS AND RECOMMENDATIONS

5.1 CONCLUSIONS

Based on this study, the following conclusions are drawn:

1. A combination of a Runge-Kutta and Adams-Moulton predictor/corrector method is successfully implemented in the numerical simulation of the phreatic profiles. It is, nevertheless, not a replacement for the more economic and efficient hybrid program.

2. An analog/hybrid simulation of the analysis of wave motion in rock-fill embankments is a viable alternative to the Finite Element and Finite Difference Methods. The adjustable integration rate associated with analog simulation represents a definite advantage over numerical integration.

3. The various methods used to calculate the Outcrop Point Movement are successful. The solutions obtained can automatically be plotted on a strip chart recorder, an XY plotter, a Tektronix graphics terminal or Decuwriter terminal.

4. Experimentation with trial cases confirm Nasser's [35] observations of increasing wave transmission to the impervious core with increasing conductivity and decreasing wave steepness and embankment width.

5. The findings of this study indicate that the maximum water level at the core falls significantly below the maximum run-up level at the outcrop section. This could lead to a more economical design than the current practice.

5.2 RECOMMENDATIONS .

Possible extensions of this work are summarized in the following recommendations:

1. The analog/hybrid technique used ought to be refined to improve the simulation. A possible approach is to resort to a backward differencing of second order accuracy. It is also worthwhile to investigate other hybrid techniques such as the hybrid method of characteristics or the scheme devised by André [2].

2. There is a definite need for a review acquainting Civil Engineers with the advantages of available hybrid techniques. Such a review should focus on the classification of the techniques in terms of the minimum size of the hybrid system required, the type of hardware needed, the expected time of computation and the simplicity of implementation.

3. The analysis of the Outcrop Point Movement should be adopted to simulate the exit conditions of a continuous breakwater. The introduction

of the vertical velocity at the outcrop section in the hybrid simulation would lead to a definite improvement.

For the class of nonlinear waves considered in this study, a better approximation of the seepage face could be achieved if the analysis of the outcrop point movement is based on an asymmetric external fluctuation of the input wave. This would also improve the simulation of the interior wave.

4. A challenging undertaking would be an attempt to apply an analog technique to layered dams with various geometries and porosities.

5. For a purely digital solution, it would be worthwhile to consider a Burlisch-Stoer integration method. It features from 6th to 12th order accuracy, variable step size, three possible error criteria, and is very stable for highly nonlinear problems.

APPENDIX A

OUTCROP POINT MOVEMENT

APPENDIX A

OUTCROP POINT MOVEMENT

·The wave induced unsteady non-Darcy flow under consideration in this study requires the outcrop point movement relative to the external wave as a boundary condition (Fig. A.1).

When a water wave attacks a porous structure, the wave reaches a maximum run-up position on the face of the structure and recedes to a minimum rush-down level: these maximum and minimum levels constitute the impact wave height. Experiments done by Nasser [35] show that a sine wave can be used to represent the impact water wave. Assuming a sine function to describe the external water level fluctuation, then:

$$Y_f = h_0 + A_0 \sin(\omega t) \qquad \ldots \ldots \ldots \ldots (a.1)$$

where

Y_f = elevation of the free water level at the interface with respect to the channel bottom

h_0 = mean water level

A_0 = amplitude of the water wave

ω = frequency of oscillation

t = time

Dracos [10] states that "as long as water flows into a porous body, the phreatic line and the free water level meet at the same point
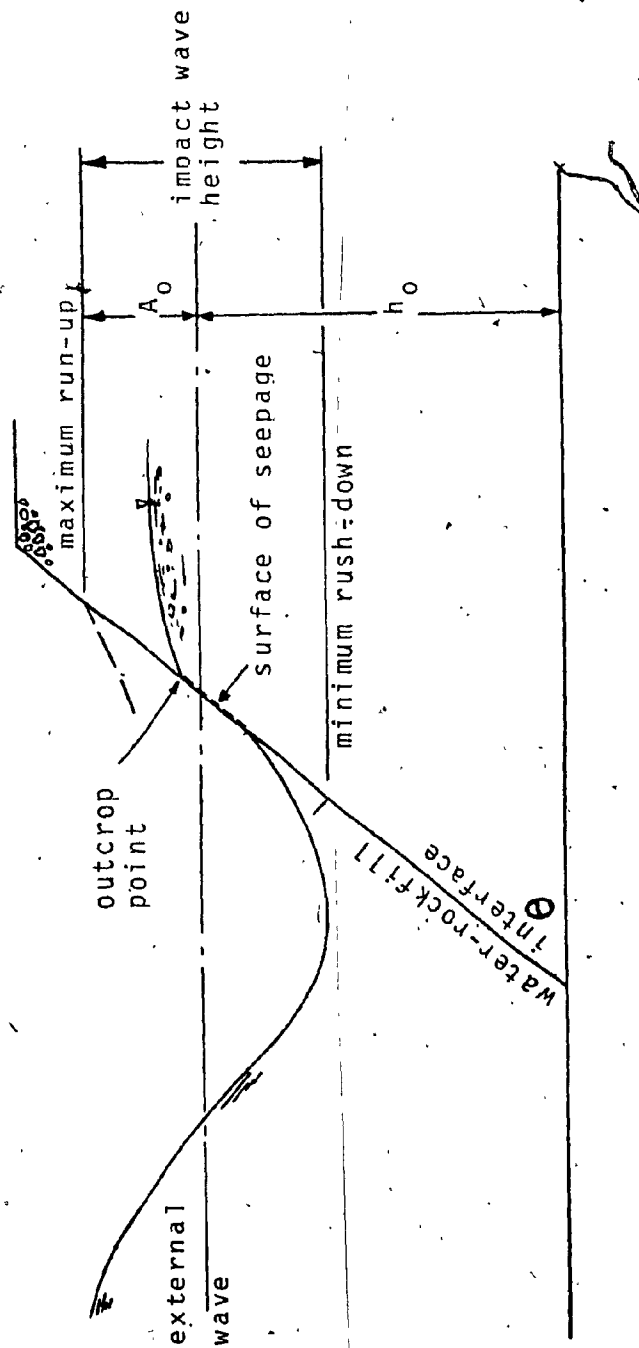
Fig. A.1. Outcrop Point as a Boundary Condition

on the boundary". When, however, the water exits from the porous body, a seepage surface may be interposed between the free water level and the phreatic line: a seepage surface will not occur unless the internal fall rate is less than the fall rate of the external water level. The vertical velocity of fluctuation, V_f, is the derivative of equation (a.1) or:

$$V_f = A_0 \cos(\omega t) \qquad \ldots \ldots \ldots \ldots \ldots \text{(a.2)}$$

And hence the maximum fall rate, V_{fmax}, is

$$V_{fmax} = \omega A_0 \qquad \ldots \ldots \ldots \ldots \ldots \text{(a.3)}$$

The maximum internal fall velocity, V, is given by Dracos as:

$$V = \frac{k}{m} \sin^2\theta \qquad \ldots \ldots \ldots \ldots \ldots \text{(a.4)}$$

where   m = porosity

k = non-Darcy hydraulic conductivity

θ = angle of inclination of the structure face with the horizontal

$k = 1/(a + bm|V|) \qquad \ldots \ldots \ldots \ldots \ldots \text{(a.5)}$

The value of V can be calculated directly from (a.4) and (a.5) to be:

$$V = \frac{1}{2} \left[\frac{-a}{bm} + \sqrt{\left(\frac{a}{bm}\right)^2 + \frac{4\sin^2\theta}{m^2 b}} \right] \qquad \ldots \ldots \ldots \ldots \text{(a.6)}$$

The drop rate of the free water level can be classified as 'slow' if

$$V_f < V = \frac{-k}{m} \sin^2\theta \qquad \ldots \ldots \ldots \ldots \ldots \text{(a.7a)}$$

or 'fast' if:

$$V_f > V = -\frac{k}{m}\sin^2\theta \qquad \ldots\ldots\ldots\ldots (a.7b)$$

a slow drop case implies that the outcrop point movement coincides with the free water level.

Comparing equations (a.7) and (a.2) and introducing the dimensionless parameter

$$W = \frac{k}{\omega A_o m} \qquad \ldots\ldots\ldots\ldots (a.8)$$

yields:

$$\cos(\omega t)/W < -\sin^2\theta \text{ for slow drop} \qquad \ldots\ldots\ldots\ldots (a.9a)$$

$$\cos(\omega t)/W > -\sin^2\theta \text{ for fast drop} \qquad \ldots\ldots\ldots\ldots (a.9b)$$

Equating the terms yields the time, t_1, during which internal and external movements coincide:

$$t_1 = \frac{1}{\omega}\cos^{-1}(-W\sin^2\theta) \qquad \ldots\ldots\ldots\ldots (a.10)$$

This now provides some information in determining the outcrop point movement (see Fig. A.2).

1. For $W\sin^2\theta > 1$, t_1 cannot exist or else it is equal to $T/2$, where T is the wave period. This condition defines a slow drop case.

2. For $W\sin^2\theta < 1$, a number of cases arise which must be studied separately.

    A. For $t < t_1$, the water is entering the porous media and therefore the outcrop point movement is identical to the movement of the free water level or region I in Fig. A.2.

- 93 -
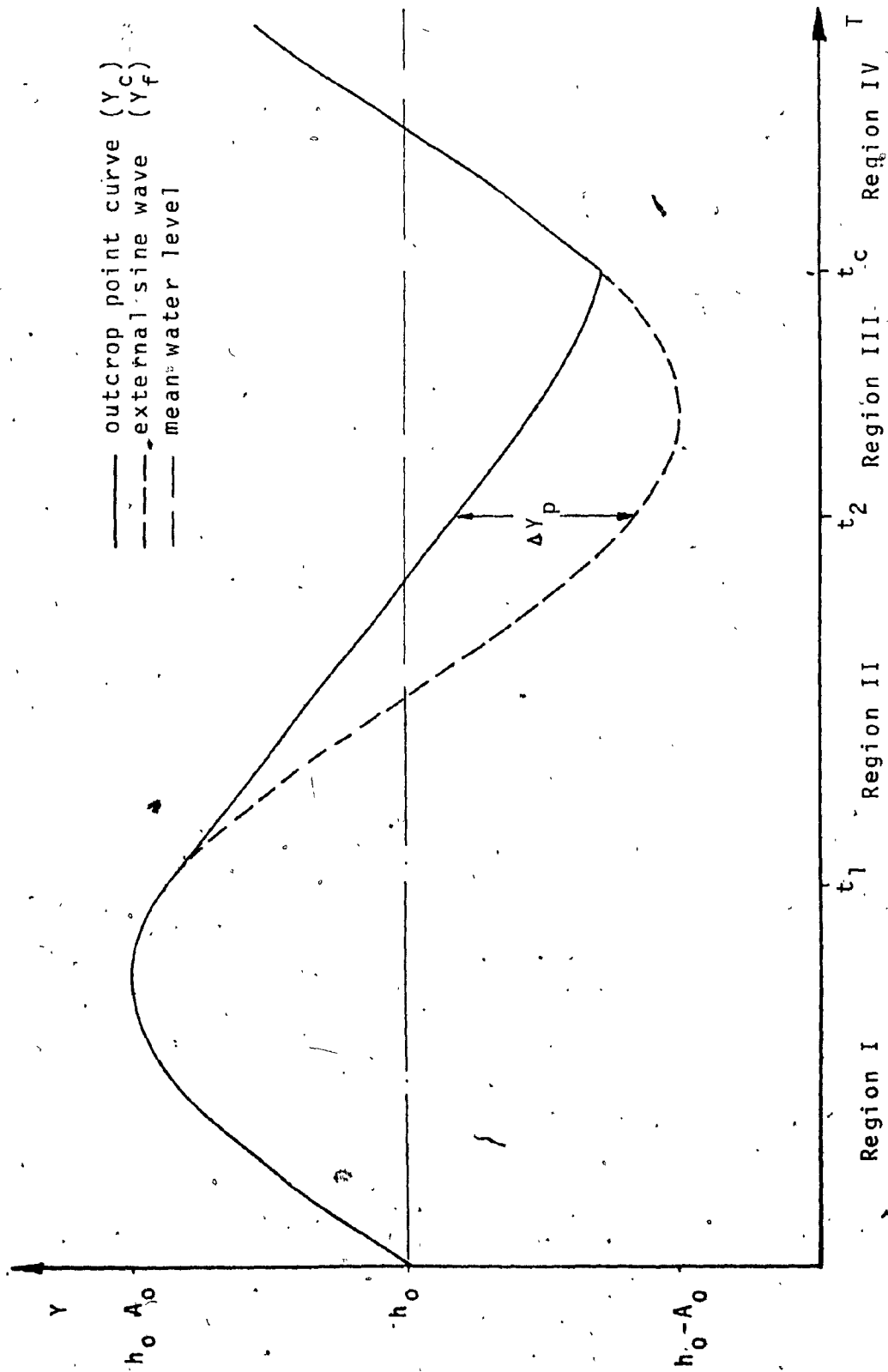
Fig. A.2. Outcrop Point Movement

B. For $t_1 < t < t_2$, the outcrop point falls at the maximum internal velocity V as represented by the slope at time t_2 in region II. Point t_1 (or $T-t_2$) is the time at which there is a maximum deviation, ΔY_p, between the outcrop point and the free water level. The equation representing this region is:

$$Y = h_0 + A_0 \sin\omega t_1 + V(t-t_1) \quad \ldots \ldots \ldots \ldots \text{(a.11)}$$

C. Region III for $t_1 < t < t_2$

At $t = t_2$, the outcrop point will have reached its maximum deviation, ΔY_p, from the free water level curve and hence the two curves will start to converge. The non-linear viscous damping effect is described by a second order differential equation:

$$\ddot{Y}_c + (a_1 + b_1|\dot{Y}_c|)\dot{Y}_c + \delta\, Y_c = \delta\, f(t) \quad \ldots \ldots \ldots \text{(a.12)}$$

where $a_1 = gma$

$\qquad b_1 = gm^2 b$

$\qquad \delta = g \sin^2\theta / \Delta Y_p$

$\qquad \Delta Y_p = 2\, Ao \sin(\omega t_1) - V(t_2 - t_1)$

$\qquad f(t) = h_0 + A_0 \sin(\omega t)$

$\qquad (\dot{\ }) \quad$ refers to the time derivative

The required initial conditions for this equation are:

$$\dot{Y}_c(t_2) = V = -\frac{k}{m} \sin^2\theta \qquad \ldots \ldots \ldots \text{(a.13)}$$

$$Y_c(t_2) = h_0 + A_0 \sin(\omega t_2) + V(t_2 - t_1) \qquad \ldots \ldots \ldots \text{(a.14)}$$

This region is the most difficult to analyze. Five solution methods were investigated and will be covered in depth.

    D.   Region IV is a repetition of Region I where the water is once again entering the porous media and hence the outcrop point rises with the free water level.

SOLUTION OF VISCOUS NON-LINEAR DAMPING EQUATION (REGION III)

Three parameters were used to analyze and describe the nature of the fast drop cases particularly in the region of non-linear viscous damping. These parameters are:

1. W, from equation (a.8), is a dimensionless parameter that varies between 0 (zero) and $1/\sin^2\theta$ for fast drop cases. The lower the value of W, the greater the damping. As W increases, the case approaches the slow drop state.

2. δ , given in equation (a.9) and possessing the units $\sec^{-2}$, is of prime importance in the analog solution because it is a pot setting. In the cases studied, its value varied between 4 and 111,000. Low values of δ represent a highly damped system whereas high values, i.e: $\delta > 800$, resemble slow drop cases.

3. A practical dimensionless percentage was developed to indicate quantitatively how much the fast drop case differed from the slow drop case. This number is given as:

$$Pk = \frac{\Delta Y_p}{2A_0} \times 100 \qquad\qquad \dots\dots\dots\dots (a.15)$$

Pk varied between 0 (zero) and 85% in the cases studied. A Pk value of zero is identical to the slow drop case. High values indicated substantial deviations from the slow drop case and therefore represented highly damped cases.

Five methods were used to get solutions in region III: MIMIC, analytic, numerical, approximation and analog. Each of these methods provided a solution for the region of viscous damping.

1. MIMIC

MIMIC is a parallel simulation language that numerically solves differential equations. Its advantage lies in the ease of programming and convenient plots of the solution. A major disadvantage of the Mimic package available at Concordia University is the inaccuracy and unreliability of the solutions. Large errors were introduced into the solution when the MIMIC program consistently determined an initial acceleration of 500 cm/sec^2 at time t_2 instead of a zero acceleration. For low values of δ, the general form of the solution curve was obtained but at high δ values, the solution broke down. With the existing software, it was not possible to obtain one continuous curve for the four regions described.

2. Numerical

Since the MIMIC simulation package was inaccurate, a Runge-Kutta fourth order method was used. An adequately small step was required ($\Delta h < .01$) to obtain any solution. A program was developed to piece together the total outcrop point curve and plot the results. The results were very good.

3. Analytic Solution

Dracos gave an analytic solution in terms of an external cosine water wave but because of an error in choosing a proper dimensionless number χ, his solution was wrong. The χ term chosen for this study yields results in close agreement with the numerical solution but exhibits large errors for cases with low δ values in sloping rockfaces. The general computer program developed gives a comparison of the analytic and numerical solutions.

The solution subject to the given initial conditions of the differential equations in region III is:

$$Y = \frac{D-C\lambda_2}{\lambda_1-\lambda_2} e^{\lambda_1(t-t_2)} - \frac{D-C\lambda_1}{\lambda_1-\lambda_2} e^{\lambda_2(t-t_2)} + h_0$$

$$+ A\sin\omega t - B\cos\omega t \qquad \ldots \ldots \ldots (a.16)$$

where $\quad \lambda_1 = -\frac{gm}{2X}\left(1 - \sqrt{x}\right) \qquad \ldots \ldots \ldots (a.17)$

$$\lambda_2 = -\frac{gm}{2X}\left(1 + \sqrt{x}\right) \qquad \ldots \ldots \ldots (a.18)$$

$$\chi = 1 - \frac{4K}{gm}\sin^2\theta \frac{\Delta Y_p}{A_0 T} \qquad \ldots \ldots \ldots (a.19)$$

$$TKG = \frac{gm\omega}{K} \qquad \ldots \ldots \ldots (a.20)$$

$$\omega = \frac{2\pi}{T} \qquad \ldots \ldots \ldots (a.21)$$

$$\delta = \frac{g\sin^2\theta}{\Delta Y_p} \qquad \ldots \ldots \ldots (a.22)$$

$$A = A_0 \; \frac{\delta(\delta - \omega^2)}{TKG^2 + (\delta - \omega^2)^2} \qquad \ldots \ldots \ldots \ldots \ldots \ldots \ldots (a.23)$$

$$B = A \; \frac{TKG}{(\delta - \omega^2)} \qquad \ldots \ldots \ldots \ldots \ldots \ldots \ldots (a.24)$$

$$C = (A_0 + A)\sin\omega t_1 + B\cos\omega t_1 + V(t_2 - t_1) \; \ldots \ldots \ldots \ldots (a.25)$$

$$D = -\omega A\cos\omega t_1 + \omega B\sin\omega t_1 + V \; \ldots \ldots \ldots \ldots \ldots \ldots (a.26)$$

χ is only a little smaller than unity so that λ_1 becomes small and λ_2 becomes a large negative number. The large negative number λ_2 causes the second term of the solution to tend to zero very fast and it can safely be disregarded. Therefore, the outcrop point movement in the viscous damping region is given by the modified equation:

$$Y = \frac{D-C}{\lambda_1-\lambda_2} \; e^{\lambda_1(t-t_1)} + A\sin\omega t - B\cos\omega t \qquad \ldots \ldots \ldots \ldots (a.27)$$

When this function equals the external sine function $(Y_c = h_0 + A_0\sin\omega t)$, then the two curves rise again as the water will be entering the porous body from the reservoir.

4. Approximate Solution

Nasser [35] found that a drop rate of about one half of the maximum fall velocity, V, would give very close values to those obtained by his finite difference solution of the damped equation.

In this study, 147 fast drop cases were analyzed to compare the actual drop rate to the maximum velocity. Since the numerical and analog results were in close agreement, the approximate slopes were calculated

from Fig. A.3 as:

$$\text{linear drop rate} = \frac{y_2 - y_3}{t_2 - t_3} \qquad \dots \dots \dots \text{(a.28)}$$

This was then compared to the maximum drop rate to determine the ratio needed:

$$\text{Ratio} = \frac{y_2 - y_3}{t_2 - t_3} \times \frac{t_1 - t_2}{y_1 - y_2} \qquad \dots \dots \dots \text{(a.29)}$$

Based on the 147 cases studied, the following information was revealed:

mean	=	0.7567
std dev.	=	2.60
highest ratio	=	.836
lowest ratio	=	.676

Therefore, an approximate solution would be to use a drop rate of 75 per cent of the maximum fall velocity rather than the half value reported by Nasser.

5. Analog Solution

The analog solution most truly represents the system in program preparation and during computer operation. Essential to the proper calculation in this simulation was the digital logic, amplitude scaling, time scaling and the proper system diagram.

The versatility of the analog computer, once properly programmed (the programming procedures are dealt with in detail in Appendix B), lies in the ease of studying the whole system or parts of it separately. A preliminary study was made to measure the effect of the linear Darcy coeffi-
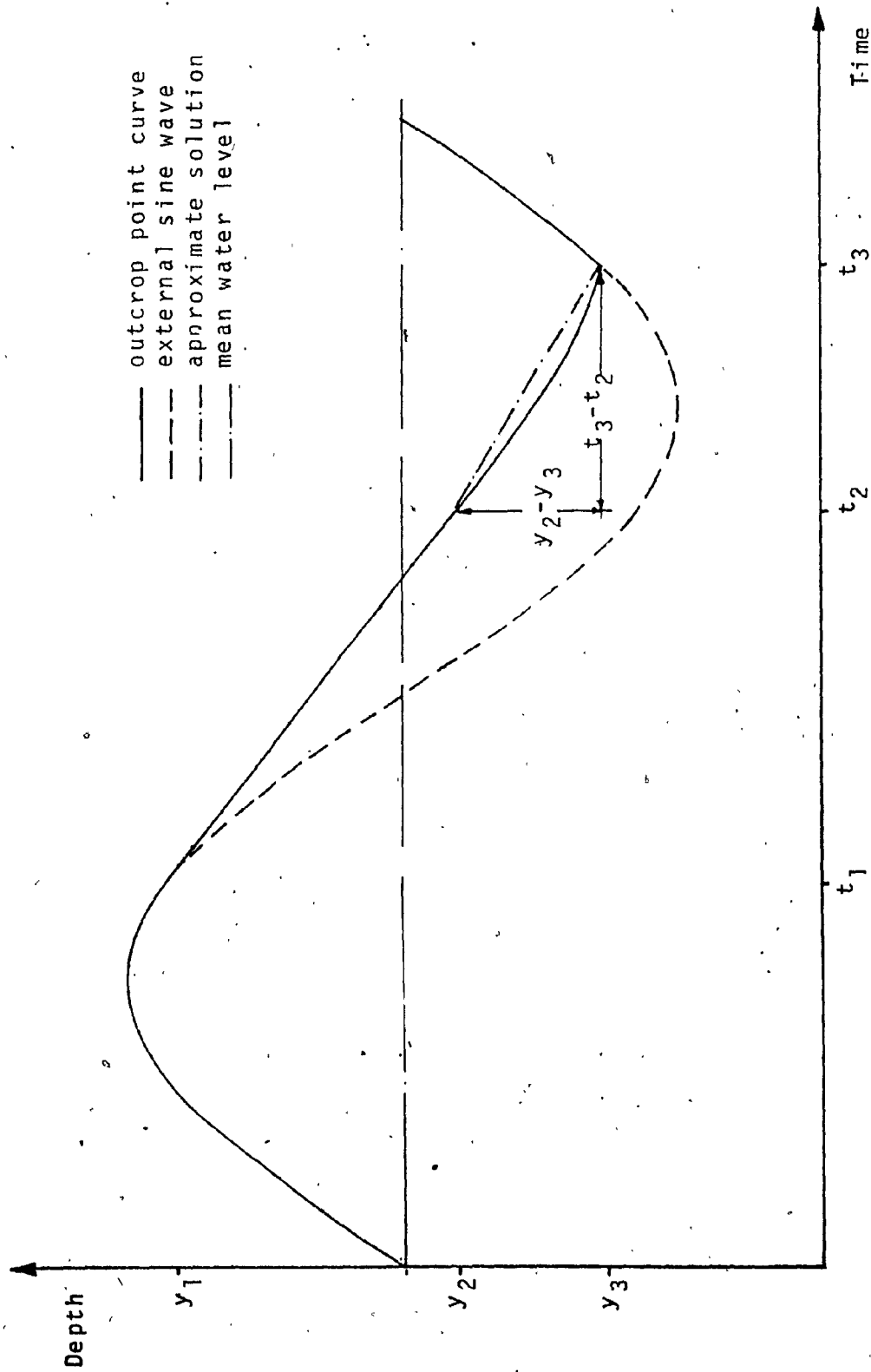
Fig. A.3. Illustration of the Approximate Solution

cient, a, in equation (a.12). In most cases 'a' was of very little signi-
ficance in the solution whereas the non-Darcy coefficient, b, was indispen-
sible. This supports the assumption that the flow is turbulent in the fast
drop cases (i.e. $i = aq + bq^2$). The more weight that is put on coefficient
b, the more turbulent the flow will become.

Because of its parallel nature, the analog computer produces con-
tinuous solutions which can be monitored on a strip chart recorder, oscil-
loscope or on an X-Y plotter. X-Y plots proved to be very helpful since
the outcrop point curve could be superimposed on the sine wave which pro-
vided an excellent basis for comparison. These plots also monitored the
difference in solution with or without certain variables such as 'a' or 'b'.
These plots were only used for final comparisons and results. Intermediate
results were obtained on the strip chart recorder.

After proper scaling, a vast range of cases were studied, from
sloping dams with low δ values of 4 to vertical breakwaters with values of δ
as high as 111,000. Figures A.4 to A.11 show the difference between the
outcrop point movement and the input sine wave for varying values of δ.
High values of δ approach the slow drop case. The author believes that
since deviations of 5% are not uncommon in the field, simulating fast drop
cases with very high values of δ might be very impractical. It is sugges-
ted that a cut-off factor be introduced so that any transition drop cases
(fast drop cases sufficiently close to slow drop cases) can be treated in
a special manner. For Pk less than 5%, the differences between Y_c and Y_f
curves are negligible as can be seen in Figures A.12 to A.15.

The main disadvantage of the continuous or analog solution is
that it is scaled and hence its accuracy at any point is only as good as

CASE 0-16.

M= .3500
A= .0100
B= .0210
THETA= 28.5650 (DEGREES)
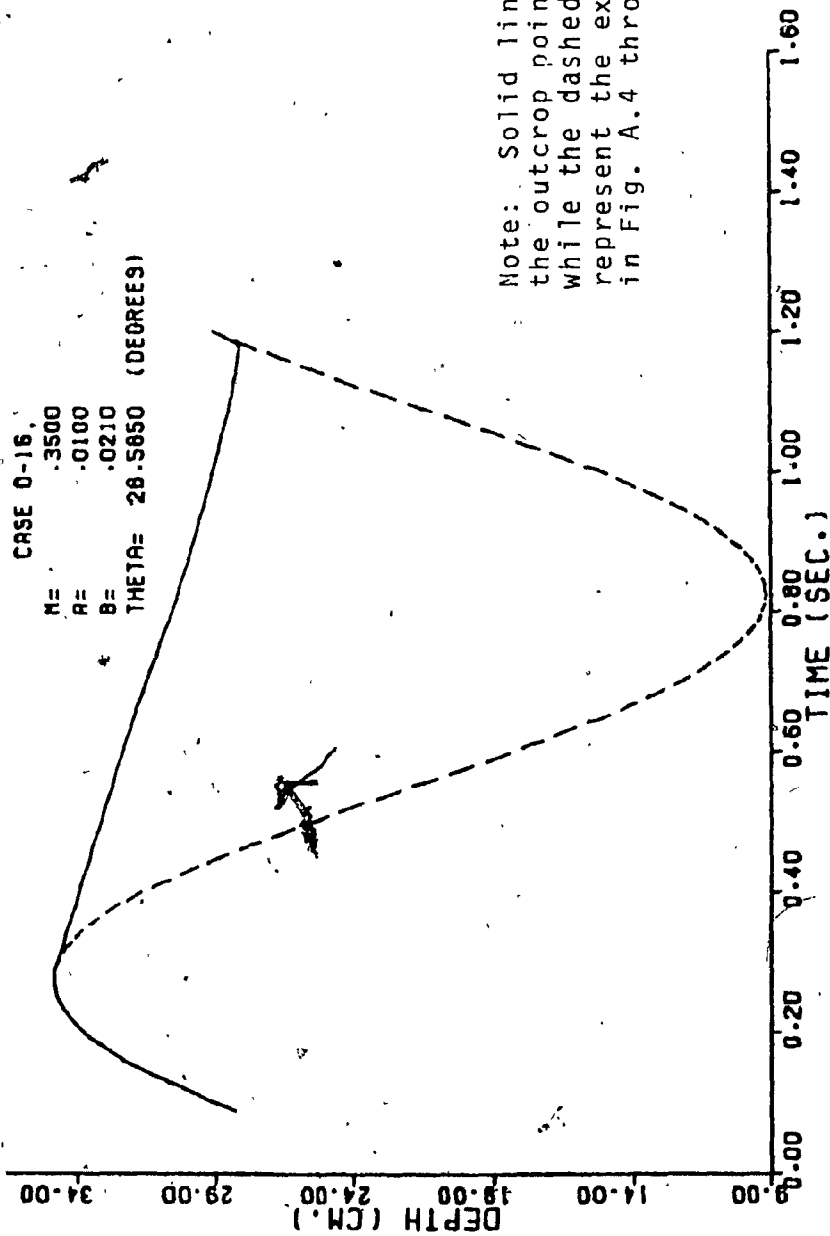
Note: Solid lines represent
the outcrop point movement,
while the dashed lines
represent the external waves
in Fig. A.4 through A.15.

Fig. A.4. Outcrop Point Movement for δ= 9.22
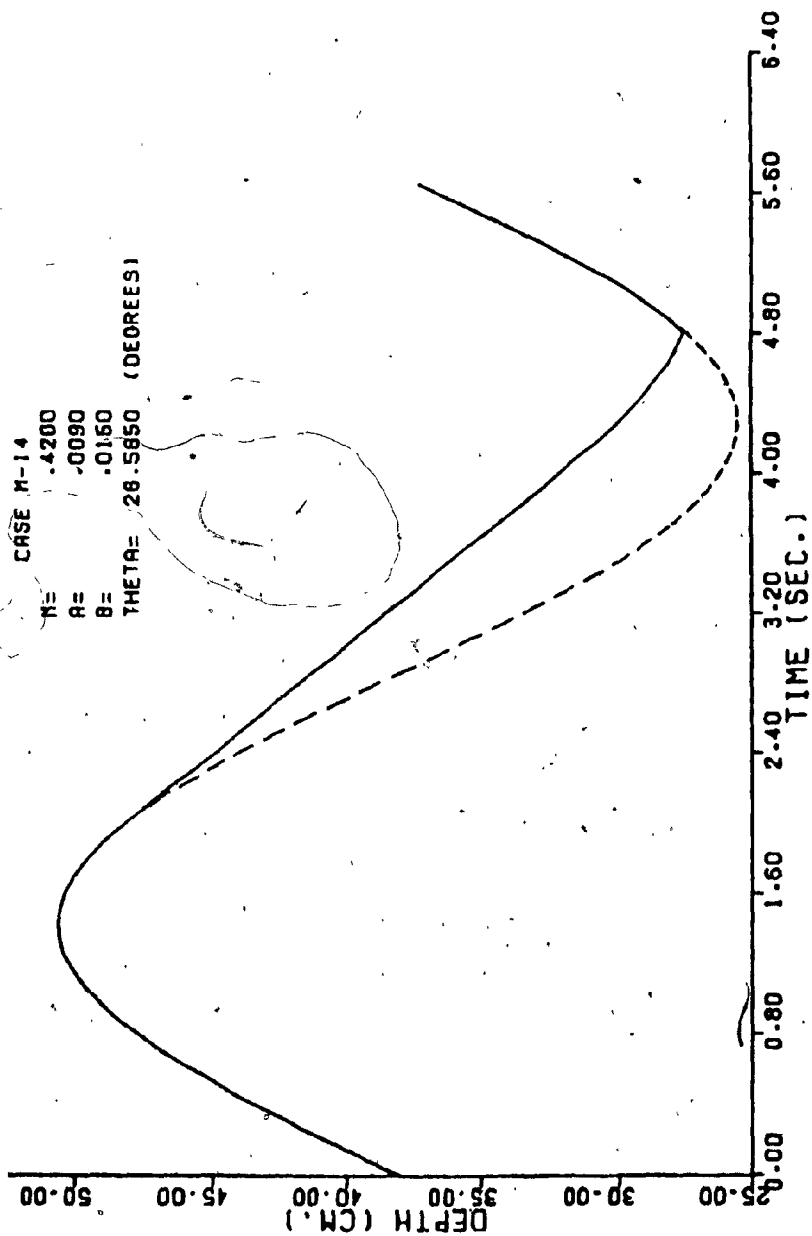
DEPTH (CM.)

TIME (SEC.)

CASE M-14

N= .4200
A= .0090
B= .0160
THETA= 28.5850 (DEGREES)

DEPTH (CM.)

TIME (SEC.)

Fig. A.5. Outcrop Point Movement for δ=30.4

CASE G-6

M=   .4820
A=   .0170
B=   .0330
THETA= 90.0000 (DEGREES)

DEPTH (CM.)

8.00   16.00   24.00   32.00   40.00   48.00

TIME (SEC.)

0.00   0.20   0.40   0.60   0.80   1.00   1.20   1.40   1.60

Fig. A.6. Outcrop Point Movement for δ= 40.

CASE C-4
M=   .4320
A=   .0090
B=   .0160
THETA= 90.0000 (DEGREES)

DEPTH (CM.)

TIME (SEC.)
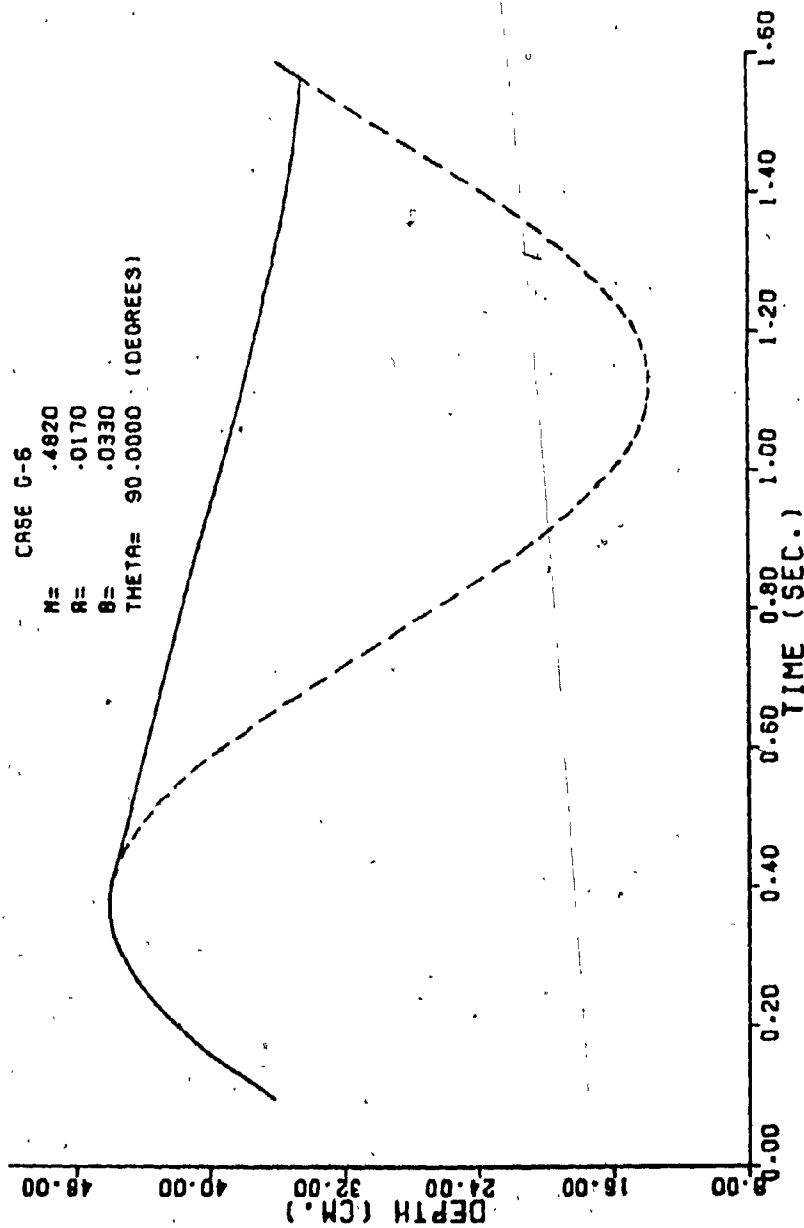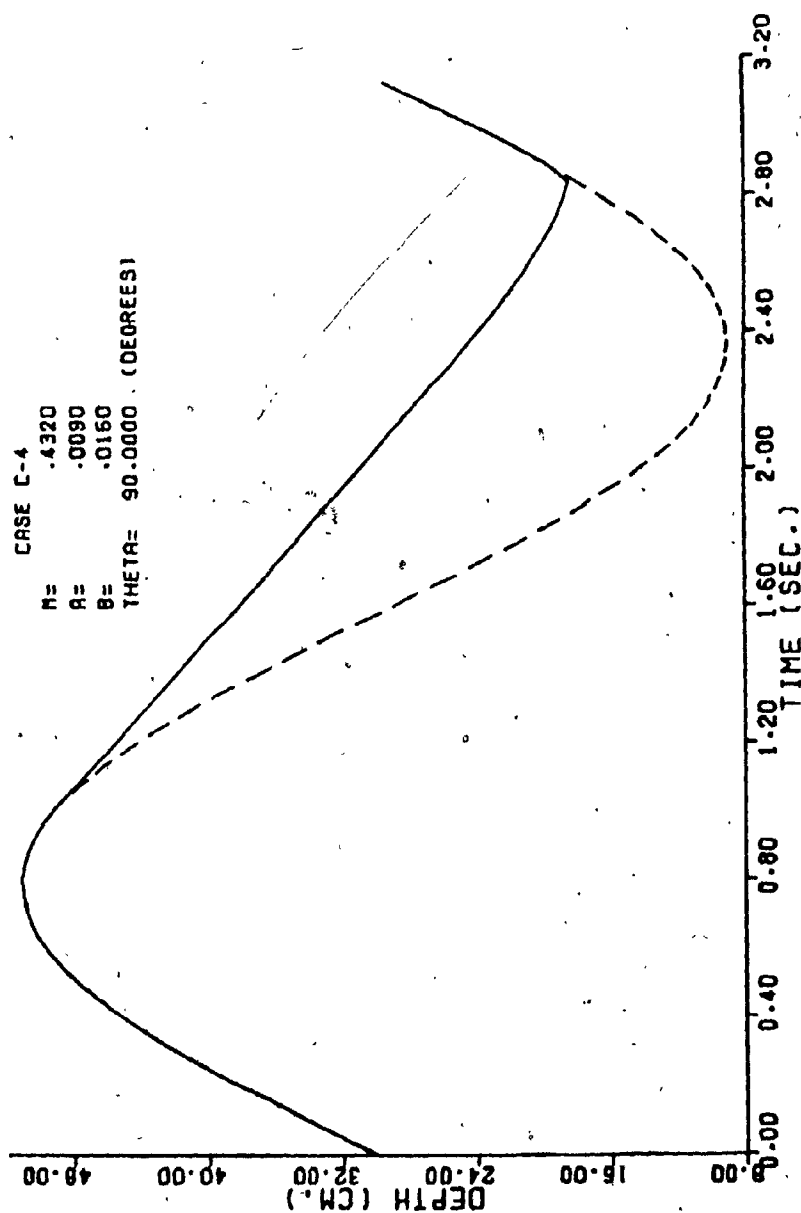
Fig. A.7. Outcrop Point Movement for δ= 56.

Fig. A.8. Outcrop Point Movement for δ=143.

CASE A-2

M=   .4900
A=   .0040
B=   .0050
THETA= 90.0000 (DEGREES)

DEPTH (CM.)

TIME (SEC.)

Fig. A.9. Outcrop Point Movement for δ= 305.

CASE H-2

M= .4860
A= .0170
B= .0330
THETA= 90.0000 (DEGREES)
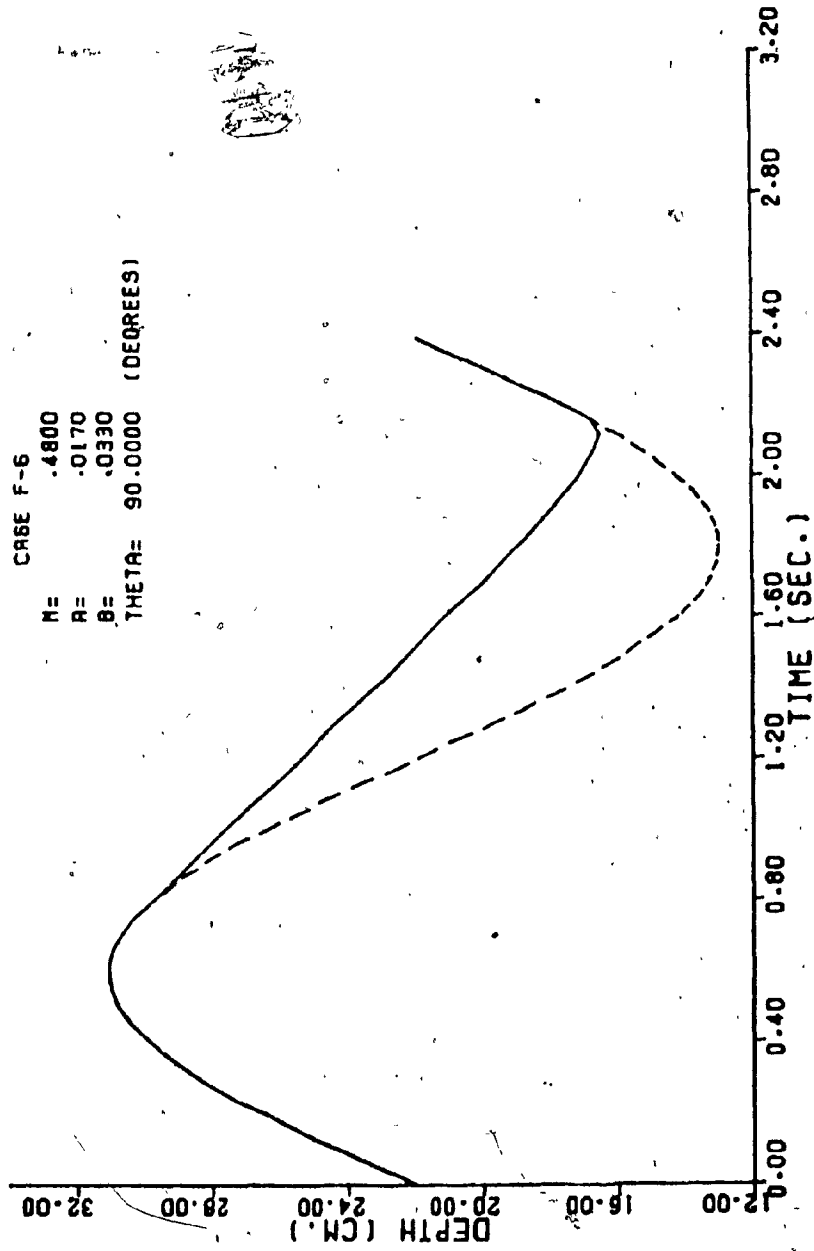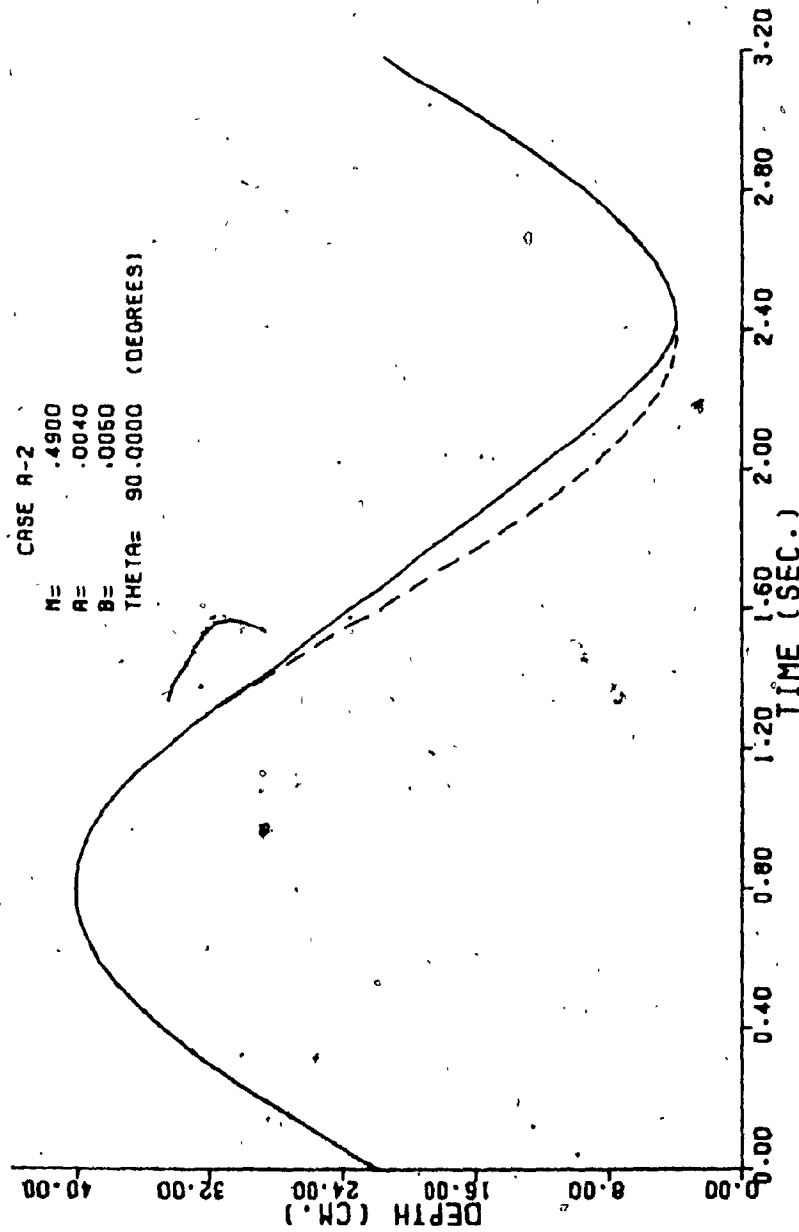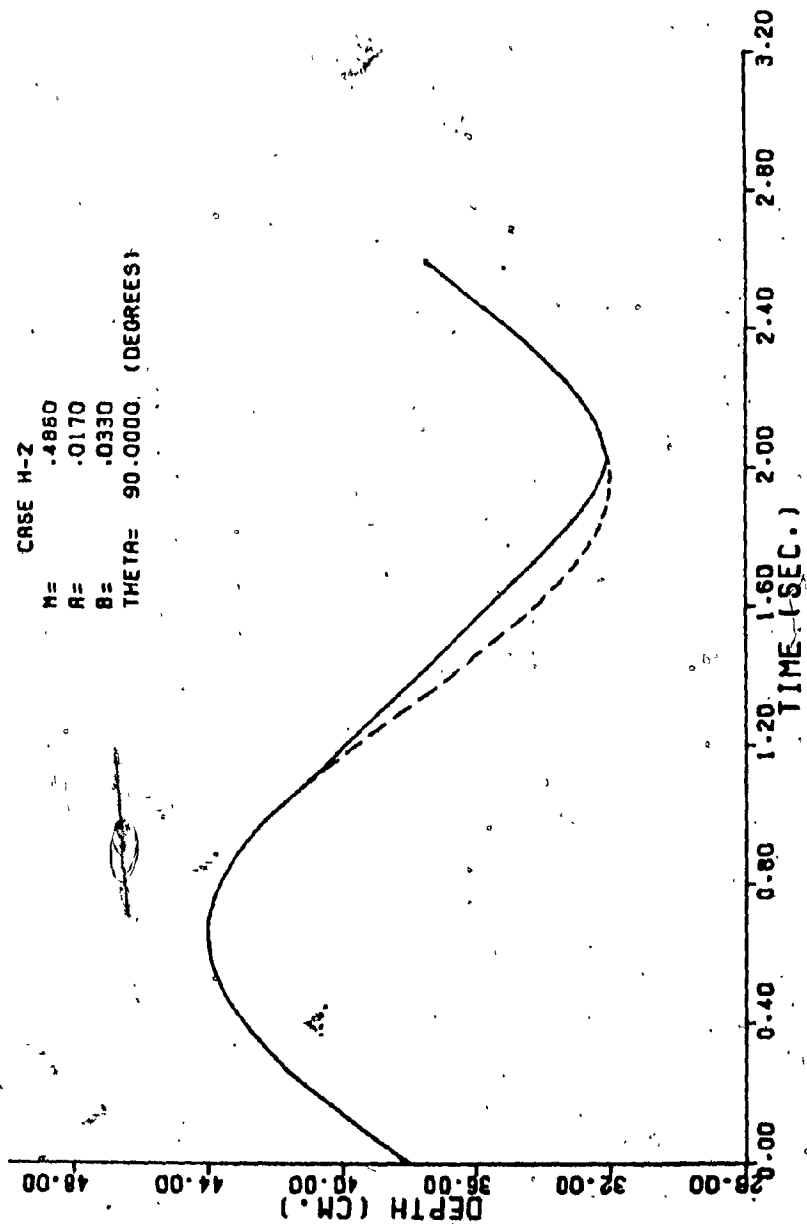
Fig. A.10. Outcrop Point Movement for δ= 702.

CASE H-9

M= .4860
A= .0170
B= .0930
THETA= 90.0000 (DEGREES)
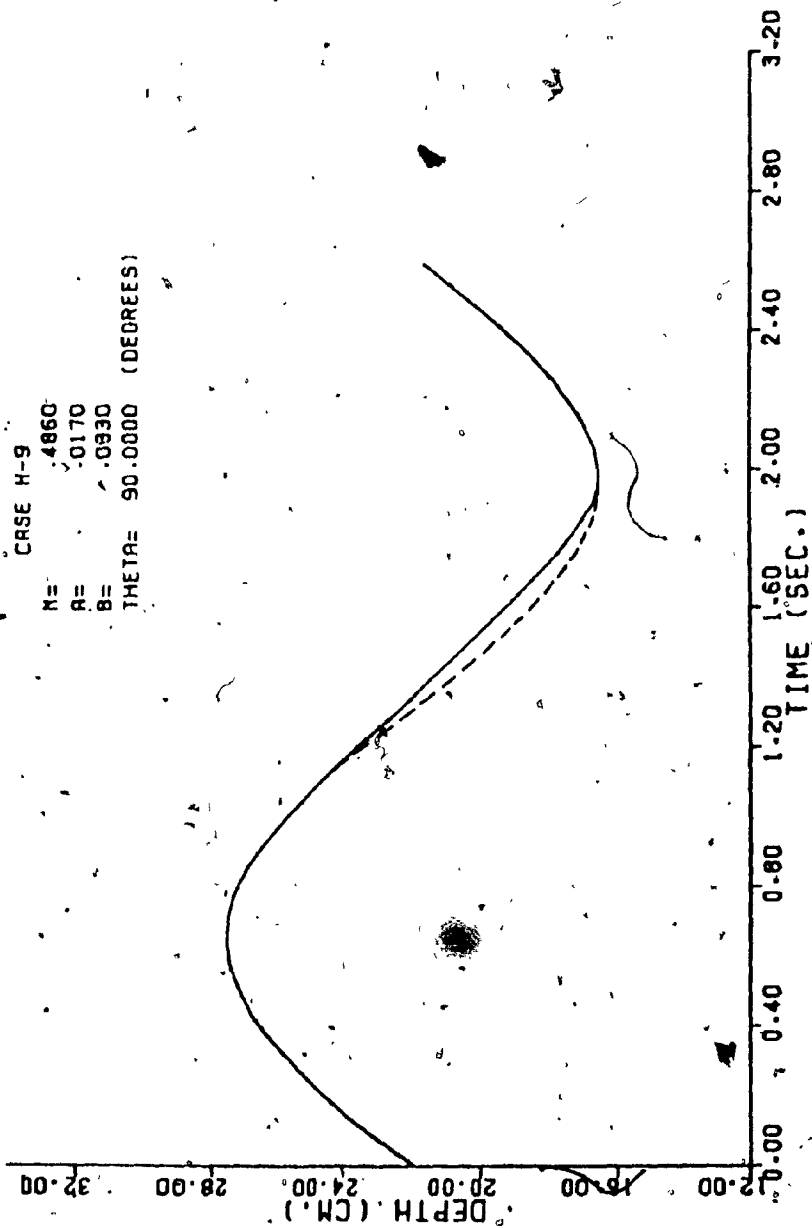
Fig. A.11. Outcrop Point Movement for δ=.1221.

DEPTH (CM.)

TIME (SEC.)

CASE I-6

M=   -.3760
A=   .0100
B=   .0210
THETA= 90.0000   (DEGREES)

DEPTH (CM.)

TIME (SEC.)

0.00   0.80   1.60   2.40   3.20   4.00   4.80   5.60   6.40

8.00   16.00   24.00   32.00   40.00   48.00
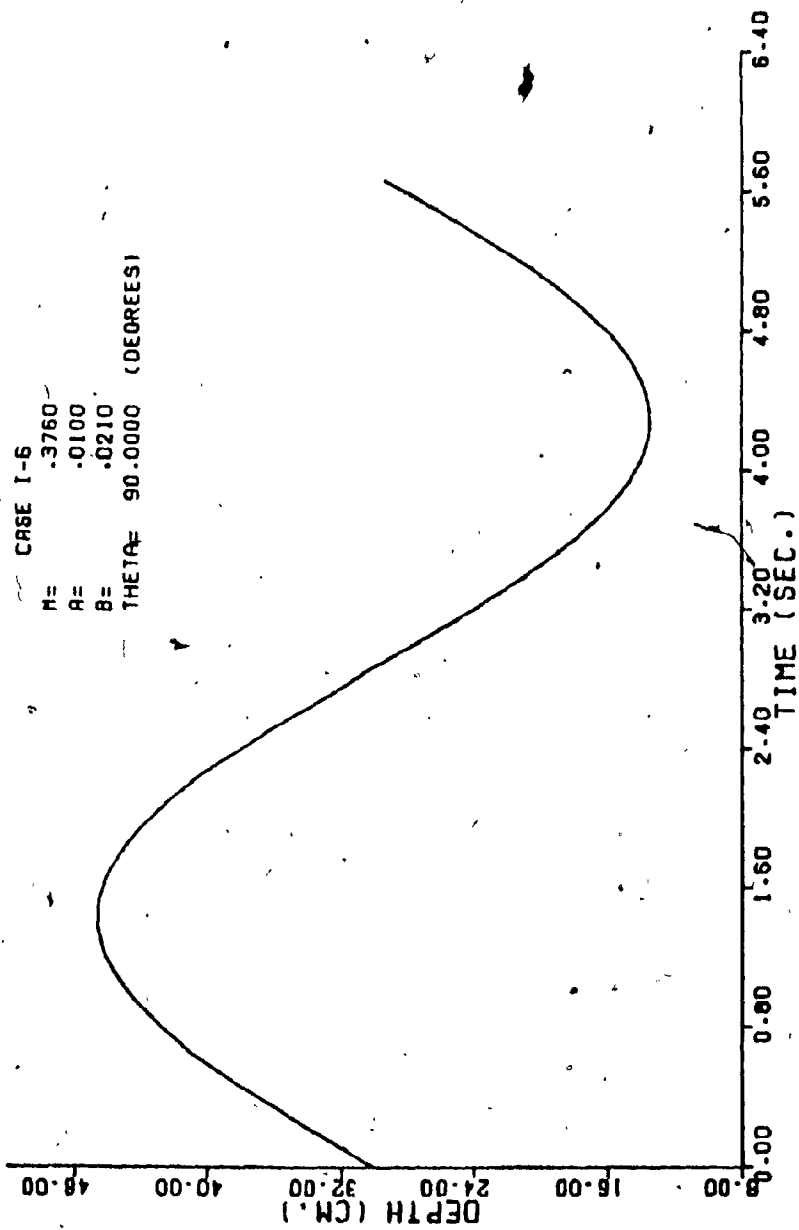
Fig. A.12.   Outcrop Point Movement for $P_k = .31\%$

CASE J-3

M=   .3720
A=   .0100
B=   .0210
THETA= 90.0000   (DEGREES)
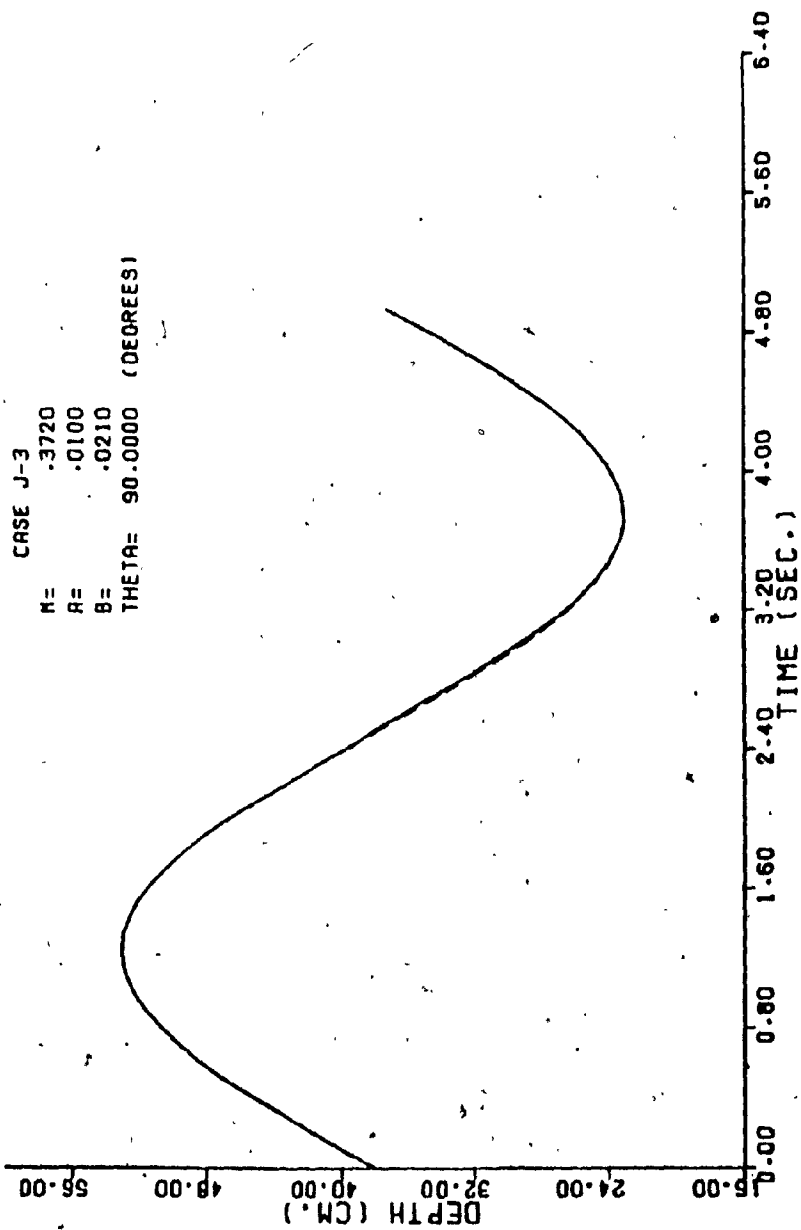
Fig. A.13. Outcrop Point Movement for $P_k = 1.04\%$
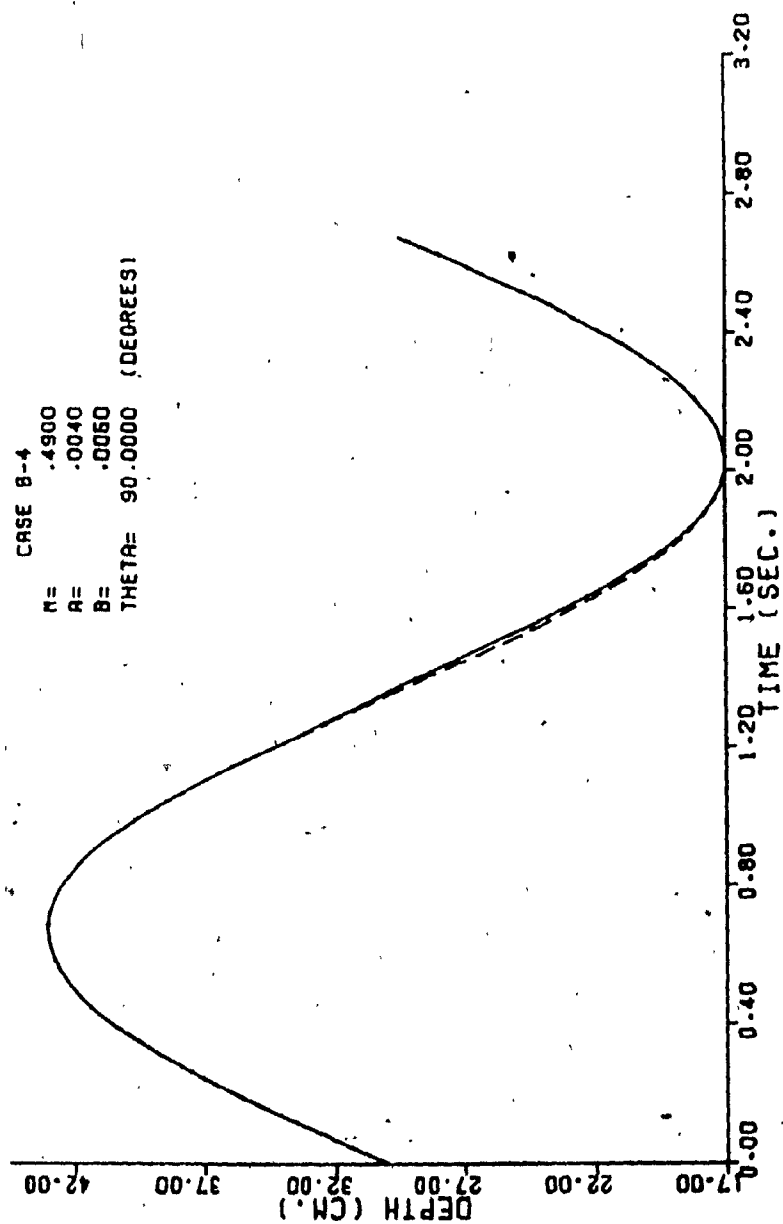
Fig. A.14. Outcrop Point Movement for $P_k = 1.85\%$

CASE B-4

M= .4900
A= .0040
B= .0060
THETA= 90.0000 (DEGREES)

CASE L-8

M= .4600
A= .0040
B= .0060
THETA= 26.5850 (DEGREES)
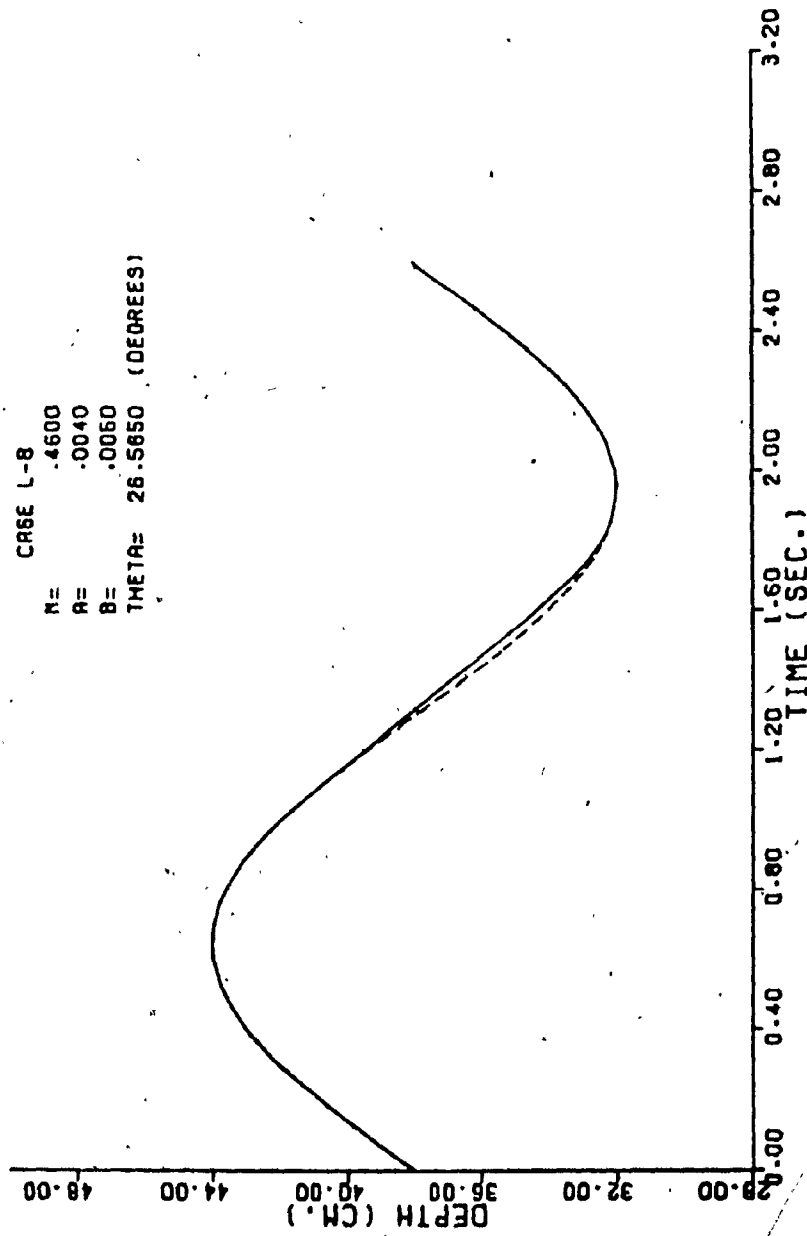
Fig. A.15. Outcrop Point Movement for $P_k = 3.5\%$

the accuracy of the components and the method of interpreting a point. Nevertheless, the solution can usually be read accurately to four decimal places. This is more than adequate for comparison with numerical and analytical solutions.

6. Comparison of Results

Meaningful comparison of the methods is best based on the point where the Y_c curve meets the Y_f curve. The analog solution yields one distinct point of intersection because of the continuous nature of the solution whereas the numerical and analytical methods provide solutions at distinct points which may or may not be the points of intersection. The step sizes for the digital methods were determined such that about 51 points would represent the total outcrop point curve (this provided a convenient graphical plot on an 8 1/2 by 11 sheet of paper). For example, fast drop cases with periods of 5.0 and 1.7 seconds would have print-out step sizes of .1 and .035 seconds respectively. Therefore, most of the discrepancies between the analog and digital techniques can be attributed to this factor of uncertainty of the digital intersection point. The Runge-Kutta method used has some inherent errors due to approximation but these are of the order of Δh^4. The actual step size Δh was always less than .01 so that these errors are negligible. The analog errors can generally be attributed to the accuracy of the components (.1 - 1%) and in the proper scaling of the recording device. A 2 - 4% error may be expected.

A brief comparison of seven cases studied shows the mean, standard deviation and the correlation coefficient for the intersection points by the analog, analytic and numeric techniques. The correlation coefficient suggests

a good correlation between the three methods even though some cases showed a wide variance (Table A.1).

In review, the analog yielded the best graphical solutions (i.e. provided the superimposed curves) whereas the numerical solution provided discrete points. The analytic solution would be most useful if one part of the curve needed to be studied more closely. The approximate solution would yield a good first approximation of the differential damped portion of the curve. Each method contributes worthwhile information to the study of the outcrop point movement.

TABLE A.1

COMPARISON OF ANALOG, ANALYTIC AND NUMERIC ANALYSIS FOR POINT t_c

Case Studied	Period (T)	Method	Coordinates		Mean and Std. Dev.		Correlation Coefficient (R)
			Time (t_c)	Depth (y)	Time (t)	Depth (y)	
B-1	1.4	Analog	1.338	34.970	1.339	34.190	.7165
		Analytic	1.330	32.925	.010	1.106	
		Numeric	1.350	34.676			
C-1	2.5	Analog	1.825	13.650	1.856	13.568	-.8989
		Analytic	1.875	13.552	.027	.076	
		Numeric	1.869	13.501			
N-7	2.52	Analog	2.550	22.730	2.534	22.662	.9542
		Analytic	2.495	22.177	.034	.454	
		Numeric	2.556	23.078			
A-2	3.2	Analog	2.350	3.150	2.417	3.787	.9943
		Analytic	2.460	4.142	.058	.553	
		Numeric	2.440	4.070			
0-4	3.28	Analog	3.450	48.130	3.400	45.286	.9988
		Analytic	3.313	39.821	0.760	4.734	
		Numeric	3.439	47.907			
D-6	3.6	Analog	2.910	15.300	2.921	15.326	.9996
		Analytic	2.916	15.312	.015	.035	
		Numeric *	2.9385	15.366			
D-7	5.5	Analog	4.400	4.500	4.205	4.195	.9762
		Analytic	4.125	4.050	1.455	.264	
		Numeric	4.180	4.036			

APPENDIX B

ANALOG SOLUTION OF OUTCROP POINT MOVEMENT

APPENDIX B

ANALOG SOLUTION OF OUTCROP POINT MOVEMENT

Programming the outcrop point problem on the analog computer required special circuit diagrams, digital logic, scaling and various other steps. This appendix recapitulates the basic steps involved in setting up the problem.

A. SYSTEM EQUATIONS AND DIAGRAMS

Three basic equations comprise the generation of the outcrop point curve: (the parameters were previously defined)

$$Y_f = h_0 + A_0 \sin(\omega t) \quad \dots \dots \dots \dots \dots \dots \dots \text{(b.1)}$$

$$Y_1 = h_0 + A_0 \sin(\omega t_1) + V(t-t_1) \quad \dots \dots \dots \dots \dots \text{(b.2)}$$

$$\ddot{Y}_c = (a_1 + b_1|\dot{Y}_c|)Y_c + \delta Y_c = \delta f(t) \quad \dots \dots \dots \dots \text{(b.3)}$$

Figure B.1 shows the complete analog diagram which incorporates the above equations. To obtain one continuous curve, digital logic was required to operate the two track/store devices and three comparators. The first equation was simulated by the components in box A (Fig. B.2). At the first time constant, t_1, the value of Y_f was stored and the multiplying circuit (box B) took over to simulate equation (b.2). At the second time constant, t_1, the value of Y_1 was stored and the second-order differential
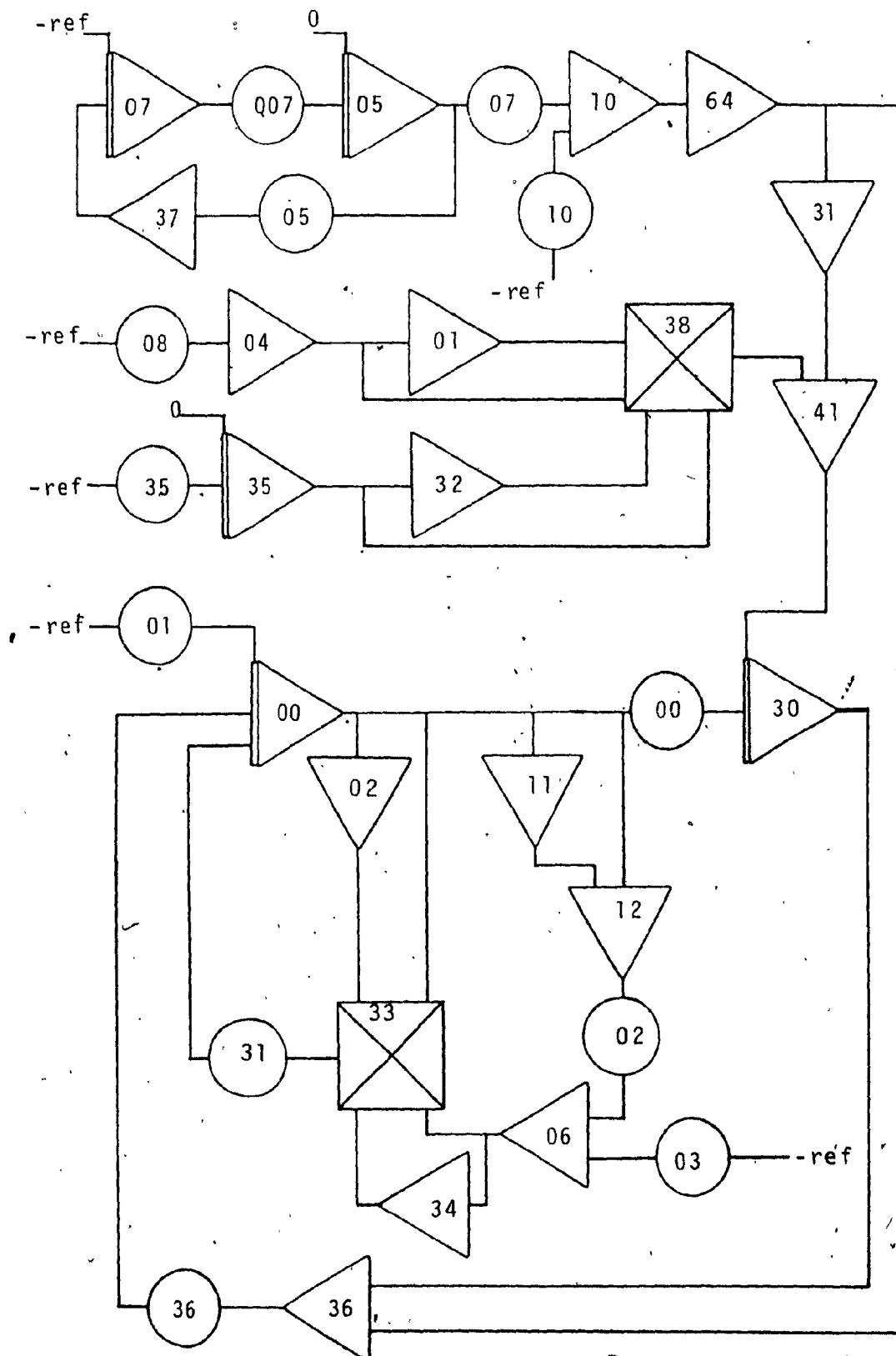
Fig. B.1 Analog Circuit Diagram for Outcrop Point Movement
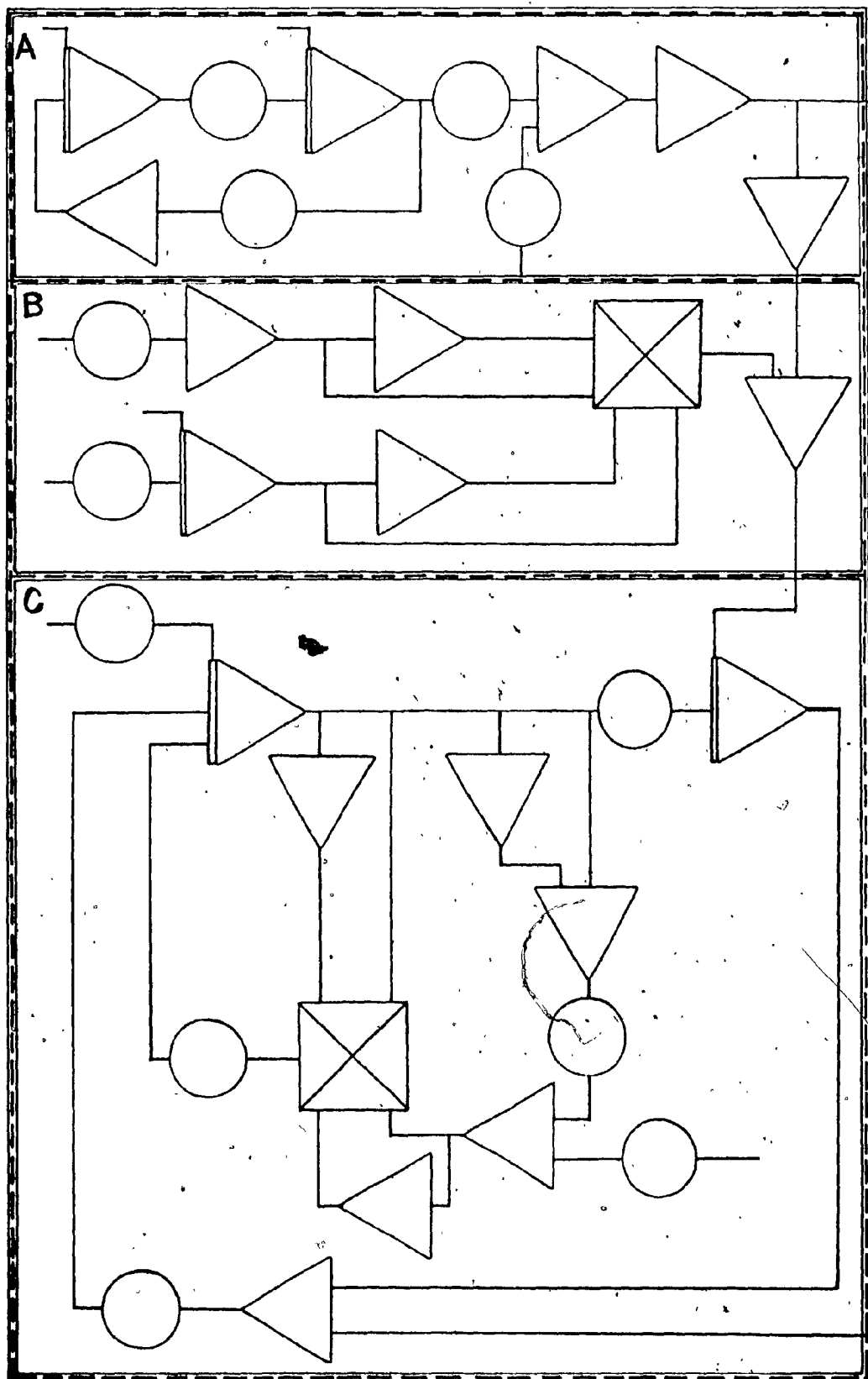
Fig. B.2   Components of the Outcrop Point Equations.

damping circuit (box C) began operating. A comparator was used to compare the signals out of amplifiers A65 and A30 so that when the value of Y_f was greater than Y_c, the first equation took over once again (Fig. B.3). This represented the rising water wave.

B. DIGITAL LOGIC

Figure B.3 shows the basic logic diagram to control the operation of the computer. Two additional comparators were needed to ensure switching at the proper time constants. The logic hardware to operate the amplifiers (i.e., A00, A30, A35) and the track/stores (i.e., T31, T41), has two holes: one for initial conditions (IC) and the other for operate (OP). When the OP lead is high, the amplifier goes into the operate mode. This is essential for the differential damping circuit where integrators A00 and A30 should not operate before the second time constant t_1.

C. AMPLITUDE SCALING

Analog computers have a range of 10 volts reference (sometimes 100 volts) but the variables are scaled to values in machine units (1 machine unit = reference voltage). The original differential equation was modified after introducing the appropriate scale factors to yield:

$$\ddot{Y}_c = -\frac{1}{K_1}\left(a_1 + \frac{b_1}{K_1}\mid K_1\dot{Y}_c\mid\right)K_1\dot{Y}_c - \frac{\delta}{K_0}\left(K_0 Y_c - K_0 Y_f\right) \quad \ldots \ldots \text{(b.4)}$$

where $K_1 = (1 \text{ machine unit})/(\dot{Y}_{c\,max})$

  $K_0 = (1 \text{ machine unit})/(Y_{c\,max})$

K_0 and K_1 were determined automatically within the general program developed after it was noted that $\dot{Y}_{c\,max} = V$ and $Y_{c\,max}$ is always less
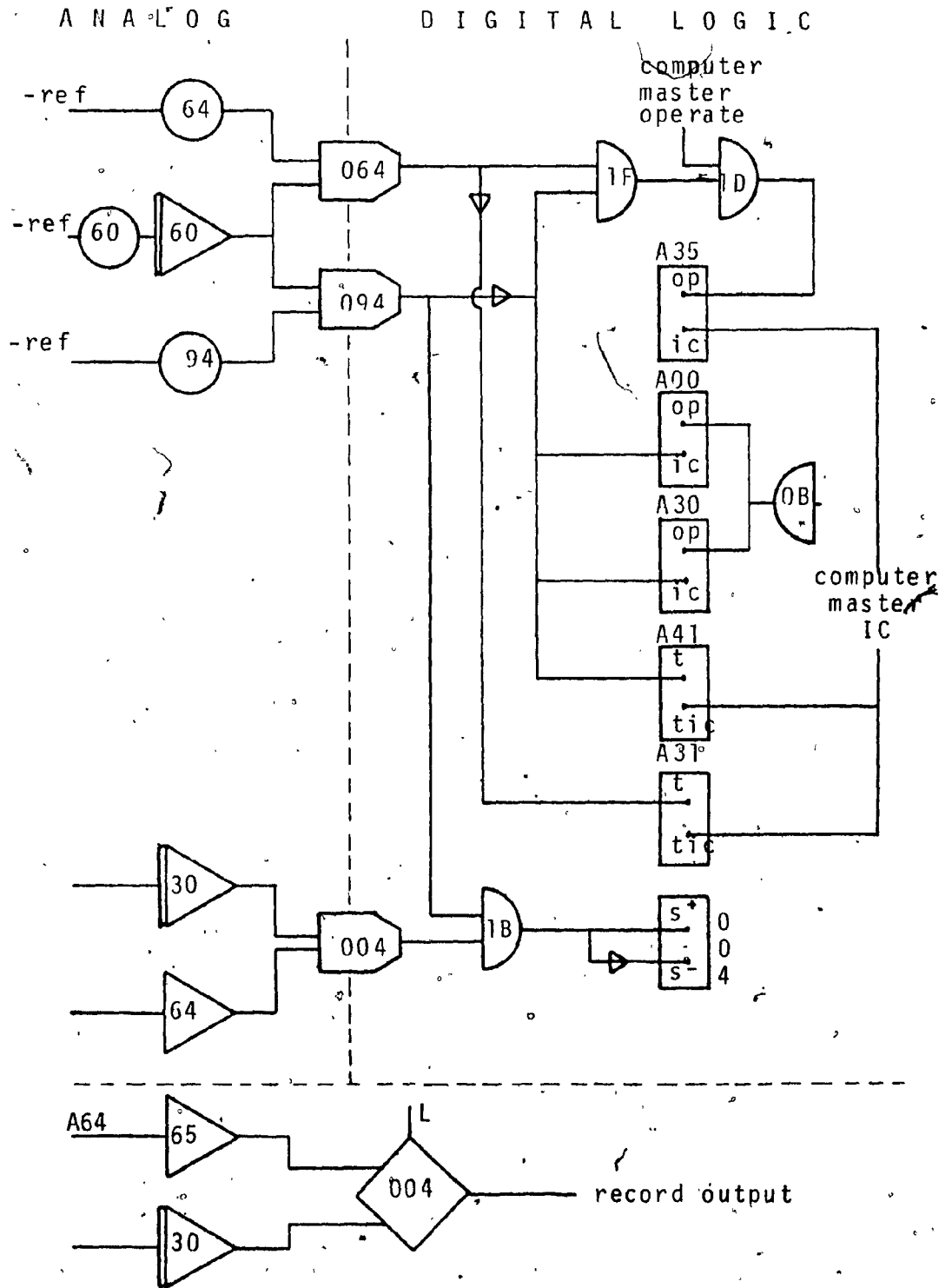
Fig. B.3 Digital Logic Diagram

than $h_0 + A_0$. To be on the safe side, the values of K_1 and K_0 were determined respectively as:

$$K_1 = 1/\left(INT((V + 7.5)/5*5\right) \qquad \ldots \ldots \ldots \ldots (b.5)$$

$$K_0 = 1/\left(INT((h_0 + A_0 + 5)/5)*5\right) \qquad \ldots \ldots \ldots \ldots (b.6)$$

(INT is the integer value of the number).

D. TIME SCALING

The generalized form of a linear second order differential equation (similar to the non-linear equation (b.3) is given as:

$$\ddot{Y} + 2\alpha\omega_n \dot{Y} + \omega_n^2 Y = \omega_n^2 f(t) \qquad \ldots \ldots \ldots \ldots (b.7)$$

where

α = damping ratio

ω_n = undamped natural frequency

$\omega = \omega_n \sqrt{1-\alpha^2}$ damped natural frequency of oscillation

Equations with ω_n in the range $0.1 < \omega_n < 10$ usually have solution rates suitable for recording on strip chart and X-Y recorders. For systems outside of this range, a time scale factor, β, should be chosen such that $0.1 < (\omega_n/\beta) < 10$.

The integration rate is proportional to the gain of the integrator. Therefore, time scaling is simply a gain-adjusting operation for all the integrators by the same amount $(1/\beta)$. When $\beta = 1$, computer time and real time are one and the same; when β is smaller than unity, the solution rate is speeded up; when $\beta > 1$ the solution rate is slowed down.

Comparing equations (b.3) and (b.4), it can be seen that $\omega_n = \sqrt{\delta}$ and therefore the following time scaling constants were used:

$$0 < \delta < 81 \qquad \beta = 1$$
$$81 < \delta < 4000 \qquad \beta = 10$$
$$\delta > 4000 \qquad \beta = 100 \qquad \dots\dots\dots : \quad \text{(b.8)}$$

It is to be noted that time scaling was only required for the second order differential damping segment of the system. The frequency of the rest of the system was dictated by the frequency term, ω, in the forcing function $Y_f = h_0\, A_0 \sin(\omega t)$. No time scaling was necessary here since the frequency was always less than 10 cps.

E. ADDITIONAL SCALING

Reasonable potentiometer settings are in the range of .05 to .95. Two pot settings created additional problems in that their values were always much greater than unity. The first pot in question, P36, had a value of $\dfrac{\delta}{\beta}\dfrac{K_1}{K_0}$ which varied enormously since δ varied from 4 to 111,000. Also pot P03 proved troublesome with a setting of b_1/K which yielded values ranging from 20 to 115. To circumvent these problems, these pots were reduced to settings less than unity and then the appropriate gains on amplifiers A00 and A30 were adjusted. Integrators have gains of 1 and 10 but in the digital logic there is space provided for pins which when inserted into the F slot, increases the gain by 10, into the MS slot increases the gain by 1000, and into both slots increases the gain by 10,000. This was very important in the scaling of the circuit. Table B.1 shows examples of scaling for a wide range of δ values.
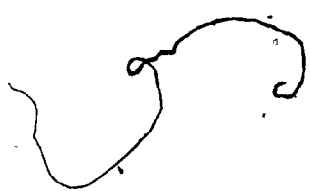
TABLE B.1
SAMPLES OF ANALOG SCALING OF P36 AND PO2

Case Studied	β	δ	Pot Settings		Gains From		Pins On	
			P36	PO2	P36	PO2	A00	A30
B-1	1	37	70	41	10	10	F	–
J-5	1	75	165	72	–	1/10	MS	–
D-6	10	158	32	68	–	–	MS	F
F-5	10	426	.99	112	–	10	MS	F
C-1	10	1075	151	69	10	–	MS	F
H-10	10	1222	180	115	–	–	F-MS	F

F. STATIC CHECK

Before running any problem on an analog computer, a static check was performed to see that the analog components functioned up to par. Basically, this involved putting arbitrary values on the pots and following the circuit to check what theoretical outputs could be expected at any amplifiers. These calculated values were then checked against the outputs measured on the analog computer while in the static test mode. The programmer could thereby determine whether certain components were faulty or locate an error in patching. Table B.2 and Fig. 4 show the calculations of a sample static check.

The beauty of the analog computer becomes evident once the circuit is in operation. The programmer can tap the solution at any point in the system, freeze the system and note the values at all points in the system, and modify the parameters to search for an optimal solution. Although the solution is restricted to a scaled four-digit accuracy, that is sufficient for most preliminary engineering analysis or design.

TABLE B-2
SAMPLE STATIC CHECK

Amplifier	Function	Calculated Values		Measured Values	
		Derivative	Amplifier	Derivative	Amplifier
A00	integ	.3400	.5000	.3413	.5000
A01	inv		-.2000		-.2000
A02	inv		-.5000		-.5000
A04	inv		.2000		.2000
A05	integ	.5000	.0000	.5023	.0000
A06	sum		-.2500		-.2500
A07	integ	.0000	1.0000	.0001	.9999
A10	sum		.3000		.3000
A30	integ	.3000	-.2500	.3013	-.2500
A31	inv		.0000		.0000
A32	inv		.0000		.0000
A33	mult		-.1250		-.1255
A34	inv		.2500		.2501
A35	integ	-.1000	.0000	-.1004	.0000
A36	sum		.5500		.5500
A37	inv		.0000		.0000
A38	mult		.0000		.0001
A41	sum		.0000		.0000
A60	integ		.0000		.0000
A64	inv		-.3000		-.3000

integ = integration

inv = inversion

mult = multiplication

sum = summation
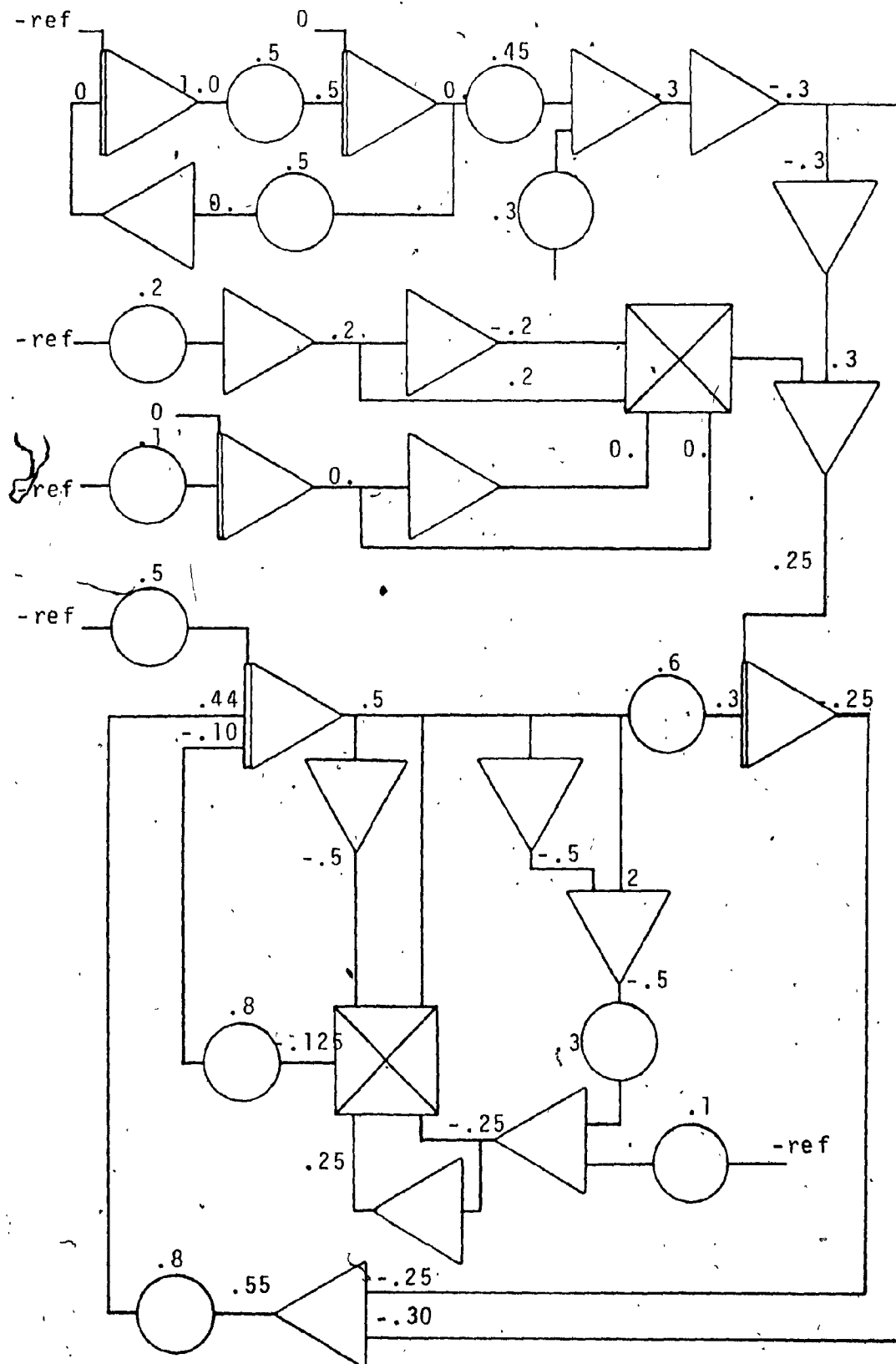
Fig. B.4 Static Check Circuit Diagram

APPENDIX C

A NOTE ON ANALOG AND ANALOG/HYBRID COMPUTERS [27, 28, 44]

APPENDIX C

A NOTE ON ANALOG AND ANALOG/HYBRID COMPUTERS [27, 28, 44]

Electronic differential analyzers (EDA) commonly referred to as analog computers comprise only a small segment of the vast analog simulation field. Most people are familiar with scale models and their value in estimating real conditions. Special purpose mathematical models are often confined to research where the governing equations of one physical system are used to simulate another system. Electronic analog computers are classified as general purpose because of their more inherent mathematical nature (Fig. C.1).

Analog computers, as referred to in this thesis, implement mathematical relations between physical variables with electronic computing elements that operate simultaneously. Each element can perform a mathematical operation such as addition, subtraction, multiplication, division, and integration with respect to time. The solutions are measured voltages at any point of interest within a circuit. A circuit or program is established by interconnecting various computing elements with wires called "patch cords".

Analog computers exhibit many features that render it suitable for simulation. There is a close correspondence between the real and the simulated problem not only in the solution but in the solution technique.
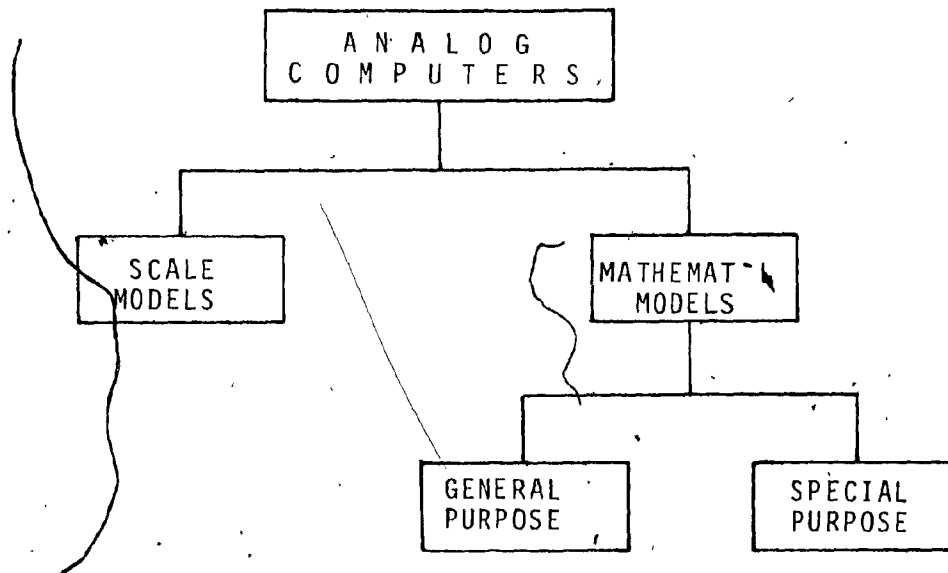
Fig.C1.a   Computation by Analogy
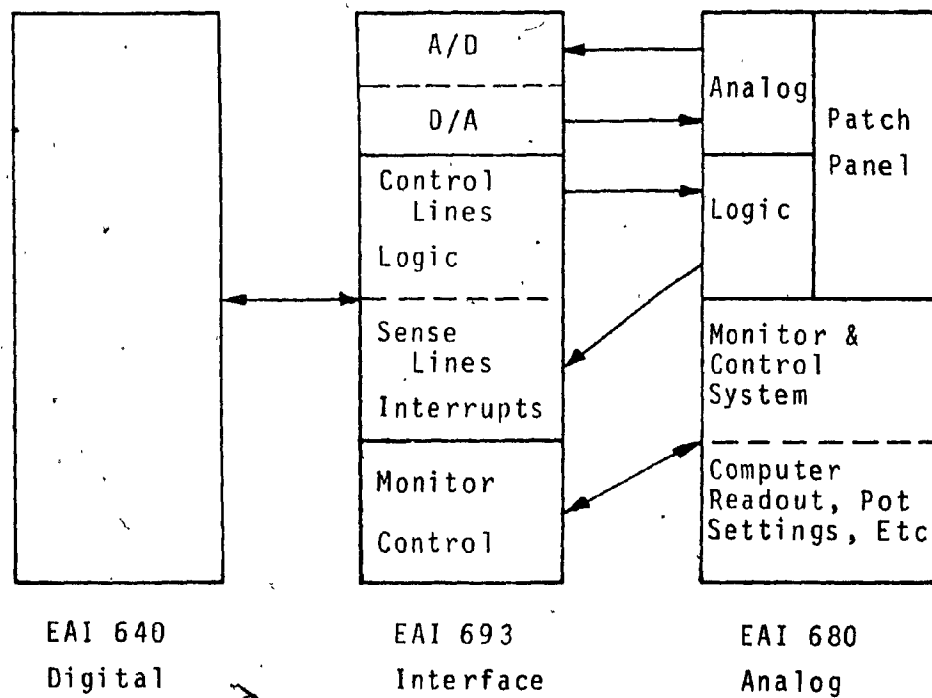
Fig.C1.b   EAI 690 Hybrid Computer System

The components of the system operate in parallel and thus the answers are immediately available. Corrections and adjustments to parameters are easily made, thereby enhancing the flexibility of man-machine interaction. The integrating capability and the continuous nature of output are important advantages for analog computers.

Despite its advantages, the analog computer has lost ground to the digital computer because it is not as accurate (limited to .01% for each elementary operation), it is defficient in memory storage and it lacks the capability to perform logic operations. Hybrid computers have combined the advantages of both computers, ie. accuracy, memory, programmability, speed, flexibility, and decision making capability. They have sophisticated interface systems that not only transfer analog and digital signals but allow the digital program to control the analog system. Perfunctory manual operations are executed automatically, such as setting pots. The digital program could also control successive simulation runs with recorded results, optimizing parameters during the runs, etc.

The hybrid computer is an invaluable simulation tool. Once the basic components are understood, they are not too difficult to program. The rest of this Appendix describes the basic analog and hybrid components found on the EAI 690 which was used in the present study.

References 4, 12, 13, 14, 21 and 61 can be consulted to get further descriptions of the components described below.

ANALOG COMPONENTS

1. Potentiometers (Pots) (Fig. C.2)

Pots are used to multiply a given voltage by a constant between zero and unity. They consist of a resistance with one end grounded and a sliding contact. They have a resolution of 0.01 per cent and can thus be set to four decimal digits. Pots can be either hand-set or servo-set, ie. set by a servo-mechanism within the analog computer. It is recommended maintaining pot values between 0.25 and .80.

2. Operational Amplifiers (Fig. C.3)

The operational amplifier is the basic functional unit in an electronic analog computer. The fundamental equation governing the output of an operational amplifier is:

$$V_o = - Z_f \cdot \frac{V_i}{Z_i} \qquad \dots \dots \dots \dots \dots (C.1)$$

where Z_i = input impedance

Z_f = feedback impedance

V_i = input voltage

V_o = output voltage

By varying the input and feedback impedances, the output is forced to behave in some desired way. These operational amplifiers find application in inverters, summers, integrators, high-gain amplifiers and track/store units. They will automatically invert the sign of an input voltage.
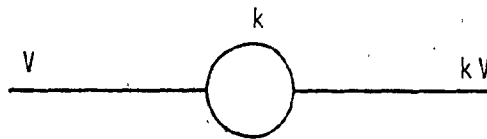
Fig. C.2   Potentiometer Symbol
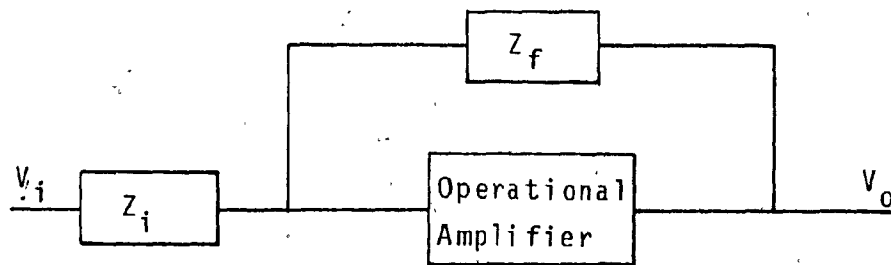
Fig. C.3.   Operational Amplifier Circuit
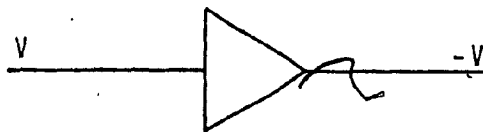
Fig. C.4.   Inverter Symbol
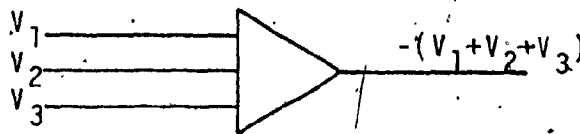
Fig. C.5.   Summer Symbol

3. <u>Inverters (Fig. C.4)</u>

Inverters change the sign of the incoming voltage(s) and can thus be used for subtraction, ie. a voltage is inverted and then added to other voltages.

4. <u>Summers (Fig. C.5)</u>

Summers will algebraically sum the incoming voltages and invert the sign. Most summers have up to six inputs with gains of 1 and 10. These components are controlled to give four-figure accuracy.

5. <u>High Gain Amplifiers (Fig. C.6)</u>

These are basically summers with their feedback resistances removed. They are only used when external feedback is provided. The output voltage is such that the sum of the input voltages must be equal to zero.

6. <u>Integrators (Fig. C.7)</u>

This component differs from a summer in that its feedback component is a capacitor instead of a resistor. It will integrate a sum of voltages and invert the sign. It is, therefore, of immense value in solving differential equations. The EAI 680 is equipped with four different feedback capacitor values for every integrator. This is useful in solving problems with a wide range of time constants, for high-speed repetitive and iterative operation, etc. The integrator can be charged to an initial voltage to represent the initial conditions of the differential equation.

7. Multipliers (Fig. C.8)

The two most common methods of multiplying voltages in general-purpose analog computers are servo-multiplication and quarter-square, biased-diode multiplication.

Servo-mechanisms are closed loop control devices that control in accordance with input signal loads that are coupled to the output. They are basically following devices that must respond quickly and precisely to changes in inputs. A servomultiplier is an electromechanical servo which provides products of analog variables.

The EAI 680 uses quarter-square multipliers. The name stems from the identity:

$$xy = \frac{1}{4}\left[(x+y)^2 - (x-y)^2\right] \qquad \dots \dots \dots \dots \dots (C.2)$$

The quarter-square multiplier contains two squaring networks: one to generate the first term on the right hand side of the identity and the other to generate the second term. This requires four input signals ($\pm x$, $\pm y$) to satisfy all possible outputs. The output signal may or may not be inverted depending on the arrangement of the input signals.

8. Track/Store Device (Fig. C.9)

This device provides some memory capability to the analog compu-ter. It is controlled by digital logic in such a fashion that it behaves as a regular summer while in the tracking mode and holds the output con-stant in the store mode. Arbitrary initial conditions can be inputted.

$$V_1, V_2, V_3 \qquad (V_1 + V_2 + V_3 = 0)$$
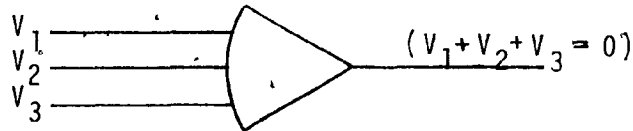
Fig. C.6. High Gain Amplifier Symbol

$$V_{ic}, \quad \dot{V} \qquad -V_{ic} - \int_0^{\tau} V d\tau$$
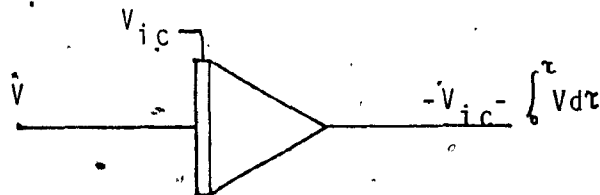
Fig. C.7.   Integrator Symbol

$$X, \ -X \qquad \pm xy$$
$$y, \ -y$$
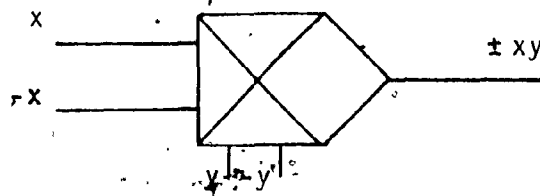
Fig. C.8. Multiplier Symbol

$$V \qquad TS \qquad -V$$
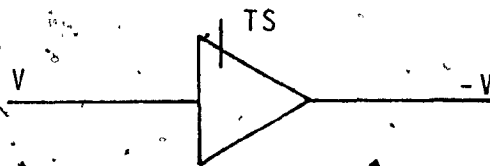
Fig. C.9.   Track/Store Symbol
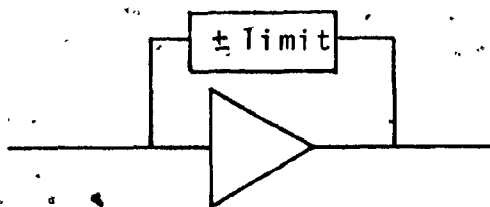
$$\pm \text{limit}$$

Fig. C.10. Limiter Symbol

9. Limiters (Fig. C.10)

This device basically sets a range in which the output voltage can exist. It is helpful in ensuring a circuit does not overload or in finding absolute values of voltages.

DIGITAL LOGIC ELEMENTS

1. Comparator (Fig. C.11)

The comparator compares the sum of two analog voltages and produces a high digital output signal (binary 1) when their sum is positive and a low signal (binary 0) when their sum is negative. In the outcrop problem, comparators were used to control the timing sequence and yield a continuous curve.

2. Digital Inverter (Fig. C.12)

This component produces the binary complement of the input digital signal, ie. when the input is high, the output is low and vice versa.

3. And Gate (Fig. C.13)

The And gate performs the fundamental logic multiplication operation. Both inputs must be high for the output to be high. Either the direct or the inverted output may be selected.

4. Digital-Analog Relay Switch (Fig. C.14)

This provides for the logical switching of two analog inputs. A high digital signal closes the switch and a low signal opens the switch. The logic control input is terminated on the digital patch panel.

Fig. C.11. Comparator Symbol

Fig. C.12. Digital Inverter Symbol
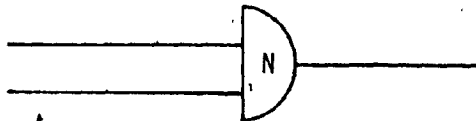
Fig. C.13. And Gate Symbol
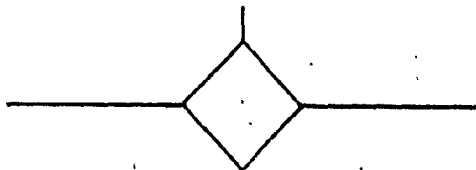
Fig. C.14. Relay Switch Symbol

(Note: N denotes address)

INTERFACE COMPONENTS (Fig. C.15)

1. Senselines

Senselines are flip-flops controlled by digital logic signals on the analog console that can be interrogated by the digital computer.

2. Control Lines

Control lines represent flip-flops located on the analog-logic panel that can be set and reset by the digital computer.

3. Analog/Digital (A/D) Converters

Analog/Digital converters are devices which translate pulses having an amplitude proportional to an analog voltage into the binary-coded equivalent of this amplitude.

4. Digital/Analog (D/A) Converters

Digital/Analog (D/A) Converters are devices which accept input data in binary form and generate an analog voltage proportional to the binary number.

5. Interrupts

Interrupts serve almost the same purpose as the sense-lines. When the input generated is high, an interrupt is set at the leading edge. Once triggered, the EAI 640 branches to whatever location is specified by the pointer stored in the interrupt trap cell. The users program is executed.

if X = S, then a sense line

= C, then a control line

= I, then an interrupt line

Analog/Digital Converter

Digital/Analog Converter

Fig. C.15.   Interface Symbols

APPENDIX D

COMPUTER PROGRAMS

APPENDIX D

COMPUTER PROGRAMS

Four programs were developed for this study. The first one is a Mimic simulation of the Outcrop Point Movement; however, since certain features of the Mimic package did not work, the results were not reliable and one continuous output curve could not be obtained. The variables used are consistent with those of the study except that P is utilized as the period of oscillation. Sample inputs are given at the end of the listing and include the seven essential parameters, a, b, m, θ, P, A_0, h_0. A partial sample output is included.

The second program, "PROGRAM WAVE", was developed as a substitute for the Mimic program. It is interactive in nature and has various options available to the programmer. The program first determines whether a case is slow or fast drop. If the latter case applies, the program prints out all the pertinent constants and parameters necessary for the analysis of the outcrop point movement, otherwise the program stops. These calculations are determined in Subroutine "Fast". Included in the subroutine is an option to printout the pot settings needed for the analog simulation and the appropriate scale factors. The potentiometer addresses and its corresponding values are printed out.

Subroutine "Differ" contains a Runge-Kutta 4th order technique to solve the second order differential damping equation (region III in Figure A.2, Appendix A) numerically. Only the step size and the printout

APPENDIX D

COMPUTER PROGRAMS

Four programs were developed for this study. The first one is a Mimic simulation of the Outcrop Point Movement; however, since certain features of the Mimic package did not work, the results were not reliable and one continuous output curve could not be obtained. The variables used are consistent with those of the study except that P is utilized as the period of oscillation. Sample inputs are given at the end of the listing and include the seven essential parameters, a, b, m, θ, P, A_0, h_0. A partial sample output is included.

The second program, "PROGRAM WAVE", was developed as a substitute for the Mimic program. It is interactive in nature and has various options available to the programmer. The program first determines whether a case is slow or fast drop. If the latter case applies, the program prints out all the pertinent constants and parameters necessary for the analysis of the outcrop point movement, otherwise the program stops. These calculations are determined in Subroutine "Fast". Included in the subroutine is an option to printout the pot settings needed for the analog simulation and the appropriate scale factors. The potentiometer addresses and its corresponding values are printed out.

Subroutine "Differ" contains a Runge-Kutta 4th order technique to solve the second order differential damping equation (region III in Figure A.2, Appendix A) numerically. Only the step size and the printout

frequency have to be specified.

Subroutine "Analyt" contains the analytic and approximate solutions also corresponding to Region III of the Outcrop Point Movement. A printout of the comparison of the numerical, analytic and approximate solution is optional. The analytic solution is not very accurate for certain sloping cases but is much more accurate than Dracos' solution as given in his paper [10].

Subroutine "Fitcurv" joins the various Regions of the Outcrop Point Movement to yield one complete period of oscillation. The printout of the numerical solution is optional. Two different plotting routines are available for the program, one to yield a digital plot that will fill an 8 1/2 x 11 sheet of paper and another that will yield a Calcomp plot on a Tektronix terminal. Figures A.4 through A.15 were obtained using the latter method.

Subroutine "POTS" determines the pot settings needed for the analog circuit of the main analog/hybrid program. Sample outputs of this program illustrating its various options are included at the end.

The third program, "PROGRAM ODE", can be used as a subroutine and added to the previous program. This program has two variations that will yield the solution of the family of phreatic profiles within the rock-fill for one complete wave period. It uses the outcrop point movement determined in the previous program as the boundary conditions. The program uses a Runge-Kutta 4th order method to calculate the first four values of the integration whereupon an Adams-Moulton Predictor/Corrector Method is utilized to continue the solution. This method is adopted to reduce the number of function calls to the derivative function DERFN. The program uses a bisector search method to converge to the solution. Tape 5 is used

as input, Tape 6 yields the solution profiles at each time increment, Tape 7 contains the values of the gradient of the W_1 and W_2 curves at all times and space locations and Tape 8 stores the intermediate profile calculations for each iteration. An option is included to manually guess the profile solution.

The other variation of the program is a non-dimensionalized form which would overcome the limitations of units, and decrease the problem of determining adequate numerical integration intervals. At present, the program is not fully operational. The need for this program emerges from the fact that the proper scaling factors for the analog program are not known in advance and hence they must be determined. The numerical integration consumes too much computer time to be viable as a solution technique (ranging from 51 secs. for a 100 steps of a unit embankment to about 160 secs. for 700 integration steps). This is where the economy of the analog/ hybrid computer solution becomes apparent.

The fourth program is the hybrid program that will yield the phreatic line profiles. The program is interactive in that it asks the programmer to read in the proper data. It controls the operation mode of the analog computer and contains options for the amount of printout the programmer feels is necessary. Once the program yields a solution, the computer pauses and gives the operator an opportunity to plot the solution on an x-y plotter.

The analog solution can be obtained without the aid of the digital control but the method would be awkward and very time consuming. This is due to the fact that the solution for any particular time increment is determined in an iterative manner.

```
*
*
*      MIMIC SIMULATION OF THE OUTCROP POINT MOVEMENT
*
*      CONSTANTS AND PARAMETERS AND THEIR DEFINITIONS
*      PAR(A,B,M,THETA)
*      PAR(P,HO,AO)
*      A    = DARCY COEFFICIENT
*      B    = NON-DARCY COEFFICIENT
*      M    = POROSITY
*      THETA = ANGLE OF INCLINATION OF ROCKFILL
*      P    = PERIOD OF OSCILLATION
*      HO   = MEAN WATER LEVEL
*      AO   = AMPLITUDE OF IMPACT WAVE
*
*      IMPORTANT QUANTITIES NEEDED IN THE SYSTEM EQUATIONS
*
       G          =980.6
       PI         =3.14159
       ABM        =A/(B*M)
       ST         =SIN(THETA)
       DIS        =SQR((ABM*ABM+4.*ST*ST)/(M*M*B))
*                 MAXIMUM INTERNAL VELOCITY (V)
       V          =(-DIS+ABM)/2.
*                 COEFFICIENT OF PERMEABILITY RELATING TO V (K)
       K          =1./(A+B*M*ABS(V))
*                 FREQUENCY OF THE WAVE (OM)
       OM         =2.*PI/P
*                 MAXIMUM DEVIATION BETWEEN EXTERNAL AND INTERNAL WAVES
       DELYP      =2.*AO*SIN(OM*TSR)+V*(TSRI-TSR)
*                 OTHER IMPORTANT QUANTITIES
       AI         =G*M*A
       BI         =G*M*M*B
       W          =K*P/(2.*PI*M*AO)
       DEL        =G*ST*ST/DELYP
*                 IMPORTANT TIME CONSTANTS (TSR,TSRI)
       TSR        =ACS(-M*ST*ST)/OM
       TSRI       =P-TSR
*
*
*      EQUATIONS DEFINING THE SYSTEM
*
       YF         =HO+AO*SIN(OM*T)
       YFI        =HO+AO*SIN(OM*TSR)+V*(TSRI-TSR)
       YF2        =HO+AO*SIN(OM*(T+TSRI))
NOTIJ  YC         =HO+AO*SIN(OM*TSR)+V*(T-TSR)
       DAMP       =-(AI+BI*ABS(DYCI))*DYCI-DEL*YCI+DEL*YF2
       DYCI       =INT(DAMP,V)
       YCI        =INT(DYCI,YFI)
```

```
*
*                    LOGIC TO PIECE TOGETHER THE OUTCROP POINT CURVE
*
           IFLAG     =FSW(T-TSR+.05,TRUE,FALSE,FALSE)
           NIFLG     =NOT(IFLAG)
  IFLAG    YC        =YF
           JFLAG     =FSW(T-TSRI,FALSE,TRUE,TRUE)
           NJFLG     =NOT(JFLAG)
           NOTIJ     =AND(NIFLG,NJFLG)
  JFLAG    JOIN      =YCI-YF
  JFLAG    KFLAG     =FSW(JOIN,TRUE,FALSE,FALSE)
  KFLAG    YC        =YF
           NKFLG     =NOT(KFLAG)
           NOTJK     =AND(JFLAG,NKFLG)
  NOTJK    YC        =YCI
*
           FIN(T,4.5)
           DTMAX     =.01
           DTMIN     =.005
           DT        =.1
*
*                    OUTPUT
                     HDR(T,YF,YC,YCI,DAMP,DYCI)
                     OUT(T,YF,YC,YCI,DAMP,DYCI)
                     PLO(T,YF,YC,YCI,DAMP,DYCI)
                     TTP(  MOVEMENT OF OUTCROP POINT)
                     TTY(EXTERNAL SINE WAVE AND OUTCROP)
                     TTX(TIME-SECONDS)
                     END
*
*                    SAMPLE INPUT DATA.
*
  .009       .015        .43       1.5708
  5.5        22.         18.
  .009       .015        .432      1.5708
  2.5        22.         8.5
  .009       .015        .443      1.5708
  5.1        39.         15.5
*EOR
```

```
      PROGRAM WAVE(INPUT,OUTPUT,TAPE6=OUTPUT,TAPE14)
      COMMON /BL1/M,G/BL2/A,B/BL4/THETA,DELYP,K,K1/BL6/H,N/BL7/XL
      COMMON /BL3/HO,AO,TSR1,TSR,V,OMEGA,WANT(5),DEL,T,KO
      COMMON /BL5/APRIME,BPRIME,YO1,CASE
      DIMENSION X(300),YC(300)
      REAL M,K,KC,K1,CASE

C     INPUT THE NECESSARY DATA (INTERACTIVELY)
C     --------------------------------------------
    1 PRINT 2
      READ 3,CASE
      READ *,M,A,B,THETA,T,HO,AO
      IF(M.EQ.1.)STOP
      IF(THETA.NE.90) GO TO 5
      PRINT 4
      READ *,XL
    5 THETA=THETA*3.14159/180.
      WRITE(14,10) CASE,M,A,B,XL,HO
      TRY=T/50
      PRINT 6,TRY
      READ *,H,N
      PRINT 7
      READ *, WANT(1),WANT(2),WANT(3),WANT(4),WANT(5)
      CALL FAST
      CALL DIFFER(X,YC)
      CALL SERIAL(X,YC)
C     GO TO 1

    2 FORMAT(1H1,10X,*ENTER IN FREE FORMAT AND IN ORDER, EACH OF*,
     +/,11X,*THE FOLLOWING QUANTITIES**,/,15X,*1.  A TITLE*
     +* FOR THE CASE UNDER STUDY*,/,19X,*(MUST BE ENTERED ON A*,
     +* SEPARATE LINE)*,/,15X,*2.  POROSITY (IF M=1, THE*
     +* PROGRAM STOPS)*,/,15X,*3.  A  (DARCY COEFFICIENT)*,/,15X,
     +*4.  B (NON-DARCY COEFFICIENT)*,/,15X,*5.  SLOPE OF THE DAM*
     +* INCLINE (IN DEGREES)*,/,15X,*6.  PERIOD OF OSCILLATION*,/,15X,
     +*7.  MEAN WATER LEVEL*,/,15X,*8.  WAVE AMPLITUDE*)
    3 FORMAT (A10)
    4 FORMAT(/,11X,*ENTER THE LENGTH OF ROCKFILL*)
    6 FORMAT(/,11X,*FOR THE NUMERICAL SOLUTION, ENTER THE STEP SIZE*
     +* (H<.01)*,/,11X,*AND THE FREQUENCY OF PRINTOUT (INTEGER) SO THAT*
     +* THEIR*,/,11X,*PRODUCT IS *,F7.5)
    7 FORMAT(/,11X,*ENTER 1 FOR EACH OF THE FEATURES DESIRED *,
     +*(OTHERWISE ENTER 0)*,/,15X,*A.  POT SETTINGS*,/,15X,
     +*B.  COMPARISON OF NUMERICAL AND ANALYTIC RESULTS*,/,15X,
     +*C.  ANALOG SCALING OF OUTPUT*,/,15X,
     +*D.  NUMERICAL OUTCROP POINT MOVEMENT*,/,15X,
     +*E.  PLOT OF OUTCROP POINT MOVEMENT*,/,
     +11X,*A SAMPLE INPUT IS  1,0,1,1,0*)
   10 FORMAT(3X,A10,F8.3,2F8.4,F8.1,F8.1)
      END
```

```
      SUBROUTINE FAST
      COMMON /BL1/M,G/BL2/A,B/BL4/THETA,DELYP,K,K1
      COMMON /BL3/H0,A0,TSR1,TSR,V,OMEGA,WANT(5),DEL,T,K0
      COMMON /BL5/APRIME,BPRIME,YC1,CASE
      REAL M,K,K0,K1,CASE
C     CALCULATION OF FAST DROP PARAMETERS
C     -------------------------------------------
      G=980.6
      ABM=A/(B*M)
      V=-(-ABM+(ABM**2.+4.*SIN(THETA)**2./(M*M*B))**.5)/2.
      K=1/(A+B*M*ABS(V))
      W=K*T/(6.28319*M*A0)
      IF(ABS(W*SIN(THETA)**2).GT.1.)GO TO 20
      O1=K1=INT((ABS(V)+7.5)/5)*5.
      Q0=K0=INT((H0+A0+5)/5)*5.
      IF(K0.LT.K1) K0=K1
      K0=1/K0
      K1=1/K1
      TSR=T/6.28319*ACOS(-W*SIN(THETA)**2)
      APRIME=G*M*A
      BPRIME=G*M*M*B
      OMEGA=2.*3.14159/T
      TSR1=T-TSR
      DELYP=2.*A0*SIN(OMEGA*TSR)+V*(TSR1-TSR)
      DEL=G/DELYP*SIN(T-ETA)**2.
      YF1=H0+A0*SIN(OMEGA*TSR)
      YC1=YF1+V*(TSR1-TSR)
      YFC1=H0+A0*SIN(OMEGA*TSR1)
      ACCEL=-(APRIME+BPRIME*ABS(V))*V-DEL*YC1+DEL*YFC1
      PK=DELYP*50/A0

C     PRINTOUT OF RELEVANT FAST DROP PARAMETERS
C     -------------------------------------------
      PRINT 8,CASE,A,APRIME,B,BPRIME,T,TSR,M,TSR1,G,
     +K,THETA,OMEGA,A0,YF1,H0,DELYP
      PRINT 23,YC1,V,ACCEL
      PRINT 24,W,DEL,PK

      IF(WANT(1).EQ.C) RETURN

C     DETERMINING THE POT SETTINGS AND SCALE FACTORS
C     -------------------------------------------
      BETA=1.
      IF(DEL.GT.81) BETA=10
      IF(DEL.GT.4000) BETA=100
      P00=1/BETA*K0/K1
      P01=K1*ABS(V)
      P02=BPRIME/K1
      P03=APRIME
      P05=P07=OMEGA
      P07=K0*A0
      P08=K0*ABS(V)
```

```
      P10=K0*H0
      P31=1/BETA
      P35=.1
      P36=1/BETA*K1/K0*DEL
      P62=.1
      P64=TSR/10
      P94=TSR1/10

C     PRINTOUT OF SCALED POT SETTINGS
C     --------------------------------
      WRITE(6,200) Q0,Q1,BETA,P00,P01,P02,P03,P05,Q07,P07,P08,P10,P31,
     +P35,P36,P62,P64,P94
      RETURN
   20 PRINT 21

    8 FORMAT(1H1,/,T37,A10,//,T20,*G I V E N*,T51,*CALCULATED*,/,
     +T20,9(1H-),T51,10(1H-),//,T12,*A =*,T30,F8.4,T44,
     +*APRIME =*,T61,F8.4,/,T12,*B =*,T30,F8.4,T44,
     +*BPRIME =*,T61,F8.4,/,T12,*PERIOD =*,T30,F8.4,T44,
     +*TSR =*,T61,F8.4,/,T12,*POROSITY =*,T30,F8.4,T44,
     +*TSR1 =*,T61,F8.4,/,T12,*GRAVITY =*,T30,F8.4,T44,
     +*HYD. COND.(K) =*,T61,F8.4,/,T12,*SLOPE (RAD) =*,T30,F8.4,T44,
     +*FREQUENCY =*,T61,F8.4,/,T12,*AMPLITUDE (A0) =*,T30,F8.4,T44,
     +*TANGENT PT. =*,T61,F8.4,/,T12,*DEPTH (H) =*,T30,F8.4,T44,
     +*MAX. DEVIATION =*,T61,F8.4,/)
   21 FORMAT(/,11X,*SORRY, THIS IS NOT A FAST DROP CASE!*,//,11X,
     +57(1H*))
   23 FORMAT(11X,*Y(0) = *,F8.4,2X,*VEL(0) = *,F8.4,2X,
     +*ACCEL(0) = *,F10.4,/)
   24 FORMAT(T12,*W =    *,F8.4,2X,*DEL = *,F11.4,2X,
     +*PK (%)    =*,F10.4,//,11X,57(1H*))
  200 FORMAT(//,T22,*POT*,T30,*SETTING*,T45,*K0 = 1/(*,F3.0,*)*,/,
     +T22,*---*,T30,*-------*,T45,*K1 = 1/(*,F3.0,*)*,/,T45,*BETA = *,
     +F4.0,/,T22,*P00*,T27,F10.4,/,T22,*P01*,T27,F10.4,/,
     +T22,*P02*,T27,F10.4,/,T22,*P03*,T27,F10.4,/,
     +T22,*P05*,T27,F10.4,/,T22,*Q07*,T27,F10.4,/,
     +T22,*P07*,T27,F10.4,/,T22,*P08*,T27,F10.4,/,
     +T22,*P10*,T27,F10.4,/
     +T22,*P31*,T27,F10.4,/,T22,*P35*,T27,F10.4,/,
     +T22,*P36*,T27,F10.4,/,T22,*P62*,T27,F10.4,/,
     +T22,*P64*,T27,F10.4,/,T22,*P94*,T27,F10.4,//,11X,57(1H*))
      RETURN
      END
```

```
      SUBROUTINE DIFFER(X,YDOT)
C     --------------------------------------------------------
C     SUBROUTINE TO CALCULATE THE NUMERICAL SOLUTION
C.    BY A RUNGE-KUTTA-4 METHOD AND TO COMPARE IT TO
C.    AN APPROXIMATE ANALYTIC SOLUTION
C     --------------------------------------------------------
C     COMMON /BL3/H0,A0,XIN,TSR,PIN,W,WANT(5),DEL,T,Q0
      COMMON /BL5/A,B,YIN,CASE/BL6/H,N
      DIMENSION X(300),Y(300),YDOT(300),YC(300).
      REAL K1,K2,K3,K4,L1,L2,L3,L4,K,M,CASE

      ACCEL(P,X,Y)=-(A+B*ABS(P))*P+DEL*(H0+A0*SIN(W*X)-Y)

      IF(WANT(3).EQ.0) Q1=Q0=1
      IF(WANT(2).EQ.0) GOTO 115
      PRINT 110,H,N

C     NUMERICAL FRAMEWORK FOR SECOND ORDER DIFFERENTIAL EQUATION
C     --------------------------------------------------------
  115 X(1)=XX=X0=XIN
      Y(1)=YY=Y0=YIN
      YDOT(1)=P=P0=PIN
      KOUNT=0
      1 = N
  125 KOUNT=KOUNT+1
      K1=H*P
      L1=H*ACCEL(P,XX,YY)
      XX=X0+H/2
      YY=Y0+K1/2
      P =P0+L1/2
      K2=H*P
      L2=H*ACCEL(P,XX,YY)
      YY=Y0+K2/2
      P =P0+L2/2
      K3=H*P
      L3=H*ACCEL(P,XX,YY)
      XX=X0+H
      YY=Y0+K3
      P =P0+L3
      K4=H*P
      L4=H*ACCEL(P,XX,YY)
      K1=(K1+2*K2+2*K3+K4)/6
      L1=(L1+2*L2+2*L3+L4)/6
      XX=X0=X0+H
      YY=Y0=Y0+K1
      P =P0=P0+L1
      IF(KOUNT.LT.I) GO TO 125
      J=KOUNT/N+1
      X(J)=XX
      Y(J)=YY
```

```
      YDOT(J)=P
      IF(XX.GE.(1.1*T)) GO TO 150
      I = I + N
      GOTO 125
  150 CALL ANALYT(X,Y,YDOT,J)

  110 FORMAT(/,26X,*SECOND ORDER DIFFERENTIAL DAMPING*,//,
     +T12,*FOR H =*,F7.5,*   AND N =*,I4,/,T59,*% DIFF*,/
     +T14,*TIME*,T22,*NUM*,T31,*ANAL*,T39,*APPROX*,T49,*YDOT*,
     +T57,*ANAL*,T63,*APPROX*,/)
      RETURN
      END




      SUBROUTINE ANALYT(X,Y,YDOT,J)
      COMMON /BL1/M,G/BL3/H0,A0,TSR1,TSR,V,W,WANT(5),DEL,T,Q0
      COMMON /BL4/THETA,DELYP,K,Q1
      DIMENSION X(300),Y(300),YDOT(300)
      REAL K,M
C     APPROXIMATE ANALYTICAL SOLUTION
C     --------------------------------
      TK=K/(W*M)
      TKG=G/TK
      CHI=1-(4*K*SIN(THETA)**2*DELYP)/(G*M*A0*T)
      XLAMDA1=-G*M*(1-(CHI**.5))/(2*CHI)
      XLAMDA2=-G*M*(1+CHI**.5)/(2*CHI)
      COEFFA=A0*DEL*(DEL-W**2)/(TKG**2+(DEL-W**2)**2)
      COEFFB=COEFFA*TKG/(DEL-W**2)
      COEFFC=(A0+COEFFA)*SIN(W*TSR)+COEFFB*COS(W*TSR)+V*(TSR1-TSR)
      COEFFD=-W*COEFFA*COS(W*TSR)+W*COEFFB*SIN(W*TSR)+V
      PART1=(COEFFD-COEFFC*XLAMDA2)/(XLAMDA1-XLAMDA2)
      PART5=(COEFFD-COEFFC*XLAMDA1)/(XLAMDA1-XLAMDA2)
      IF(WANT(2).EQ.0) GOTO 176
      DO 170 I=1,J
      TIME=X(I)
      PART2=PART1*EXP(XLAMDA1*(TIME-TSR1))
      PART3=PART5*EXP(XLAMDA2*(TIME-TSR1))
      PART4=H0+COEFFA*SIN(W*TIME)-COEFFB*COS(W*TIME)
C     ZC=PART2-PART3+PART4
C     ZC=PART2+PART4
      DIFF=(Y(I)-ZC)*100/Y(I)
      SINE=H0+A0*SIN(W*TIME)
C     APPROXIMATE SOLUTION
C     --------------------
      APPROX=H0+A0*SIN(W*TSR)+V*(TSR1-TSR)+.75*V*(TIME-TSR1)
      DIFF2=(APPROX-Y(I))*100/Y(I)
      PRINT 175,X(I),Y(I)*Q0,ZC*Q0,APPROX*Q0,YDOT(I)*Q1,DIFF,DIFF2
      IF(SINE.GT.Y(I))GOTO 176
  170 CONTINUE
  176 CALL FITCURV(X,Y,YDOT,MM)
  175 FORMAT(T12,F6.4,4(1X,F8.4),2(1X,F6.2))
      RETURN
      END
```

```fortran
      SUBROUTINE FITCURV(X,Y,YC)
C     ------------------------------------------------
C     SUBROUTINE TO FIT TOGETHER THE VARIOUS COMPONENTS
C     OF THE OUTCROP CURVE TO GET ONE CONTINUOUS CURVE
C     ------------------------------------------------
      COMMON /BL3/H0,A0,TSR1,TSR,V,W,WANT(5),DEL,T,KO/BL6/H,N
      COMMON /BL8/H
      DIMENSION X(300),Y(300),YC(350),TIME(350)
      REAL KO
      DO 23 I=1,150
   23 YC(I)=0.
      TIME(1)=0.
      YC(1)=H0
      H=H*N
      DT=H
      I=L=1
      YT1=H0+A0*SIN(W*TSR)
      YT2=Y(1)
C     ------------------------------------------------
C     THE RISING PART OF THE OUTCROP POINT
C     ------------------------------------------------
   38 I=I+1
      TIME(I)=TIME(1)+H*(I-1)
C     ------------------------------------------------
C     THE MAXIMUM FALL RATE OF THE OUTCROP POINT
C     ------------------------------------------------
      IF(TIME(I).GE.TSR) GOTO 48
      YC(I)=H0+A0*SIN(W*TIME(I))
      GOTO 38
   48 YC(I)=H0+A0*SIN(W*TSR)+V*(TIME(I)-TSR)
      I=I+1
      TIME(I)=TIME(1)+H*(I-1)
      IF(TIME(I).GE.TSR1) GOTO 60
      GOTO 48
C     ------------------------------------------------
C     NON-LINEAR DIFFERENTIAL VISCOUS DAMPING
C     ------------------------------------------------
   60 TIME(I)=X(L)
      YC(I)=Y(L)
      YSIN=H0+A0*SIN(W*TIME(I))
      IF((YC(I)-YSIN).LE.0.) GO TO 74
      I=I+1
      L=L+1
      GOTO 60
C     ------------------------------------------------
C     THE OUTCROP POINT RISES AGAIN WITH THE EXTERNAL WAVE
C     ------------------------------------------------
   74 TYC=TIME(I)
      YTC=H0+A0*SIN(W*TYC)
      IF(TYC.GT.T) GO TO 87
   75 YC(I)=H0+A0*SIN(W*TIME(I))
```

```
        I=I+1
        TIME(I)=TIME(1)+H*(I-1)
        IF(TIME(I).GT.T) GOTO 90
        GOTO 75
  87    II=I
        YC(I)=H0+A0*SIN(W*TIME(I))
        L=II-INT(T/H)-1
        GOTO 93
  90    II=I-1
        L=1
  93    PRINT 95,TSR,YT1,TSR1,YT2,TYC,YTC
        WRITE(14,105) TSR,YT1,TSR1,YT2,TYC,YTC
        IF(WANT(4).EQ.0) GOTO 97
        PRINT 96
  97    DO 100 J=L,II
        M=J-L+1
        X(M)=TIME(M)=TIME(J)
        YF=(H0+A0*SIN(W*TIME(J)))*K0
        YC(M)=YC(J)*K0
        IF(WANT(4).EQ.0) GOTO 100
        PRINT 99,M,TIME(M),YF,YC(M)
 100    CONTINUE
        CALL DOTS(DT)
        DO 102 I=2,M
 102    WRITE(14,101) TIME(I)-TIME(I-1),YC(I)
        IF(WANT(5).EQ.0) RETURN
        CALL PLOT(Y,YC,TIME,M,55,0)

  95    FORMAT(///T28,*T1 = *,F8.4,T44,*Y(T1) = *,F8.4,/
       +T28,*T2 = *,F8.4,T44,*Y(T2) = *,F8.4,/
       +T28,*TC = *,F8.4,T44,*Y(TC) = *,F8.4)
  96    FORMAT(1H1,/,T21,*I*,T32,*TIME*,T44,*SINE WAVE*,
       +T60,*OUTCROP*,//)
  99    FORMAT(19X,I2,3(5X,F10.4))
 101    FORMAT(5X,2(F10.4,5X))
 105    FORMAT(/T5,*T1 =*,F8.4,T25,*Y(T1)=*,F8.4,/
       +T5,*T2 =*,F8.4,T25,*Y(T2)=*,F8.4,/
       +T5,*TC =*,F8.4,T25,*Y(TC)=*,F8.4)
        RETURN
        END
```

```
      SUBROUTINE PLOT(ITY,Y,Z,N,XSCALE,IPRINT)
C     ------------------------------------------------------------
C     PROGRAM TO PLOT A SET OF X-VERSUS-Y VALUES
C     X IS THE SYMBOL USED TO MARK THE POINT OF INTERSECTION
C     Y IS THE DEPENDENT VARIABLE ARRAY
C     Z IS THE INDEPENDENT VARIABLE ARRAY
C     N IS THE NUMBER OF DATA POINTS IN EACH ARRAY
C     XSCALE IS THE NUMBER OF COLUMNS USED TO PRINT THE X SCALE
C     IPRINT EQUALS 1 IF THE SCALED DATA POINTS ARE TO BE PRINTED OUT
C     ------------------------------------------------------------
      DIMENSION Y(N),Z(N),TY(300),LINE(132),ITY(300),TX(300)
      REAL LINE,BLANK,DOT,MARK
      INTEGER XSCALE,XSCAL1
      DATA BLANK,DOT,MARK/1H ,1H.,1H*/
C     ------------------------------------------------------------
C     CREATE TEMPORARY STORAGE FOR ARRAYS (A=TY AND B=TX GENERALLY)
C     ------------------------------------------------------------
      DO 100 I=1,N
         TY(I)=Y(I)
 100     TX(I)=Z(I)
C     ------------------------------------------------------------
C     FIND THE MINIMUM AND MAXIMUM ELEMENTS IN EACH ARRAY
C     ------------------------------------------------------------
      XMIN=YMIN=10.**10
      XMAX=YMAX=-10.**9
      DO 500 I=1,N
         IF(TX(I).GT.XMAX) XMAX=TX(I)
         IF(TY(I).GT.YMAX) YMAX=TY(I)
         IF(TX(I).LT.XMIN) XMIN=TX(I)
         IF(TY(I).LT.YMIN) YMIN=TY(I)
 500  CONTINUE
      PRINT 987,XMIN,XMAX,YMIN,YMAX
C     ------------------------------------------------------------
C     SCALE ELEMENTS IN X ARRAY IF NEGATIVE OR LESS THAN ONE
C     ------------------------------------------------------------
      DO 601 I=1,N
 601  TX(I)=TX(I)-XMIN+1.0
      XMAX=XMAX-XMIN+1.0
      XMIN=1.0
C     ------------------------------------------------------------
C     SCALE ELEMENTS IN Y ARRAY IF NEGATIVE OR LESS THAN ONE
C     ------------------------------------------------------------
      DO 602 I=1,N
 602  TY(I)=TY(I)-YMIN+1.0
      YMAX=YMAX-YMIN+1.0
      YMIN=1.0
C     ------------------------------------------------------------
C     FORM THE SCALING RATIOS FOR X AND Y AXES
C     ------------------------------------------------------------
      RANGEY=YMAX-YMIN
      RANGE2=XSCALE-1
      RANGEX=XMAX-XMIN
      PRINT 988,RANGEX,RANGE2,RANGEY
C     ------------------------------------------------------------
C     SCALE THE ELEMENTS OF THE ARRAYS
```

```
      CO 700 I=1,N
         TX(I)=1.0+(TX(I)-XMIN)*RANGE2/RANGEX
 700     TY(I)=10.0+(TY(I)-YMIN)*70./RANGEY
C     ------------------------------------
C.    PLOT THE SCALED DATA ARRAYS
C     CREATE AND PRINT THE Y AXIS AS DOTS
C     ------------------------------------
      DO 398 I=1,9
 398  LINE(I)=BLANK
      DO 400 I=10,83
 400  LINE(I)=DOT
      WRITE(6,401)(LINE(I),I=1,83)
C     ------------------------
C     INITIALIZE PRINT VECTOR
C     ------------------------
      DO 402 J=1,83
 402  LINE(J)=BLANK
      LINE(10)=DOT
      XSCAL1=XSCALE+1
      II=1
      DO 800 I=1,XSCAL1
      LL=1
      K5=0
 802  JJ=TX(II)
      IF(JJ.NE.I) GO TO 801
      K5=1
      KK=TY(II)
      LINE(KK)=MARK
      ITY(LL)=KK
      LL=LL+1
      II=II+1
      MM=TX(II)
      IF(MM.EQ.I) GO TO 802
 801  WRITE(6,401)(LINE(IJK),IJK=1,80)
      IF(K5.EQ.0) GO TO 805
      LL1=LL-1
      DO 804 NN=1,LL1
      ITY1=ITY(NN)
 804  LINE(ITY1)=BLANK
 805  K5=0
      LINE(10)=DOT
 800  CONTINUE
      IF(IPRINT.NE.1) GO TO 900
      DO 901 I=1,N
 901     WRITE(6,902) I,TX(I),TY(I)
 900  CONTINUE

 401  FORMAT(1H ,83A1)
 902  FORMAT(I5,2F15.7)
 987  FORMAT(1H1,9X,*XMIN=*,F9.4,4X,*XMAX=*,F9.4,4X,*YMIN=*,F9.4,4X/
     +*YMAX=*,F9.4)
 988  FORMAT(/,10X,*RANGEX =*,F13.4,*   RANGE2 =*,F13.4,
     +*   RANGEY =*,F12.4,//)
      RETURN
      END
```

```
      SUBROUTINE POTS(OT)
C     THIS SUBROUTINE WILL GIVE THE PROPER POT SETTINGS
C     FOR THE HYBRID PROGRAM DEVELOPED
C     ---------------------------------------------------
      COMMON /BL1/M,G/BL2/A,B/BL7/XL
      REAL M

      P00=P31=1/6.
      P01=P36=1/(50*OT)
      P02=P32=.75
      P03=P33=M
      P06=PJ8=1.9612*M
      P10=A
      P12=3J*B
      P30=P35=.25
      FACTOR=1.
      IF(XL.GE.10.) FACTOR=10.
      P60=.1/FACTOR
      P65=XL/(10*FACTOR)
      WRITE(14,5) P00,P30,P01,P31,P02,P32,PC3,P33,P06,P35,
     +P08,P36,P10,P60,P12,P65
    5 FORMAT(/T5,*P00=*,F8.4,T25,*P30 = *,F8.4,
     +/T5,*P01=*,F8.4,T25,*P31 = *,F8.4,/T25,*P02 = *,F8.4,
     +T25,*P32 = *,F8.4,/T5,*P03=*,F8.4,T25,*P33 - *,F8.4,
     +/T5,*P06=*,F8.4,T25,*P35 = *,F8.4,/T5,*P08=*,F8.4,
     +T25,*P36 = *,F8.4,/T5,*P10=*,F8.4,T25,*P60 = *,F8.4,
     +/T5,*P12=*,F8.4,T25,*P65 = *,F8.4//)
      RETURN
      END
```

```
      PROGRAM ODE (INPUT,OUTPUT,TAPE5,TAPE6,TAPE7,TAPE8)
C     SOLUTION TO FIRST ORDER DIFFERENTIAL EQUATION BY RUNGE-KUTTA
      DIMENSION WW2(4),WW1(4),RESULTS(701,6),TIME(52),DEPTH(52)
      REAL M

C     DEFINE DERIVATIVE FUNCTION

      DERFN(Y,Z,YM1)=-1./(.75*Y+.25*Z)*(M*(Y-YM1)/DT+.5*G*(A+B*
     +ABS(Y+Z)/2)*(Y+Z)*M*M)

C     READ IN PARAMETERS
      ISTEP=1
      PRINT 202
C     READ IN TAPES
      READ(5,*) M,A,B,XL,H0,PTA,PTB,U
      PRINT *,20H INPUT T1,H1,T2,H2,T
      READ *,T1,H1,T2,H2,T
      DO 15 J=1,52
   15 READ(5,*) TIME(J),DEPTH(J)
      IMAX=701
      H=XL/(IMAX-1)
      I10=(IMAX-1)/10
      IM1=IMAX-1
      G=980.6
      FAC=16*M*M*G
      WRITE(7,210)

C     DEFINE THE CONDITIONS AT INITIAL TIME
      W10=2*M*(G*H0)**.5
      W11=2*M*(G*H1)**.5
      W12=2*M*(G*H2)**.5
      TYME=C.
      GO TO 2
    1 PTA=U+1.5
      PTB=U-1.5

C     MOVE ON TO THE NEXT TIME INCREMENT
    2 PRINT 203
      DT=TIME(ISTEP)
      TYME=TYME+DT
      IF(TYME.GT.T) STOP
      IF(TYME.LE.T1) W10=(W10*(T1-TYME)+W11*TYME)/T1
      IF(TYME.GT.T1.AND.TYME.LE.T2) W10=(W11*(T2-TYME)+W12*(TYME-T1))
     +                                 /(T2-T1)
      IF(TYME.GT.T2) W10=(W12*(T+T1-TYME)+W11*(TYME-T2))/(T+T1-T2)
      W20=-W10
      IF(DT.LE.0) STOP
      C=(G*DEPTH(ISTEP))**.5
      ICOUNT=1
      GO TO 4
```

```fortran
C     DEFINE THE LIMITS AND THE INITIAL VALUE OF THE VELOCITY U
    3 DO 13 I=1,IMAX,IM1
   13 PRINT 200,RESULTS(I,1),(RESULTS(I,J),J=2,6)
      PRINT 204
      READ *, PTA,PTB,U
      IF(PTA.EQ.100) STOP
      ICOUNT=1
    4 X0=0
      I=1

C     COMPUTE FOUR VALUES BY RUNGE-KUTTA AND PRINT OUT

      WW1(1)=W1=U+2*M*C
      WW2(1)=W2=U-2*M*C
      CALL STORE(RESULTS,X0,W1,W2,FAC,M,I,IMAX)
      DO 10 I=2,4
      FK11=+DERFN(W1,W2,W1O)
      FK12=+DERFN(W2,W1,W2O)
      FK21=+DERFN(W1+.5*FK11,W2+.5*FK12,W1O)
      FK22=+DERFN(W2+.5*FK12,W1+.5*FK11,W2O)
      FK31=+DERFN(W1+.5*FK21,W2+.5*FK22,W1O)
      FK32=+DERFN(W2+.5*FK22,W1+.5*FK21,W2O)
      FK41=+DERFN(W1+FK31,W2+FK32,W1O)
      FK42=+DERFN(W2+FK32,W1+FK31,W2O)
      X0=X0+H
      WW1(I)=W1+H*(FK11+2.*FK21+2.*FK31+FK41)/6.
      WW2(I)=W2+H*(FK12+2.*FK22+2.*FK32+FK42)/6.
      W1=WW1(I)
      W2=WW2(I)
      CALL STORE(RESULTS,X0,W1,W2,FAC,M,I,IMAX)
   10 CONTINUE
      F1=DERFN(WW1(1),WW2(1),W1O)
      F2=DERFN(WW1(2),WW2(2),W1O)
      F3=DERFN(WW1(3),WW2(3),W1O)
      F4=DERFN(WW1(4),WW2(4),W1O)
      F6=DERFN(WW2(1),WW1(1),W2O)
      F7=DERFN(WW2(2),WW1(2),W2O)
      F8=DERFN(WW2(3),WW1(3),W2O)
      F9=DERFN(WW2(4),WW1(4),W2O)
      WRITE(7,211) ISTEP,ICOUNT,F1,F6,F2,F7,F3,F8,F4,F9
      I=4

C     ADAMS-MOULTON PREDICTOR/CORRECTOR METHOD

   30 I=I+1
      PW1=W1+H*(55*F4-59*F3+37*F2-9*F1)/24
      PW2=W2+H*(55*F9-59*F8+37*F7-9*F6)/24
      F5=DERFN(PW1,PW2,W1O)
      F0=DERFN(PW2,PW1,W2O)
      CW1=W1+H*(9*F5+19*F4-5*F3+F2)/24
      CW2=W2+H*(9*F0+19*F9-5*F8+F7)/24
      W1=CW1+19*(PW1-CW1)/270
      W2=CW2+19*(PW2-CW2)/270
```

```
      X0=X0+H
      F1=F2
      F2=F3
      F3=F4
      F4=DERFN(W1,W2,W10)
      F6=F7
      F7=F8
      F8=F9
      F9=DERFN(W2,W1,W20)
      IF(I/I10*I10.EQ.I) WRITE(7,212) I,F4,F9
      CALL STORE(RESULTS,X0,W1,W2,FAC,H,I,IMAX)
      IF(I.LT.IMAX) GOTO 30

C     BISECTOR SEARCH FOR THE CORRECT VELOCITY FOR
C     THE BOUNDARY VALUES PROBLEM

      R=(W1+W2)/2
      IF(ABS(R).LE..01) GOTO 40
      IF(R) 25,25,32
C     LOWER LIMIT IS ADJUSTED UPWARDS
C     ------------------------------------
   25 PTB=U
      GO TO 35
C     UPPER LIMIT IS ADJUSTED DOWNWARDS
C     ------------------------------------
   32 PTA=U
C     THE NEW VELOCITY IS COMPUTED
C     ------------------------------------
   35 U=(PTA+PTB)/2
      ICOUNT=ICOUNT+1
      DO 37 I=1,IMAX,I10
   37 WRITE(8,201) (RESULTS(I,J),J=1,6)
      IF(ICOUNT.LE.10) GO TO 4
      PRINT 47
      GO TO 3

C     SUCCESS!!  YOU HAVE CONVERGED TO A SOLUTION
C     PREPARE TO MOVE ON TO THE NEXT VALUE
   40 WRITE(6,42) ISTEP,ICOUNT
      WRITE(6,60)
      DO 44 I=1,IMAX,I10
      WRITE(8,214) RESULTS(I,1),RESULTS(I,2)
   44 WRITE(6,200) RESULTS(I,1),(RESULTS(I,J),J=2,6)
      ISTEP=ISTEP+1
      GO TO 1
```

```
C     FORMAT STATEMENTS

42 FORMAT(//,* STEP NO. *,I3,* REQUIRED *,I3,* ITERATIONS*/)
47 FORMAT(//* SOMETHING IS WRONG.  YOU ARE NOT CONVERGING*,
  +* FAST ENOUGH.*/* TRY READING IN A NEW VALUE OF U*/)
60 FORMAT (7X,*X*,12X,*Y*,14X,*U*,13X,*C*,12X,*W1*,12X,*W2*,/)
200 FORMAT (F10.4,3X,F14.7,4(3X,F10.4))
201 FORMAT(6(2X,G1C.3))
202 FORMAT(/* ENTER POROSITY(H), COEFFICIENTS(A,B), LENGTH(XL),*,
  +/*   MEAN WATER LEVEL(H0), UPPER AND LOWER LIMITS OF VELOCITY,*,
  +/*    AND THE INITIAL GUESS FOR THE VELOCITY(U)*/)
203 FORMAT(/* ENTER THE INCREMENT AND THE NEW INITIAL HEIGHT*/)
204 FORMAT(/* ENTER NEW UPPER AND LOWER LIMITS*,
  +* AND THE ACTUAL VELOCITY*/)
210 FORMAT(1H1,5X,*THIS TAPE7 GIVES THE VALUES OF THE DERIVATIVE*,
  +/6X,*AT EACH STEP OF THE INTEGRATION.  THIS OF VALUE FOR THE*,
  +/6X,*ANALOG/HYBRID SIMULATION.*/6X,60(1H-))
211 FORMAT(/5X,*STEP NO.*,I4,4X,*ITERATION NO.*,I4,//,
  +15X,*1*,5X,2G14.7/15X,*2*,5X,2G14.7/15X,*3*,5X,
  +2G14.7/15X,*4*,5X,2G14.7)
212 FORMAT(13X,I3,5X,2G14.7)
214 FORMAT(10X,F5.2,3X,F10.4)
215 FORMAT(*-------- STEP NO. *,I4,* -------- ITERATION NO. *,
  +I4,* ----------*)
    END
```

```
      SUBROUTINE STORE(RESULTS,X0,W1,W2,FAC,PORE,NUM,IMAX)
      DIMENSION RESULTS(IMAX,6)
      RESULTS(NUM,1)=X0
      RESULTS(NUM,2)=(W1-W2)**2/FAC
      RESULTS(NUM,3)=(W1+W2)/2
      RESULTS(NUM,4)=(W1-W2)/(4*PORE)
      RESULTS(NUM,5)=W1
      RESULTS(NUM,6)=W2
      RETURN
      END
```

PAGE 1   ANALOG/HYBRID SIMULATION OF NON-DARCY FLOW
                IN ROCKFILL STRUCTURES

```
C      DEVELOPED BY PETER KOTIUGA WITH THE HELP OF DAVID HARGREAVES.
C
C      THIS PROGRAM CALCULATES THE PHREATIC SURFACES OF THE WAVE
C      MOTION WITHIN ROCKFILL STRUCTURES USING A CSDT HYBRID
C      APPROACH.  THE CONTINUITY AND MOMENTUM EQUATIONS HAVE BEEN
C.     TRANSFORMED TO THEIR CHARACTERISTIC FORM AND ARE INTEGRATED
C      SIMULTANEOUSLY.  BECAUSE IT IS A BOUNDARY-VALUE PROBLEM,
C      AN ITERATIVE BISECTOR SEARCH METHOD HAS BEEN IMPLEMENTED
C      TO YIELD A SOLUTION AT EACH TIME FRAME.  AN OPTION TO PLOT
C      THE PHREATIC SURFACE AT EACH TIME FRAME IS GIVEN AND THEN
C      THE VARIABLES ARE UPDATED.  THE SOLUTION IS OBTAINED FOR
C      ONE COMPLETE WAVE PERIOD.

       COMMON T1,H1,T2,H2,EPS,SCALE
       REAL M

C      SELECT ANALOG CONSOLE
       CALL QSHYIN(IER,680)
       CALL QSC(1,IER)

C      PLACE ANALOG IN POT COEFFICIENT MODE
       CALL QSPC(IER)
       CALL QHCLL(1,.FALSE.,IER)

C      ENTER THE PARAMETERS
       TYPE 10
  10   FORMAT(60H ENTER THE PERIOD, M.W.L., POROSITY, EPSILON  ,/,
      +50H ENTER THE SCALE FACTOR (ABOUT 300) ,/)
       ACCEPT 15,T,HC,M,EPS,SCALE
       TYPE 15,T,HC,M,EPS,SCALE
  15   FORMAT(2F5.2,2F6.4,F6.1)
       TYPE 20
  20   FORMAT(60H ENTER T1,H1,T2,H2 (4F10.4) ,/)
       ACCEPT 25,T1,H1,T2,H2
       TYPE 25,T1,H1,T2,H2
  25   FORMAT(4F10.4)
       G=980.6

       CALL PHREA(G,T,HO,M)
       STOP
       END
```

PAGE 2   SUBROUTINE TO SOLVE FOR THE PHREATIC PROFILES


```
      SUBROUTINE PHREA(G,T,H0,M)
      DIMENSION HIN(4),HOUT(2)
      COMMON T1,H1,T2,H2,EPS,SCALE
      LOGICAL SENSW
      REAL M

      W0=2.*M*SQRT(G*H0)/SCALE
      W1=2.*M*SQRT(G*H1)/SCALE
      W2=2.*M*SQRT(G*H2)/SCALE
      TIME=0.
C     READ IN IMPORTANT PARAMETERS
   17 TYPE 20
   20 FORMAT(60H ENTER THE NEW TIME INCREMENT AND DEPTH',/)
      ACCEPT 25,DT,YN
      TYPE 25,DT,YN
   25 FORMAT(2F8.4)
      IF(YN.LE.0.) RETURN
      TYPE 30
   30 FORMAT(60H ENTER RANGE OF VELOCITIES AND INITIAL',
     +2CH GUESS',/)
      ACCEPT 35,VELA,VELB,VEL
   35 FORMAT(3F4.1)

C     DEFINING THE INITIAL VALUES
      CEL=2.*M*SQRT(G*YN)/SCALE
      VELA=VELA/SCALE
      VELB=VELB/SCALE
      VEL=VEL/SCALE
      WIN(1)=VEL+CEL
      WIN(2)=VEL-CEL
      IF(TIME.GT.T) RETURN
      IF(TIME.LE.T1) WIN(3)=(W0*(T1-TIME)+TIME*W2)/T1
      IF(TIME.GT.T1.AND.TIME.LE.T2) WIN(3)=(W1*(T2-TIME)+TIME*W2)/1
      IF(TIME.GT.T2) WIN(3)=(W2*(T1+T-TIME)+TIME*W1)/(T1+T)
      WIN(4)=-WIN(3)
C     INTEGRATE ON THE ANALOG COMPUTER
   40 CALL RUN(WIN,HOUT)

C     BISECTOR SEARCH MEHTOD TO SEEK SOLUTION
      VELN=(HOUT(1)+HOUT(2))/2.
      IF(.NOT.SENSW(1)) GO TO 45
      YIN=((WIN(1)+WIN(2))*SCALE/(4.*M*G))**2.
      YOUT=((HOUT(1)+HOUT(2))*SCALE/(4.*M*G))**2.
      UIN=(WIN(1)+WIN(2))/2.
      CIN=(WIN(1)-WIN(2))/(4.*M)
      COUT=(HOUT(1)-HOUT(2))/(4.*M)
```

PAGE 3 SUBROUTINE TO SOLVE FOR THE PHREATIC PROFILES

```
      TYPE 70,TIME,YIN,UIN,CIN,YOUT,VELN,COUT
   70 FORMAT(/,12X,7HTIME = ,F6.2,/,2X,5HY(0)=F8.4,5X,5HU(0)=,F7.4,
     +5X,5HC(0)=,F8.3;/,2X,5HY(L)=,F8.4,5X,5HU(L)=,F7.4,5HC(L)=,
     +F8.3)
   45 IF(ABS(VELN).LE.EPS) GO TO 55
      IF(VELN.LT.0.) VELB=VELN
      IF(VELB.GT.0.) VELA=VELN
      VEL=(VELA+VELB)/2.
      WIN(1)=VEL+CEL
      WIN(2)=VEL-CEL

      CALL QWBDAR(WIN,1,2,IER)
      GO TO 40

C     PLOT THE CURVE FOR THE PRESENT TIME FRAME
   55 PAUSE 01
      CALL PUN(WIN,WOUT)
      PAUSE 02

C     GO TO THE NEXT TIME FRAME
      TIME=TIME+DT
      GO TO 17
      END
```

```
PAGE  4    SUBROUTINE TO TRANSFER ANALOG AND DIGITAL SIGNALS

          SUBROUTINE RUN(WIN,WOUT)
          DIMENSION WIN(4),WOUT(2)
          LOGICAL LVAL

C         SET THE DACS AND TRANSFER SIGNALS
          CALL QW3DAR(WIN,1,4,IER)
          CALL QSTDA

C         PLACE ANALOG IN IC MODE
          CALL QSIC(IER)

C         LOOP TO DETERMINE A PHREATIC SURFACE
          CALL QSDLYR(500.,IER)
          CALL QSOP(IER)
          CALL QRSLL(LVAL,0,IER)
   45     CALL QRSLL(LVAL,0,IER)
          IF(.NOT.LVAL) GO TO 45

C         READ THE A/D CHANNELS
          CALL QR9ADR(WOUT,1,2,IER)
          CALL QSIC(IER)
          RETURN
          END
```

```
      PROGRAM ODE(INPUT,OUTPUT,TAPE5,TAPE6,TAPE7,TAPE8)
C     SOLUTION TO FIRST ORDER DIFFERENTIAL EQUATION BY RUNGE-KUTTA
      DIMENSION WW2(4),WW1(4),RESULTS(101,6)
      COMMON GHO,XL
      REAL M

C     DEFINE DERIVATIVE FUNCTION

      DERFN(Y,Z,YM1)=-M/(.75*Y+.25*Z)*((Y-YM1)/DT+.5*(GMAT+.5*
     +              GMBL*ABS(Y+Z))*(Y+Z))

C     READ IN PARAMETERS
      ISTEP=1
      PRINT 202
      READ(5,*) M,A,B,XL,H0,PTA,PTB,U
      PRINT 201
      READ *, T1,H1,T2,H2,T
      PRINT*, 44H   ENTER THE VALUE OF TOLERANCE ON VELOCITY
      READ*,EPS
      IMAX=101
      I10=(IMAX-1)/10
      IM1=IMAX-1
      H=1./(IMAX-1)
      G=980.6
      FAC=16*4*M*G
      GHO=(G*H0)**.5
      GMAT=G*M*A*T
      GMBL=G*M*B*XL
      PTA=PTA/GHO
      PTB=PTB/GHO
      U=U/GHO
      WRITE(7,210)

C     DEFINE THE CONDITIONS AT INITIAL TIME

      W10=2*M
      W11=(2*M*(G*H1)**.5)/GHO
      W12=(2*M*(G*H2)**.5)/GHO
      TIME=0
      GO TO 2
    1 PTA=U+1.5
      PTB=U-1.5

C     READ IN THE INCREMENT AND THE NEW INITIAL HEIGHT

    2 PRINT 203
      READ(5,*) DT,H1
      TIME=TIME+DT
      DT=DT/T
      IF(TIME.GT.T) STOP
      IF(TIME.LE.T1) W10=(W10*(T1-TIME)+W11*TIME)/T1
```

```
      IF(TIME.GT.T1.AND.TIME.LE.T2) W10=(W11*(T2-TIME)+W12*(TIME-T1)
     +                                  /(T2-T1)
      IF(TIME.GT.T2) W10=(W12*(T1+T-TIME)+W11*(TIME-T2))/(T+T1-T2)
      W20=-W10
      C=(G*H1)**.5/GHO
      ICOUNT=1
      PRINT*,4HW10=,W10,8H  TIME= ,TIME
      GO TO 4
    3 DO 13 I=1,IMAX,IM1
   13 PRINT 200,RESULTS(I,1),(RESULTS(I,J),J=2,6)

C     DEFINE THE LIMITS AND THE INITIAL VALUE OF THE VELOCITY U

      PRINT 204
      READ *,PTA,PTB,U,OPT
      IF(U.GT.60) STOP
      PTA=PTA/GHO
      PTB=PTB/GHO
      U=U/GHO
      ICOUNT=1
    4 X0=0
      I=1

C     COMPUTE FOUR VALUES BY RUNGE-KUTTA AND PRINT OUT

      WW1(I)=W1=U+2*M*C
      WW2(I)=W2=U-2*M*C
      CALL STORE(RESULTS,X0,W1,W2,FAC,M,I,IMAX)
      DO 10 I=2,4
      FK11=+DERFN(W1,W2,W10)
      FK12=+DERFN(W2,W1,W20)
      FK21=+DERFN(W1+.5*FK11,W2+.5*FK12,W10)
      FK22=+DERFN(W2+.5*FK12,W1+.5*FK11,W20)
      FK31=+DERFN(W1+.5*FK21,W2+.5*FK22,W10)
      FK32=+DERFN(W2+.5*FK22,W1+.5*FK21,W20)
      FK41=+DERFN(W1+FK31,W2+FK32,W10)
      FK42=+DERFN(W2+FK32,W1+FK31,W20)
      X0=X0+H
      WW1(I)=W1+H*(FK11+2.*FK21+2.*FK31+FK41)/6.
      WW2(I)=W2+H*(FK12+2.*FK22+2.*FK32+FK42)/6.
      W1=WW1(I)
      W2=WW2(I)
      CALL STORE(RESULTS,X0,W1,W2,FAC,M,I,IMAX)
   10 CONTINUE
      F1=DERFN(WW1(1),WW2(1),W10)
      F2=DERFN(WW1(2),WW2(2),W10)
      F3=DERFN(WW1(3),WW2(3),W10)
      F4=DERFN(WW1(4),WW2(4),W10)
      F6=DERFN(WW2(1),WW1(1),W20)
      F7=DERFN(WW2(2),WW1(2),W20)
      F8=DERFN(WW2(3),WW1(3),W20)
      F9=DERFN(WW2(4),WW1(4),W20)
```

```
      WRITE(7,211) ISTEP,ICOUNT,F1,F6,F2,F7,F3,F8,F4,F9
      I=4

C     ADAMS-MOULTON PREDICTOR/CORRECTOR METHOD

30    I=I+1
      PW1=W1+H*(55*F4-59*F3+37*F2-9*F1)/24
      PW2=W2+H*(55*F9-59*F8+37*F7-9*F6)/24
      F5=DERFN(PW1,PW2,W10)
      F0=DERFN(PW2,PW1,W20)
      CW1=W1+H*(9*F5+19*F4-5*F3+F2)/24
      CW2=W2+H*(9*F0+19*F9-5*F8+F7)/24
      W1=CW1+19*(PW1-CW1)/270
      W2=CW2+19*(PW2-CW2)/270
      X0=X0+H
      F1=F2
      F2=F3
      F3=F4
      F4=DERFN(W1,W2,W10)
      F6=F7
      F7=F8
      F8=F9
      F9=DERFN(W2,W1,W20)
      IF(I/I10*I10.EQ.I) WRITE(7,212) I,F4,F9
      CALL STORE(RESULTS,X0,W1,W2,TAU,M,I,IMAX)
      IF(I.LT.IMAX) GOTO 30

C     BISECTOR SEARCH FOR THE CORRECT VELOCITY FOR
C     THE BOUNDARY VALUES PROBLEM

      R=(W1+W2)/2
      IF(OPT.EQ.1) GO TO 38
      IF(ABS(R).LE.EPS) GOTO 40
      IF(R) 25,25,32

C     LOWER LIMIT IS ADJUSTED UPWARDS
C     ----------------------------------------
25    PTB=U
      GO TO 35
C     UPPER LIMIT IS ADJUSTED DOWNWARDS
C     ----------------------------------------
32    PTA=U
C     THE NEW VELOCITY IS COMPUTED
C     ----------------------------------------
35    U=(PTA+PTB)/2
      ICOUNT=ICOUNT+1
      DO 37 I=1,IMAX,I10
37    WRITE(8,199) (RESULTS(I,J),J=1,6)
      IF(ICOUNT.LE.10) GO TO 4
      PRINT 47
      GO TO 3
```

```fortran
   38 PRINT 150,U*GHO,R*GHO
  150 FORMAT(*VELOCITY GUESS =*,G14.7,*   VELOCITY AT CORE =*,
     +G14.7/*   INPUT 1 IF SATISFIED, 2 TO TRY AGAIN, 3 TO STOP*)
      ICOUNT=ICOUNT+1
      READ *,DECIDE
      IF(DECIDE.EQ.3) STOP
      IF(DECIDE.EQ.1) GO TO 40
      PRINT*, 25H INPUT THE NEW VALUE OF U
      READ *, U
      U=U/GHO
      GO TO 4

C     SUCCESS!!  YOU HAVE CONVERGED TO A SOLUTION
C     PREPARE TO MOVE ON TO THE NEXT VALUE
C     ------------------------------------------------
   40 WRITE(6,42) ISTEP,ICOUNT
      WRITE(6,60)
      DO 44 I=1,IMAX,I10
      WRITE(8,214) RESULTS(I,1),RESULTS(I,2)
   44 WRITE(6,200) RESULTS(I,1),(RESULTS(I,J),J=2,6)
      ISTEP=ISTEP+1
      GO TO 1

   42 FORMAT(//,* STEP NO. *,I3,* REQUIRED *,I3,* ITERATIONS*/)
   47 FORMAT(//* SOMETHING IS WRONG.  YOU ARE NOT CONVERGING*.
     +* FAST ENOUGH.*/* TRY READING IN A NEW VALUE OF U*/)
   60 FORMAT(7X,*X*,12X,*Y*,14X,*U*,13X,*C*,12X,*W1*,12X,*W2*,/)
  199 FORMAT(6(2X,G11.4))
  200 FORMAT(F10.4,3X,F14.7,4(3X,F10.4))
  201 FORMAT(/* ENTER THE VALUES OF TIME AND DEPTH AT THE*/
     +* TWO TIME CONSTANTS T1 AND TC FROM THE OUTCROP ANALYSIS*/
     +* AND THE PERIOD OF OSCILLATION, T*/)
  202 FORMAT(/* ENTER POROSITY(M), COEFFICIENTS(A,B), LENGTH(XL),*,
     +/* MEAN WATER LEVEL(HO), UPPER AND LOWER LIMITS OF VELOCITY,
     +/* AND THE INITIAL GUESS FOR THE VELOCITY(U)*/)
  203 FORMAT(/* ENTER THE INCREMENT AND THE NEW INITIAL HEIGHT*/)
  204 FORMAT(/* INPUT (A) UPPER LIMIT, (B) LOWER LIMIT,*
     +* (C) GUESSED VELOCITY, AND*/* (D) AN OPTION TO CONTROL*
     +* THE UPDATING OF THE VELOCITY (IF YES, TYPE 1)*)
  210 FORMAT(1H1,5X,*THIS TAPE7 GIVES THE VALUES OF THE DERIVATIVE*,
     +/6X,*AT EACH STEP OF THE INTEGRATION.  THIS OF VALUE FOR THE*,
     +/6X,*ANALOG/HYBRID SIMULATION.*/6X,60(1H-))
  211 FORMAT(/5X,*STEP NO.*,I4,4X,*ITERATION NO.*,I4,//,
     +15X,*1*,5X,2G14.7/15X,*2*,5X,2G14.7/15X,*3*,5X,
     +2G14.7/15X,*4*,5X,2G14.7)
  212 FORMAT(14X,I3,5X,2G14.7)
  214 FORMAT(10X,F5.2,3X,F10.4)
  215 FORMAT(*-------- STEP NO. *,I4,* -------- ITERATION NO. *,
     +I4,* ----------*)
      END
```

```
SUBROUTINE STORE(RESULTS,X0,W1,W2,FAC,PORE,NUM,IMAX)
DIMENSION RESULTS(IMAX,6)
COMMON GHO,XL
RESULTS(NUM,1)=X0*XL
RESULTS(NUM,2)=(W1-W2)**2/FAC*GHO**2
RESULTS(NUM,3)=(W1+W2)/2*GHO
RESULTS(NUM,4)=(W1-W2)/(4*PORE)*GHO
RESULTS(NUM,5)=W1*GHO
RESULTS(NUM,6)=W2*GHO
RETURN
END
```

P	HO	AO
5.64000E+00	2.29000E-01	1.70000E-01

t	YF	YC	YCL	NEED	DYCL
0.0000E-01	2.20000E-01	2.20000E-01	1.37359E-01	-2.23425E-03	1.22893E-01
1.0000E-01	2.38899E-01	2.38899E-01	1.28782E-01	2.64432E+00	-1.09318E-01
2.0000E-01	2.57564E-01	2.57564E-01	1.18109E-01	4.20613E+00	-1.04398E-01
3.0000E-01	2.75761E-01	2.75763E-01	1.07955E-01	5.86862E+00	-9.98707E-00
4.0000E-01	2.93270E-01	2.93270E-01	9.81923E-00	7.69811E+00	-9.31039E-20
5.0000E-01	3.09305E-01	3.09390E-01	9.30956E-00	9.80500E+00	-8.43811E-00
6.0000E-01	3.23355E-01	3.25355E-01	9.13335E-00	1.24016E+01	-7.33318E-00
7.0000E-01	3.39534E-01	3.39534E-01	7.47342E-00	1.59848E+01	-5.92555E-00
8.0000E-01	3.52231E-01	3.52231E-01	6.69640E-00	2.21810E+01	-4.05328E-00
9.0000E-01	3.62895E-01	3.63299E-01	6.69667E-00	4.15426E+01	-1.15426E-00
1.0000E+00	3.72577E-01	3.72570E-01	5.84010E-00	2.27553E+01	-1.12040E+00
1.1000E+00	3.79960E-01	3.79940E-01	7.27811E-00	1.28247E+01	3.53014E-00
1.2000E+00	3.85367E-01	3.85367E-01	7.84790E-00	1.10075E+01	5.02249E+00
1.3000E+00	3.85724E-01	3.85724E-01	8.52334E-00	9.93450E-20	6.27357E+00
1.4000E+00	3.89995E-01	3.89995E-01	9.30335E-00	9.12033E-00	7.31737E-00
1.5000E+00	3.89147E-01	3.89147E-01	1.01795E-01	8.40753E-00	8.25864E-00
1.6000E+00	3.46209E-01	3.86209E-01	1.11350E-01	7.72942E-00	9.14475E-00
1.7000E+00	3.81200E-01	3.81200E-01	1.21676E-01	7.05357E-00	9.95148E-00
1.8000E+00	3.74210E-01	3.74210E-01	1.32706E-01	6.36271E-00	1.05907E-01
1.9000E+00	3.65300E-01	3.65300E-01	1.44376E-01	5.64700E-00	1.13617E-01
2.0000E+00	3.54585E-01	3.52693E-01	1.56609E-01	4.90052E-00	1.19626E-01
2.1000E+00	3.42000E-01	3.42000E-01	1.69331E-01	4.11946E-00	1.24900E-01
2.2000E+00	3.25312E-01	3.25313E-01	1.82465E-01	3.30111E-00	1.29413E-01
2.3000E+00	3.13075E-01	3.15630E-01	2.09286E-01	2.44324E-00	1.33126E-01
2.4000E+00	3.03541E-01	3.03541E-01	2.09636E-01	1.54367E-00	1.35001E-01
2.5000E+00	2.91251E-01	2.91251E-01	2.23497E-01	5.99819E-01	1.27997E-01
2.6000E+00	2.79341E-01	2.78962E-01	2.37418E-01	-3.91627E-01	1.39071E-01
2.7000E+00	2.61265E-01	2.66573E-01	2.51299E-01	-1.43526E+00	1.39178E-01
2.8000E+00	2.42674E-01	2.54384E-01	2.65035E-01	-2.53763E+00	1.38268E-01
2.9000E+00	2.23801E-01	2.42094E-01	2.78518E-01	-3.70826E+00	1.36286E-01
3.0000E+00	2.04645E-01	2.29805E-01	2.91629E-01	-4.90134E+00	1.33167E-01
3.1000E+00	1.86155E-01	2.17516E-01	3.04242E-01	-6.31951E+00	1.23207E-01
3.2000E+00	1.67844E-01	2.05227E-01	3.16223E-01	-7.81399E+00	1.16153E-01
3.3000E+00	1.50180E-01	1.92937E-01	3.27420E-01	-9.50468E+00	1.07512E-01
3.4000E+00	1.33381E-01	1.80648E-01	3.37664E-01	-1.14922E+01	9.70430E-00
3.5000E+00	1.17654E-01	1.68359E-01	3.46755E-01	-1.39776E+01	8.43617E-00
3.6000E+00	1.03097E-01	1.56070E-01	3.54440E-01	-1.74299E+01	6.97717E-00
3.7000E+00	9.01921E-00	1.43780E-01	3.60364E-01	-2.32969E+01	4.87358E-00
3.8000E+00	7.87933E-00	3.63485E-01	3.63985E-01	-3.99135E+01	1.90845E-00
3.9000E+00	6.13671E-00	3.63075E-01	3.63075E-01	-3.16450E+01	-3.47417E-00
4.0000E+00	5.55575E-00	3.58550E-01	3.58550E-01	-3.14550E+01	-5.34089E-00
4.1000E+00	5.17830E-00	3.52553E-01	3.52553E-01	-1.41128E+01	-6.61848E-00
4.2000E+00	5.00957E-00	3.45387E-01	3.45387E-01	-1.16174E+01	-7.69841E-00
4.3000E+00	5.05148E-00	3.37196E-01	3.37196E-01	-1.02094E+01	-8.56619E-00
4.4000E+00	5.30350E-00	3.28085E-01	3.28085E-01	-9.18579E-00	-9.54390E-00
4.5000E+00	5.76251E-00	3.18141E-01	3.18141E-01	-8.32559E-00	-1.03335E-01
4.6000E+00	6.42281E-00	3.07444E-01	3.07444E-01	-7.53544E-00	-1.10488E-01
4.7000E+00	7.27626E-00	2.96069E-01	2.96069E-01	-6.00312E-00	-1.16875E-01

MOVEMENT OF OUTCROP POINT
EXTERNAL SINE WAVE AND OUTCROP

RUN 2
PLOT 1

A=YF   5.0000   15.0000   25.0000   35.0000   45.0000   55.0000
B=YC   5.0000   15.0000   25.0000   35.0000   45.0000   55.0000
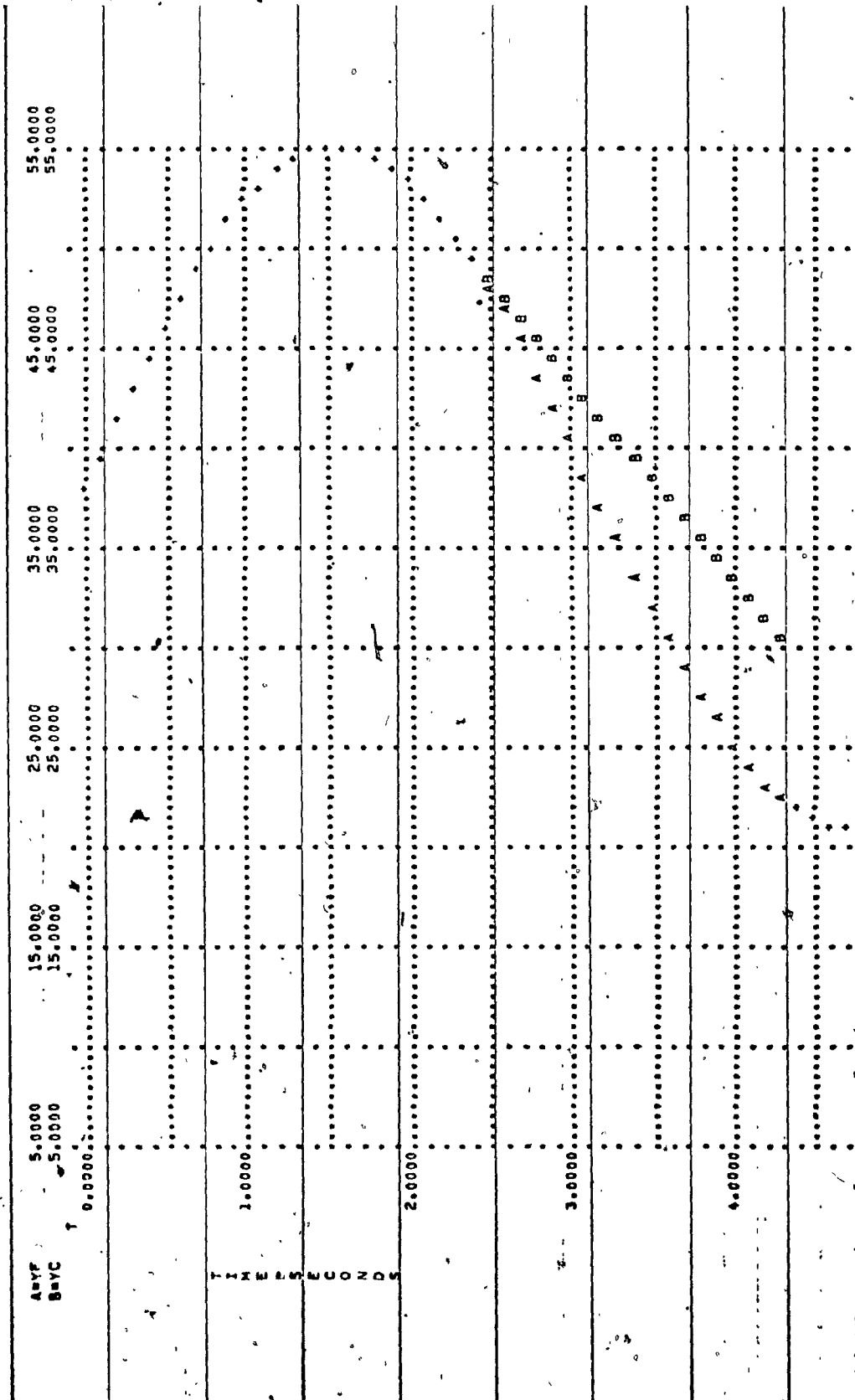
RUN 1
PLOT 1

MOVEMENT OF OUTCROP POINT
EXTERNAL SINE WAVE AND OUTCROP
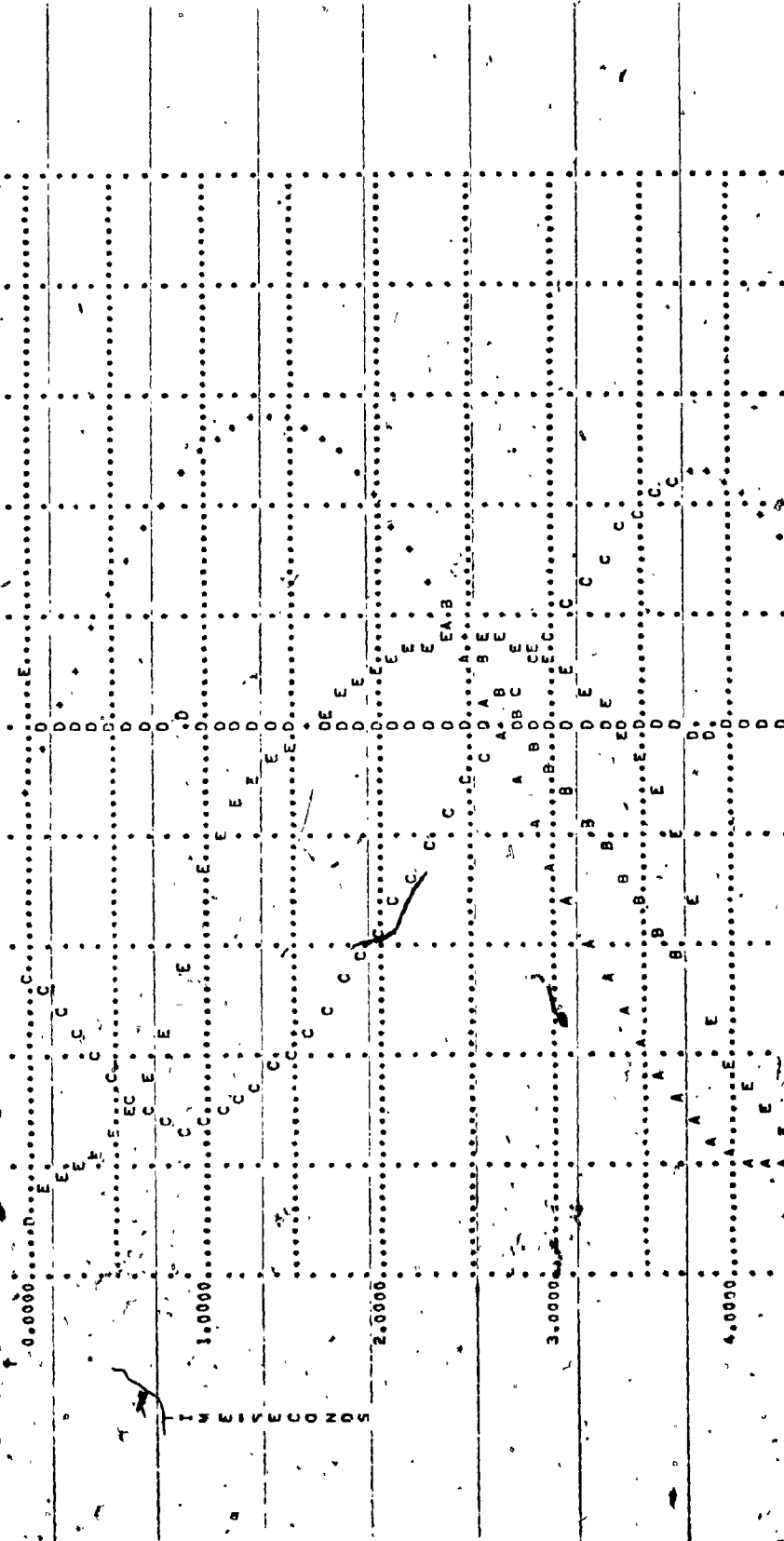
I	TIME	SINE WAVE	OUTCROP
1	0.0000	.6667	.6667
2	.0540	.7040	.7040
3	.1080	.7407	.7407
4	.1620	.7761	.7761
5	.2160	.8097	.8097
6	.2700	.8409	.8409
7	.3240	.8692	.8692
8	.3780	.8941	.8941
9	.4320	.9152	.9152
10	.4860	.9322	.9322
11	.5400	.9446	.9446
12	.5940	.9525	.9525
13	.6480	.9555	.9555
14	.7020	.9537	.9537
15	.7560	.9471	.9471
16	.8100	.9358	.9358
17	.8640	.9200	.9200
18	.9180	.9000	.9001
19	.9720	.8760	.8788
20	1.0260	.8486	.8576
21	1.0800	.8181	.8364
22	1.1340	.7850	.8152
23	1.1880	.7500	.7940
24	1.2420	.7136	.7727
25	1.2960	.6764	.7515
26	1.3500	.6390	.7303
27	1.4040	.6021	.7091
28	1.4580	.5663	.6879
29	1.5120	.5321	.6666
30	1.5660	.5002	.6454
31	1.6200	.4711	.6242
32	1.6740	.4453	.6030
33	1.7135	.4287	.5875
34	1.7675	.4096	.5663
35	1.8215	.3947	.5453
36	1.8755	.3844	.5249
37	1.9295	.3788	.5053
38	1.9835	.3781	.4868
39	2.0375	.3821	.4699
40	2.0915	.3910	.4549
41	2.1455	.4044	.4424
42	2.1995	.4223	.4331
43	2.2535	.4442	.4442
44	2.3220	.4773	.4773
45	2.3760	.5071	.5071
46	2.4300	.5395	.5395
47	2.4840	.5741	.5741
48	2.5380	.6102	.6102
49	2.5920	.6473	.6473
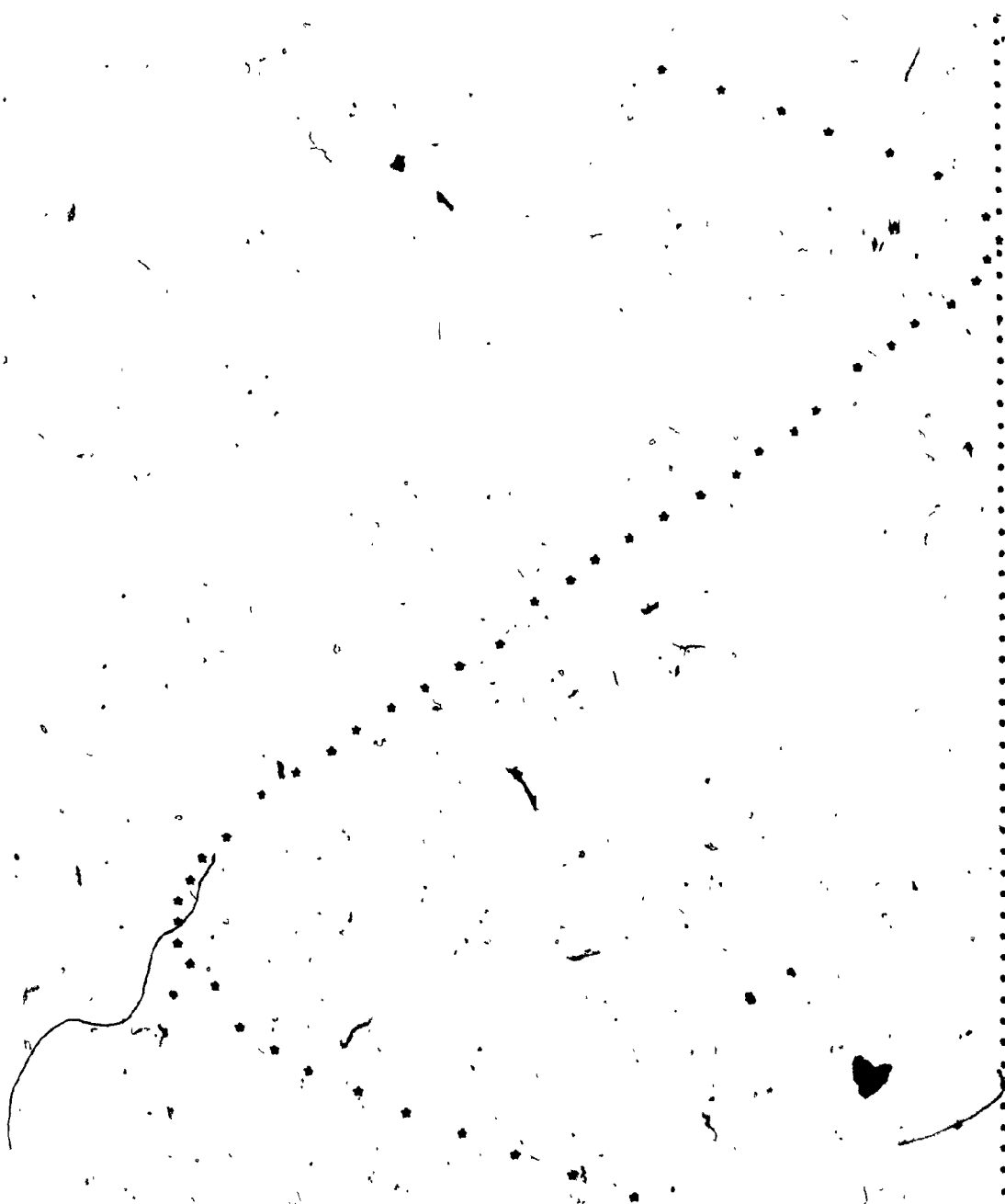
STEP NO. 1 REQUIRED 8 ITERATIONS

X	Y	U	C	W1	W2
0.0000	38.7435000	.7266	194.9150	190.1840	-186.7309
.1000	38.7122424	.6430	194.8364	190.0248	-186.7380
.2000	38.6800889	.5569	194.7553	189.8610	-186.7432
.3000	38.6531207	.4797	194.6876	189.7160	-186.7566
.4000	38.6310102	.4044	194.6319	189.5866	-186.7777
.5000	38.6131995	.3325	194.5870	189.4711	-186.8061
.6000	38.5992845	.2631	194.5519	189.3676	-186.8413
.7000	38.5889213	.1958	194.5258	189.2749	-186.8833
.8000	38.5818145	.1299	194.5079	189.1916	-186.9318
.9000	38.5777080	.0649	194.4976	189.1165	-186.9868
1.0000	38.5763765	.0003	194.4942	189.0487	-186.8460

STEP NO. 2 REQUIRED 7 ITERATIONS

X	Y	U	C	W1	W2
0.0000	39.4755000	1.3594	196.7477	192.5982	-189.8794
.1000	39.4836225	1.2001	196.5605	192.2647	-189.8645
.2000	39.3304999	1.0398	196.3861	191.9270	-189.8475
.3000	39.2709148	.8897	196.2373	191.6323	-189.8529
.4000	39.2230594	.7481	196.1176	191.3744	-189.8783
.5000	39.1854355	.6131	196.0236	191.1480	-189.9218
.6000	39.1567870	.4833	195.9519	190.9485	-189.9820
.7000	39.1360458	.3574	195.9008	190.7722	-190.0574
.8000	39.1222078	.2342	195.8656	190.6155	-190.1471
.9000	39.1146963	.1127	195.8466	190.4756	-190.2501
1.0000	39.1125314	-.0080	195.8411	190.3496	-190.3656

STEP NO. 3 REQUIRED 4 ITERATIONS

X	Y	U	C	W1	W2
0.0000	40.1847000	1.9219	198.5072	194.8709	-191.0271
.1000	40.0650509	1.6957	198.2135	194.3592	-190.9678
.2000	39.9461864	1.4676	197.9172	193.8432	-190.9079
.3000	39.8499671	1.2554	197.6708	193.3992	-190.8883
.4000	39.7737410	1.0560	197.4896	193.0159	-190.9038
.5000	39.7145712	.8668	197.3426	192.6838	-190.9502
.6000	39.6700880	.6854	197.2321	192.3949	-191.0242
.7000	39.6382704	.5097	197.1530	192.1424	-191.1229
.8000	39.6173722	.3381	197.1010	191.9203	-191.2440
.9000	39.6058450	.1690	197.0723	191.7233	-191.3853
1.0000	39.6022752	.0010	197.0634	191.5466	-191.5446

APPENDIX E

ORGANIZATION OF DATA

APPENDIX E

ORGANIZATION OF DATA

The experimental data used in this study, after Nasser (35), consists of four types of porous media: 4.4 cm, 1.7 cm, 0.7 cm crushed rock and 4.6 cm rounded quartz. There were eight parameters of particular interest for each rock type, seven of which are listed in Table E.1, along with their respective ranges: a, the linear resistance coefficient; b, the Non-Darcy resistance coefficient; m, the porosity; T, the period of oscillation; L, the length of rockfill; h_0, the mean water level; A_0 the maximum wave amplitude; and θ, the slope of the embankment.

There were 15 case groups among the four rock types. There was one sloping embankment case group for each of the four media; i.e. case groups L, M, N, O. These had a constant slope of 26.565^0 (i.e. 1:2). All the remaining cases were vertical embankments.

The data is broken down into individual cases identified by a letter designating the group followed by a number, eg. Case C-3. Each case group refers to a particular rock type that has identical a, b, m, L and θ values, as can be seen in Table E.2. Therefore only T, h_0 and A_0 vary within a group.

The case groups are divided into fast drop and slow drop cases to avoid confusion. Tables E.3 through E.9 show the pertinent variables

for the fast drop cases while Table E.10 summarizes the slow drop cases. The fast drop cases have three extra calculated parameters listed which are helpful in the analysis of the outcrop point movement: W is the dimensionless parameter that determines whether a case is fast drop, its value being necessarily less than $1/\sin^2\theta$; δ is introduced into one of the pot settings in the analog simulation and has a very wide range of values which creates scaling problems; Pk, another dimensionless number that indicates the percentage deviation of the fast drop case from the slow drop case.

To summarize, there were 224 cases studied, 165 fast drop cases and 59 slow drop. Of the 165 fast drop cases investigated, 92 had vertical embankments. Only 2 slow drop cases had sloped embankments.

TABLE E.1

PROPERTIES OF MEDIA AND RANGE OF VARIABLES

Parameter	Medium			
	4.40 cm Crushed Rock	1.70 cm Crushed Rock	0.7 cm Crushed Rock	1.60 cm Rounded Quartz
a (sec/cm)	0.004	0.009	0.017	0.010
b (sec/cm)^2	0.005	0.015	0.033	0.021
Range of:				
m	.46 - .49	.42 - .443	.45 - .486	.35 - .377
L (cm)	44.5 - 90.5	16.5 - 90.5	7 - 49	16.5 - 90.5
T (sec)	1.1 - 5.8	1.12 - 5.8	1.5 - 5.72	1.1 - 5.75
h_0 (cm)	22 - 38	22 - 38	22 - 38	22 - 38
A_0 (cm)	3.5 - 32	4 - 30	5.5 - 17.7	4 - 29
Case Groups	A,B,L	C,D,E,M	F,G,H,N	I,J,K,O

TABLE E.2

PROPERTIES OF THE TEST CASES

Group	Rock Type (cm)	L (cm)	m	a (sec/cm)	b (sec/cm)^2	θ (degrees)
A	4.4	90.5	.49	.004	.005	90
B	4.4	44.5	.49	.004	.005	90
C	1.7	90.5	.432	.009	.015	90
D	1.7	52.0	.43	.009	.015	90
E	1.7	16.5	.443	.009	.015	90
F	0.7	49.0	.48	.017	.033	90
G	0.7	21.0	.482	.017	.033	90
H	0.7	7.0	.486	.017	.033	90
I	1.6Q	90.5	.376	.010	.021	90
J	1.6Q	50.5	.372	.010	.021	90
K	1.6Q	16.5	.377	.010	.021	90
L	4.4	-	.46	.004	.005	26.56
M	1.7	-	.42	.009	.015	26.56
N	0.7	-	.45	.017	.033	26.56
O	1.6Q	-	.35	.010	.021	26.56

Q = Quartz

TABLE E.3

4.4 CM ROCK RECTANGULAR EMBANKMENT

		T (sec)	h_0 (cm)	A_0 (cm)	W	δ (sec.$^{-2}$)	P_k
A -	1	1.2	22	12	.4465	102	40.00
	2	3.2	22	18	.7938	305	8.92
	3	4.0	22	22	.8119	286	7.76
	4	3.4	22	16	.9489	2,805	1.09
	5	4.4	30	32	.6140	66	23.08
	6	3.8	30	32	.5303	49	31.12
	7	2.8	30	16	.7814	314	9.93
	8	1.2	30	12	.4465	102	40.00
	9	1.3	38	10	.5805	187	16.35
	10	1.2	38	16	.3349	57	53.05
	11	3.45	38	16	.9628	4,528	0.68
	12	5.2	38	32	.7259	111	13.75
B -	1	1.4	38	22	.2842	38	59.43
	2	3.5	38	20	.7814	252	9.75
	3	5.4	30	32	.7534	131	12.69
	4	2.7	30	13	.9274	2,038	1.85
	5	1.2	30	12	.4465	102	40.00
	6	1.2	22	10	.5358	160	30.55

Table E.4

1.7 cm ROCK RECTANGULAR EMBANKMENT

	T (sec)	h_0 (cm)	A_0 (cm)	W	δ (sec.$^{-2}$)	P_k
C - 1	2.50	22	8.5	.8528	1,075	5.35
2	3.14	22	12	.7587	361	11.31
3	4.12	22	13.5	.8849	981	3.70
4	3.15	30	21	.4349	56	41.30
5	1.70	30	5	.8859	61,673	.16
6	1.78	38	8.5	.6072	243	23.65
D - 1	3.46	38	16	.6300	142	21.65
2	2.50	38	9.5	.7666	480	11.76
3	1.80	38	7.3	.7183	470	14.30
4	1.70	30	5	.9904	111,432	.09
5	2.60	30	12	.6312	190	21.50
6	3.60	30	16	.6554	158	19.42
7	5.50	22	18	.8901	789	3.46
8	4.20	22	13	.9411	2,793	1.35
9	2.52	22	8.5	.8636	1,207	4.78
E - 1	5.10	38	15.5	.9304	1,819	1.75
2	3.50	38	16	.6185	135	22.67
3	2.50	38	10	.7069	323	15.19
4	1.80	38	6	.5655	197	27.50
5	2.60	30	15.5	.4743	86	9.30
6	3.76	30	24	.4430	51	40.40
7	4.20	22	14	.8483	624	5.62
8	2.50	22	9	.7854	575	9.45

0.7 ROCK RECTANGULAR EMBANKMENT

	T (sec)	h_0 (cm)	A_0 (cm)	W	δ (sec.$^{-2}$)	P_k
F - 1	2.21	30	10.5	.3666	95	49.00
2	4.24	30	10.5	.7034	302	15.45
3	5.64	30	11	.8931	1,345	3.32
4	5.64	22	17	.5779	109	26.45
5	4.34	22	10	.7560	426	4.50
6	2.40	22	9	.4645	143	38.00
G - 1	5.64	38	13.8	.7089	236	15.03
2	3.50	38	13.8	.4399	87	40.74
3	5.08	38	15	.5875	128	25.54
4	1.75	38	17.5	.1735	38	74.26
5	2.52	38	11	.3974	98	45.59
6	1.50	30	16	.1626	40	75.78
7	2.24	30	9.5	.4090	117	44.24
8	4.30	30	13.5	.5525	126	28.90
9	5.70	30	15	.6592	171	19.10
10	5.70	22	16.5	.5992	122	24.44
11	4.20	22	13	.5604	134	28.13
12	2.20	22	5.5	.6938	549	16.23
H - 1	1.79	38	9.5	.3241	95	94.38
2	2.63	38	6	.7541	702	11.65
3	3.82	38	10	.6572	254	19.27
4	5.12	38	14	.6292	161	21.72
5	5.70	38	13.8	.7106	239	14.90
6	5.72	30	10	.9840	25,738	0.19
7	4.17	30	9.5	.9551	446	11.57
8	2.64	30	15	.3028	57	51.06
9	2.62	22	5.5	.8195	1,221	7.30
10	4.58	22	9.5	.8294	770	6.70

TABLE E.6

1.6 CM QUARTZ RECTANGULAR EMBANKMENT

	T (sec)	h_o (cm)	A_o (cm)	W	δ (sec.$^{-2}$)	P_k
I - 1	3.46	22	11.5	.8490	765	5.57
2	2.60	22	12	.6114	175	23.31
3	1.72	38	12.5	.3883	84	46.65
4	2.45	38	11	.6285	205	21.77
5	3.45	38	15.5	.6281	145	21.80
6	5.72	30	16.5	.9783	9,812	.31
7	3.60	30	17	.5976	117	24.59
8	2.62	30	12	.6161	179	22.89
9	1.70	30	5.5	.8722	2,057	4.33
J - 1	1.70	38	15	.3233	60	54.50
2	3.48	38	16	.6204	136	22.50
3	5.00	38	15	.9507	3,163	1.04
4	5.74	30	18	.9095	1,057	2.57
5	3.60	30	20	.5134	75	32.85
6	2.65	30	12.5	.6047	164	23.93
7	1.70	30	5.5	.8816	2,306	3.86
8	4.15	22	14	.8455	607	5.77
K - 1	2.50	38	10.5	.6701	257	18.17
2	2.62	30	13	.5672	137	27.47
3	1.72	30	5	.9682	18,261	.54
4	3.46	22	13	.7491	314	12.00
5	5.60	22	18.5	.8671	577	4.59
6	1.70	22	14	.3417	67	52.22

Table E.7

4.4 cm ROCK SLOPING EMBANKMENT

	T (sec)	h_o (cm)	A_o (cm)	W	δ (sec.$^{-2}$)	P_k
L - 1	5.20	38	23	2.322	11.21	38.0
2	3.80	38	20	1.952	10.56	46.4
3	3.45	38	20	1.715	9.42	52.0
4	1.60	38	12	1.370	13.45	61.8
5	5.00	38	15.5	3.313	33.64	18.8
6	2.50	38	16	1.605	11.19	54.8
7	1.25	38	10	1.284	15.57	63.0
8	2.60	38	6	4.451	473.46	3.5
9	1.80	38	8	2.311	32.02	38.3
10	2.60	30	7	3.815	127.20	11.0
11	1.75	30	7	2.568	42.66	32.9
12	1.10	30	9	1.255	17.10	63.8
13	2.80	30	13	2.212	18.64	40.5
14	3.80	30	12	3.252	41.18	19.9
15	1.70	30	9	1.940	23.34	46.7
16	5.75	30	17	3.474	35.71	16.2
17	3.80	30	17	2.296	14.94	38.6
18	4.40	30	18	2.511	16.01	34.0
19	3.40	22	9	3.880	107.77	10.1
20	5.60	22	16	3.595	43.00	14.3
21	3.30	22	10	3.389	55.94	17.6
22	2.60	22	12	2.225	20.34	40.2
23	1.15	22	9	1.312	27.51	62.3
24	1.70	22	6	2.910	62.74	26.0
25	2.90	22	7	4.255	256.44	5.5

TABLE E.8

1.7 AND 0.7 CM ROCK SLOPING EMBANKMENTS

		T (sec)	h_o (cm)	A_o (cm)	W	δ (sec.$^{-2}$)	P_k
M -	1	5.76	22	20	1.836	9.98	49.2
	2	3.46	22	16	1.378	10.13	60.5
	3	3.16	22	14.2	1.418	11.61	59.5
	4	4.16	22	16	1.657	11.46	53.5
	5	1.12	22	11	.649	11.08	80.5
	6	2.62	22	4.5	3.711	174.17	12.5
	7	1.32	30	14.2	.592	8.41	82.1
	8	1.76	30	7	1.602	25.54	54.9
	9	2.63	30	9.5	.838	6.53	75.1
	10	2.20	30	20	.701	6.21	78.9
	11	3.27	30	20	1.042	7.06	69.5
	12	4.20	30	25	1.071	5.71	68.7
	13	5.73	30	22	1.660	8.34	53.4
	14	5.73	38	12.5	2.922	30.37	25.8
	15	5.15	38	30	1.094	4.80	68.0
	16	4.16	38	11	2.410	24.67	36.2
	17	3.30	38	28	.751	4.52	77.5
	18	1.32	38	14	.601	8.56	81.9
	19	1.78	38	15	.756	8.45	77.4
	20	2.60	38	9	1.841	22.23	49.0
N -	1	2.23	30	14.5	.603	8.27	81.8
	2	2.87	30	8.5	1.324	18.63	62.0
	3	4.10	30	10.5	1.531	16.49	56.6
	4	5.68	30	17	1.310	9.26	62.3
	5	5.68	22	15	1.485	11.31	57.8
	6	4.26	22	17.7	.944	7.68	72.2
	7	2.52	22	9.5	1.040	14.85	69.5

TABLE E.9

1.6 cm QUARTZ SLOPING EMBANKMENT

	T (sec)	h_0 (cm)	A_0 (cm)	W	δ (sec.$^{-2}$)	P_k
0 - 1	1.30	38	15	.563	7.88	82.9
2	1.72	38	14	.798	9.19	76.2
3	2.48	38	13	1.239	11.76	64.2
4	3.28	38	29	.735	4.34	78.0
5	5.15	38	16	2.091	14.19	43.2
6	5.20	38	27	2.111	14.34	42.7
7	5.72	30	19	1.956	11.14	46.3
8	4.15	30	26	1.037	5.42	69.6
9	3.60	30	22	1.063	6.47	68.9
10	1.88	30	15	.814	8.63	75.8
11	5.70	30	10.2	3.630	70.10	13.7
12	1.30	30	10	.844	13.09	74.9
13	1.70	30	8.5	1.299	18.43	62.6
14	2.62	30	8	2.128	28.94	42.3
15	2.62	22	4.5	3.782	189.87	11.5
16	1.10	22	12.8	.558	9.22	83.1
17	1.71	22	6.2	1.792	31.50	50.2
18	2.64	22	14.8	1.159	9.99	66.3
19	5.70	22	16.6	2.231	14.75	40.0
20	3.48	22	16	1.413	10.28	59.6
21	5.74	22	20	1.864	10.12	48.5

0   1.6 cm rock
    m — .350
    a — .010
    b — .021

TABLE E.10
SLOW DROP CASES

	T	$\dot{h}_{o}$	A_o
A-13	1.8	22	7
14	3.0	22	4
15	5.6	22	5
16	5.6	22	20
17	5.8	30	24
18	3.8	30	16
19	5.5	30	12
20	2.6	30	7
21	1.75	30	4
22	1.88	38	4.5
23	5.0	38	13
B-7	1.8	38	8
8	2.5	38	10
9	5.0	38	16
10	5.3	38	14
11	3.6	30	16
12	5.2	30	19
13	2.7	30	11
14	1.7	30	5.5
15	1.7	22	4
16	2.85	22	3.5
17	4.15	22	14
18	3.3	22	14
19	5.6	22	20
20	3.45	22	12

TABLE E.10 - CONT'D.

	T	h_o	A_o
C - 7	1.7	22	4
8	5.76	22	15
9	5.76	30	16
10	4.14	30	8.5
11	2.60	30	6
12	2.6	38	5.5
13	3.45	38	7
14	5.17	38	13.8
15	5.76	38	14
D -10	5.7	38	14.5
11	5.16	38	13.8
12	5.68	30	16.5
E - 9	5.7	38	15.5
10	5.6	30	10.5
11	5.8	30	15
12	5.8	22	16
I -10	5.75	22	16
11	5.7	22	15
12	2.6	22	4.5
13	1.7	22	4
14	5.08	38	14
15	5.58	38	14
16	5,7	30	9

TABLE E.10 - CONT'D.

	T	h_o	A_o
J - 9	.5.36	38	13
10	5.6	30	10
11	1.7	22	4
12	5.74	22	16
K - 7	5.72	38	14.2
8	5.18	38	14.5
9	4.2	30	10
10	5.7	30	11
11	5.74	30	16
L - 26	5.6	30	3.5
27	4.0	22	8

APPENDIX F

PHOTOGRAPHS OF THE EAI 690 HYBRID COMPUTER

APPENDIX F

PHOTOGRAPHS OF THE EAI 690 HYBRID COMPUTER

This appendix is intended to familiarize the reader with the hardware used in this study, the EAI 690 Analog/Hybrid Computer. This system comprises a digital computer EAI 640 (Fig. F.1), and interfacing unit EAI 693 (Fig. F.1) and an analog computer EAI 680 (Fig. F.2).

The EAI 640 can read or write on magnetic tape or paper tape using the teletype printer and octal converters as controlling devices. The EAI 640 can be operated as a separate unit, can be linked with the CDC Cyber processors within the University or connected to the EAI 680 Analog Computer through the EAI 693 Interfacing Unit.

The Analog Computer (Fig. F.3) consists basically of an analog patch panel, digital logic and a control panel. The control panel sets the mode and speed of operation, sets pots, contains a four-digit accurate digital voltmeter and indicates the logic components that are in operation. The digital logic consists of And Gates, comparators, switches, controls over certain operational amplifiers, etc. (Fig. F.4).

The Analog Patch Panel (Fig. F.5) consists of 120 operational amplifiers that have the capability of performing all the basic mathematical operations including integration. The facility at Concordia at present has only about 55 operational amplifiers which limits the methods

of simulation that can be applied. A colour code helps to avoid confusion in patching circuits. Table F.1 summarizes the functions of the various colours.

TABLE F.1

COLOUR CODING FOR THE EAI 640 ANALOG PATCHING PANEL

Colour	Function
Green	Input
Red	Output
Black	Ground
Yellow	Potentiometers
White	Amplifier Control Options
Brown (Striped)	Relay Switch
Red$^+$	Positive Reference Voltage
Orange$^-$	Negative Reference Voltage

Fig. F.1 — EAI 640 Digital Computer and EAI 693 Interface.
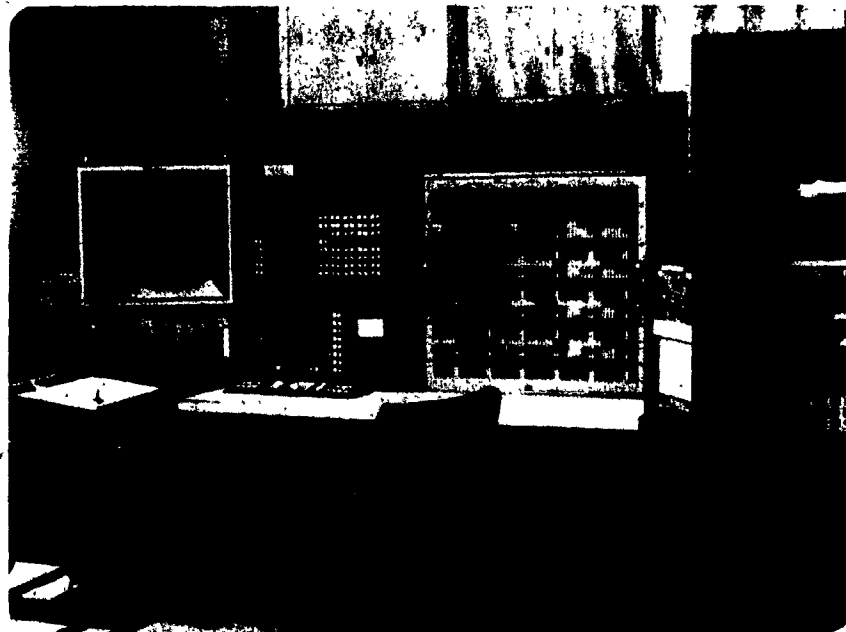

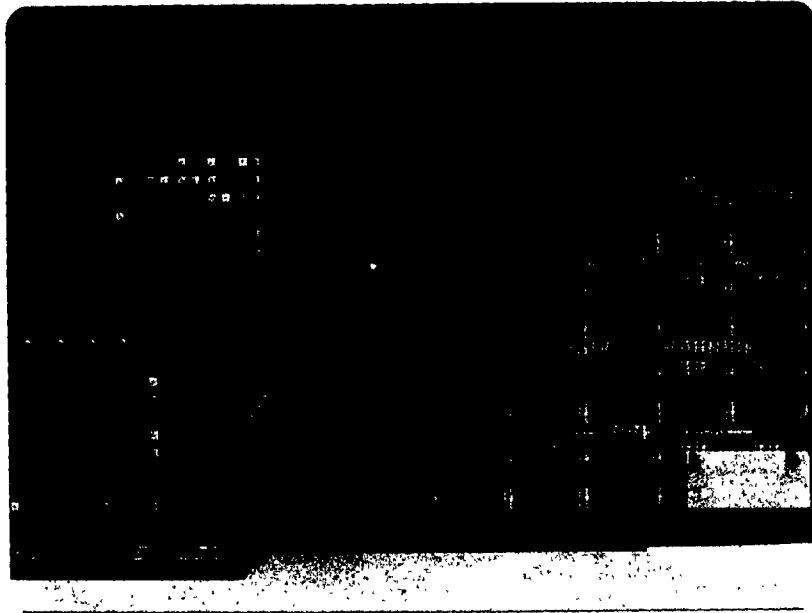*Fig. F.2 — EAI 680 Analog Computer with Peripheral Output Devices.*
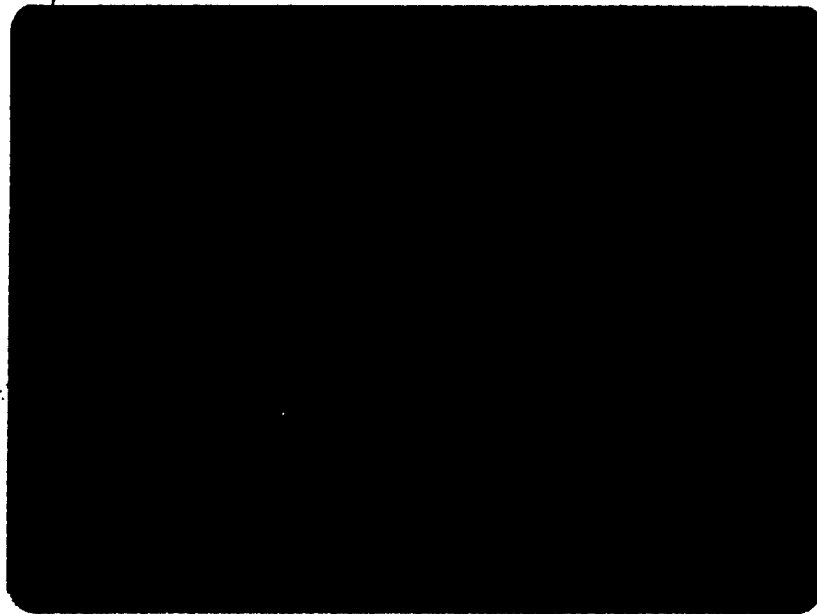
Fig. F.3 — EAI 680 Analog Console and Patch Panel.

Fig. F.4 — Typical Digital Logic Patching Trays.

Fig. F.5 — Typical Analog Patching Tray.

APPENDIX G

NOMENCLATURE

Appendix G

NOMENCLATURE

a, a_1 -   resistance coefficients

a_B, a_F -   constants

A -   constant

A_0 -   maximum amplitude

b, b_1 -   non-Darcy resistance coefficients

B -   constant

c -   celerity

C -   constant

CSDT   -   continuous-space discrete-time

D -   hydraulic depth; constant

DSCT   -   discrete-space continuous time

EDA   -   electronic differential analyzer

F	-	non-Darcy friction term; fast second
F-MS	-	fast-milli-second
$f(t)$	-	time dependent function
$f(u)$	-	square matrix of functions
g	-	acceleration due to gravity
$g(x_1 t), G$	-	forcing functions
h	-	water level
h_0	-	mean water level
Δh	-	numerical step size
i	-	hydraulic gradient
i_0	-	threshold gradient
I	-	identity matrix
IC	-	initial condition mode
j	-	index of discretized time
k	-	non-Darcy hydraulic conductivity
K_1	-	Darcy hydraulic conductivity
K_0, K	-	scaling factors
L	-	length of rockfill
L, L_B, L_F	-	operators on functions
MOC	-	Method of Characteristics

ODE	-	Ordinary Differential Equations
OP	-	Operate Mode
PDE	-	Partial Differential Equations
Pk	-	dimensionless parameter
q	-	macroscopic velocity; lateral inflow
R	-	correlation coefficient
S_f	-	friction or energy line slope
S_o	-	channel bed slope
t	-	time independent variable
t_1, t_2, t_c	-	time constants
Δt	-	time increment
T	-	period of oscillation
TKG	-	constant
u	-	horizontal pore velocity
V	-	maximum internal fall velocity
$\underline{V}$	-	actual pore velocity
V_f	-	vertical velocity
V_{fmax}	-	maximum internal fall velocity
V_i	-	input voltage
V_0	-	output voltage

W	–	vector of transformed dependent variables; dimensionless parameter
w^1, w^2	–	adjoint eigenvectors
W_1, W_2	–	characteristic independent variables
X	–	space independent variable
X_{max}	–	maximum distance
y	–	depth of water
Y_c	–	elevation of outcrop point movement
Y_f	–	elevation of free water level
ΔY_p	–	maximum deviation between Y_c and Y_f
Z_i	–	input impedance
Z_f	–	feedback impedance
α	–	characteristic direction; energy coefficient; damping ratio
β	–	characteristic direction; time scale factor
δ	–	constant
η	–	perturbation height wrt to mean water level
θ	–	interpolation factor; angle of inclination of rockfill with the horizontal
λ	–	vector of eigenvalues
χ	–	dimensionless number
ω	–	frequency of oscillation
ω_n	–	undamped natural frequency of oscillation

BIBLIOGRAPHY

BIBLIOGRAPHY

1. AHMED, N., and SUNADA, D. K., "Nonlinear Flow in Porous Media", J. of Hyd. Div., Proc. of ASCE, Vol. 95, No. HY6, Nov. 1969.

2. ANDRE, H., "Extensions to the CSDT Methods for the Hybrid Solution of Partial Differential Equations", Proc. of the 6th AICA/IFIP International Conference on Hybrid Computation. Munich, Germany, Aug. 31-Sept. 4, 1970.

3. APALOVICOVA, R., and BABIRAD, J., "Hybrid Computer Solution of Hyperbolic Partial Differential Equations", Proc. of 7th AICA International Congress. Prague, Czechoslovakia, 1973.

4. BECKEY, G.A., and KARPLUS, W.J., "Hybrid Computation". John Wiley, New York, 1968.

5. BOSGRA, O.H. and BUIS, J.P., "Hybrid Computer Solution of the Hyperbolic Equations Describing Forced-Flow Steam-Generator Dynamics", Proc. of 6th AICA/IFIP International Conference on Hybrid Computation. Munich, Germany, 1970.

6. ————. "Error Analysis of a Generalized Method of Lines for the Hybrid Solution of Partial Differential Equations", Proc. of 7th AICA International Congress. Prague, Czechoslovakia, 1973.

7. ————. "Aspects of Hybrid CSDT Difference Approximations for Partial Differential Equations", Proc. of AICA Intern. Symposium, Lehigh University, Bethlehem, Penn., June 1975.

8. ————. "The Directional Difference Method and Its Error Properties Evaluated in the Physical and Numerical Sense", Proc. of AICA Intern. Symposium. Lehigh University, Bethlehem, Pennsylvania, June 1975.

9. CHOW, V.T., "Open Channel Hydraulics". McGraw-Hill Book Co., New York, 1959.

10. DRACOS, T., "Calculation of the Movement of the Outcrop Point", Proc. XIII, Congress of IAHR, Paper D-2. Kyoto, Japan, 1969.

11. DUDGEON, C.R., "Flow of Water Through Coarse Granular Materials", Master of Engineering Thesis, University of New South Wales, 1964.

12. Electronics Associates Inc., EAI 640 Scientific Computing System, Reference Handbook, June, 1969.

13. ――――.� EAI 680 Scientific Computing System, Reference Handbook, Oct., 1966.

14. ――――.ₒ EAI 690 Hybrid Computing System, Reference Handbook, March 1969.

15. ENGELUND, F., "On the Laminar and Turbulent Flow of Ground Water through Homogeneous Sand", Transactions of the Danish Academy of Technical Science, No. 3., 1953.

16. FORCHHEIMER, P., "Wasserbewegung Durch Boden", Zeit. Ver. Deutsch. Ing., 45, 1901.

17. FUGITA, H., KEMMOCHI, Y., and BABA, K., "Simulation of Self-Excited Wave Propagation in a System with Strong Nonlinearity", Proc. of 7th AICA Intern. Congress. Prague, Czechoslovakia, 1973.

18. GENTINA, J.C., and CLERET, F., "Hybrid Computation for a Class of Partial Differential Equations", Advances in Computer Methods for PDE's, R. Vichnevetsky (ed.), Publ. AICA, 1975.

19. HANNOURA, A.A. and McCORQUODALE, J.A., "Hybrid Finite Element-Method of Characteristics Model Applied to Unsteady Nonlinear Flow in Porous Media", CSCE Specialty Conference on Computer Applications in Hydrotechnical and Municipal Engineering, Toronto, 1978.

20. HARA, H.H. and KARPLUS, W.J., "Application of Functional Optimizing Techniques for the Serial Hybrid Computer Solution of Partial Differential Equations", 1968 Fall Joint Computer Conference, AFIPS, Vol. 33, Pt. 1.

21. HAUSNER, A., "Analog and Analog/Hybrid Computer Programming", Prentice-Hall, Inc., Englewood Cliffs, N.J., 1971.

22. HENDERSON, F.M., "Open Channel Flow". MacMillan Company, New York, 1966.

23. HENRY, R.F., "Simulation of Long Waves in Branching Waterways", J. of Hyd. Div., Proc. of ASCE, Vol. 98, No. HY4, April, 1972.

24. HSU, S.K.T., and HOWE,R.M., "Preliminary Investigation of a Hybrid
    Method for Solving Partial Differential Equations", 1968
    Fall Joint Computer Conference, AFIPS, Vol..33, Pt. 1.

25. JANAC, K., "CSDT Hybrid Methods for Partial Differential Equations
    in Several Space Dimensions", Summer Computer Simulation
    Conference, Washington, D.C., July, 1976.

26. JURY, S.H., "Solving Partial Differential Equations", Industrial
    & Engineering Chemistry, Vol. 53, 1961.

27. KARPLUS, W., "Analog Simulation". McGraw-Hill, New York, 1958.

28. KORN, G.A., and VICHNEVETSKY, R., "Analog/Hybrid Computation and
    Digital Simulation", IEEE Transactions on Computers,
    Vol. C-25, No. 12, Dec., 1976.

29. KOVACS, G., "General Characterization of Different Types of Seepage",
    Proc. XIII Congress IAHR, Vol. 4. Kyoto, Japan, Sept., 1969.

30. LANE, K.S., Discussion of "Laminar and Turbulent Flow of Water
    Through Sand", Proc. ASCE, J. of Soil Mechanics Div.,
    Vol. 90, SM3, May, 1964.

31. McAVOY, T.J., "Solution of Hyperbolic Partial Differential Equations
    via a Hybrid Implementation of the Method of Characteristics",
    Simulation Journal, March, 1972.

32. McCANN, M.J.; "Simulation Techniques for Distributed Parameter Sys-
    tems", AICA Annules, No. 1., Jan., 1967.

33. McCORQUODALE, J.A., "Finite Element Analysis of Non-Darcy Flow",
    A Thesis presented to the University of Windsor in Partial
    Fulfillment of the Requirements for the Ph.D. Degree in
    Civil Engineering, Windsor, Canada, 1970.

34. McCORQUODALE, J.A., HANNOURA, A.A., and NASSER, M.S., "Hydraulic
    Conductivity of Rockfill", Journal of Hydraulic Research, 16,
    No. 2, 1978.

35. NASSER, M.S., "Theoretical and Experimental Analyses of Wave Motion
    in Rockfill Structures", A Thesis presented to the Univer-
    sity of Windsor in Partial Fulfillment of the Requirements
    for the Ph.D. degree in Civil Engineering, Windsor, Canada,
    1974.

36. NASSER, M.S., "Experimental Study of Wave Transmission", Journal of the Waterways, Harbours and Coastal Engineering Division, ASCE, Vol. 100, No. WW4, Proc. Paper 10928, Nov., 1974.

37. NASSER, M.S. and McCORQUODALE, J.A., "Wave Motion in Rockfill", Journal of the Waterways, Harbours and Coastal Engineering Division, ASCE, Vol. 101, No. WW2, Proc. Paper 11286, May, 1975.

38. NELSON, P.J., "Application of Invariant Imbedding to the Solution of PDE's by the Continuous-Space Discrete-Time Method", AFIPS Proc. of SJCC, Vol. 36, Thompson Book Co., Washington, D.C., 1970.

39. NELSON, P.J., and ALTOM, D.W., "On the Use of Invariant Imbedding Within the Continuous-Space Discrete-Time Method: Digital Simulation", Proc. 6th AICA/IFIP Intern. Conference on Hybrid Computation. Munich, Germany, Fall, 1970.

40. —————. "Hybrid Solution of Partial Differential Equations by Application of Invariant Imbedding to the Serial Method", Simulation Journal, October, 1971.

41. NG, H.C., "An Experimental Study of Steady Non-Darcy Flow in Crushed Rock". Thesis presented at the University of Windsor, Windsor, Canada, in Partial Fulfilment of the Requirements of the Degree of Master of Applied Sciences, 1969.

42. O'BRIEN, J.F., and EDGE, B.L., "A Hybrid Computer Approach to the Solution of Water Quality in an Estuary", AICA, No. 3., July 1975.

43. PAUL, R.J.A., and AHMAD, A.I.S.; "Analogue Solution of 2nd Order Hyperbolic Partial Differential Equations by Method of Continuous Characteristics", Proc. IEEE, Vol. 117, No. 6, 1970.

44. ROGERS, A.E. and CONOLLY, T.W., "Analog Computation in Engineering Design", McGraw-Hill, New York, 1960.

45. RUBIN, A.I., and KEENE, D.H., "The Future of Hybrid Computation", Simulation Journal, August, 1975.

46. SCHUCHMANN, H., "On the Simulation of Distributed Parameter Systems", Simulation Journal, June, 1970.

47. SILVEY, T.I., and BARKER, J.R., "Hybrid Computing Techniques for Solving Parabolic and Hyperbolic Partial Differential Equations", Computer Journal, Vol. 13, No. 2, May 1970.

48. SMITH, G.D., "Numerical Solution of Partial Differential Equations". Oxford University Press, London, 1965.

49. STOCKTON, A., "Hybrid Computer Solutions of the Wave Equation for Isotropic and Anisotropic Media", Summer Computer Simulation Conference, San Francisco, July, 1975.

50. VICHNEVETSKY, R., "Error Analysis in the Computer Simulation of Dynamic Systems: Variational Aspects of the Problem", IEEE Trans. on Electronic Computers, Vol. ED-16, No. 4, August 1967.

51. ————. "A New Stable Computing Method for the Serial Hybrid Computer Integration of Partial Differential Equations", 1968 Spring Joint Computer Conference, AFIPS, Vol. 32.

52. ————. "Analog/Hybrid Solution of Partial Differential Equations in the Nuclear Industry", Simulation Journal, Vol. 12, Dec., 1968.

53. ————. "Hybrid Computer Integration of Hyperbolic Partial Differential Equations by a Method of Lines", Proc. of Fourth Australian Computer Conference, Adelaide, South Australia, 1969.

54. ————. "State of the Art in Hybrid Methods for Partial Differential Equations", Proc. of 6th AICA/IFIP International Conference on Hybrid Computation, Munich, Germany, 1970.

55. ————. "Hybrid Methods for Partial Differential Equations", Simulation Journal, April, 1971.

56. ————. "Stability Charts of Methods of Lines for Partial Differential Equations", Proc. of 6th Annual Princeton Conference on Information Science and Systems, Princeton University, March, 1972.

57. ————. "Physical Criteria in Computer Methods for Partial Differential Equations", AICA Annules, Vol. 16, No. 1, Jan., 1974.

58. Vichnevetsky, R., and Tomalesky, A.W.. "A Hybrid Computer Method for the Analysis of Time Dependent River Pollution Problems", AFIPS, Spring Joint Computer Conference, 1970.

59. Vichnevetsky, R., and Tomalesky, A.W. "Computer Algorithm for Hyperbolic Equations with Application to the Simulation of Electrical-Transmission Lines", _AICA Annules_, Vol. 16, No. 2, April, 1974.

60. Ward, J.C. "Turbulent Flow in Porous Media", _J. of Hyd. Div., Proc. of ASCE_, Vol. 90, No. HY5, Sept., 1964. Closure, Vol. 92, HY4, July 1966.

61. Weyrick, R.C., "Fundamentals of Analog Computers". Prentice-Hall Inc., Engelwood Cliffs, N.J., 1969.

62. Wright, E.J. and Mufti, I.H. "Simulation of Unsteady Fluid Flow Systems using a Hybrid Computer", _Summer Computer Simulation Conference_, Vol. 1, San Francisco, July, 1975.